Multiple roles for BMP signalling in Hypothalamic Development

Aragorn Jones

A thesis submitted in partial fulfilment

of the requirements for the degree of

Doctor of Philosophy

The University of Sheffield

Faculty of Science

Department of Biomedical Science

January 2020

Table of Contents

Figure List

Tables

Abbreviations

A-P	Anterio-posterior
AEN	Anterior Extent of Neuroectoderm
AN	Anterior Neuropore
CF	Cephalic Flexure
OD	Optical Density
pAnt	Anterior Progenitors
pBHyp	Basal Hypothalamic Progenitors
PM	Prechordal Mesoderm
pMam	Mammillary Progenitors
PME	Prechordal Mesendoderm
pVT	Ventro-Tuberal Progenitors
RDVM	Rostral Diencephalic Ventral Midline
RP	Rathke's Pouch

Abstract

The hypothalamus is the central coordinator of body homeostasis but despite its indispensable function much isn't known about its development. In recent work in the embryonic chick we showed that a small group of *FGF10*-expressing progenitor cells at the ventral midline of the neural tube, termed pBHyp (basal hypothalamic progenitor) cells, give rise to the three classically defined domains of the adult basal hypothalamus: anterior, tuberal and mammillary (Fu et al., 2017). Here I show that pSMAD1/5/8, the mediator of the canonical Bone Morphogenic Protein (BMP) signalling pathway is active within rostral ventral midline cells and prefigures and predicts pBHyp cells. pSMAD1/5/8, however, is not uniformly expressed in pBHyp cells, but instead is only detected at low levels in anterior-most pBHyp cells. Using an ex vivo assay, I show that pSMAD1/5/8 and *FGF10* are induced by BMPs in a dose-dependent manner. In vivo, BMP7 is expressed at highest levels in posterior-most pBHyp cells. Together these studies suggest that pBHyp cells are pre-patterned through BMP signalling. In vivo, the first set of progenitor cells to grow from pBHyp cells are anterior progenitor cells. I show that pSMAD1/5/8 is downregulated as anterior progenitors emerge from pBHyp cells. To address whether BMP signalling must be downregulated for pBHyp cells to progress to an anterior progenitor identity, I performed gain-of-function and loss-of-function studies in vivo, implanting beads soaked in BMP7 or the BMP inhibitors, Noggin and Chordin. Ectopic BMP7 prevents the growth and development of anterior progenitors; conversely, ectopic Noggin/Chordin promotes the growth and development of anterior progenitors. Together with the ex vivo work, these interventions support a model in which the regulation of ambient levels of BMP signalling is

critical to hypothalamic development: high levels are required to establish pBHyp cells but

must then be eliminated to promote the progression of pBHyp cells to anterior progenitors.

Chapter 1: Introduction

1.1. The Hypothalamus and Hypothalamic Development

1.1.1. The Hypothalamus

The hypothalamus, located in the ventral brain, occupies just 0.3% of the adult human brain. It is an evolutionarily ancient brain region, both its organisation and resident cell types highly conserved in vertebrates (Kitamura et al., 1997; Macdonald et al., 1995; Ruiz i Altaba, 1998; Tessmar-Raible et al., 2007). Its core function is to mediate homeostasis, this is the processes by which organisms regulate their internal environment to maintain a stable and consistent equilibrium required for the organism to function properly (Cannon, 1929). To do so, the hypothalamus integrates many different signals from a variety of sensory pathways, including the peripheral body, and compares these to set points and electrical impulses. This can result in the action or inaction of behavioural, autonomic and endocrine effectors via a plethora of mechanisms; hypothalamic systems can allow for both short term or sustained reactions, dependent upon the stimulus and the response required. It is this fine-tuning that allows the hypothalamus to control homeostatic parameters such as temperature, fluid and energy balance, sleep-wake states and stress responses (Saper and Lowell, 2014), along with aggressive and sex specific behaviours (Anderson, 2016; Hashikawa et al., 2018; Li and Dulac, 2018; Yates, 2015). To achieve all of these complex and disparate functions, the

hypothalamus is made up of dozens of nuclei located around the third ventricle of the brain. Within each nucleus are collections of neurons grouped by their transcription factor expression, functional neurohormone/neuropeptidergic/enzyme expression and connections. These diverse nuclei have been the main obstacle in studying the development and function of the hypothalamus.

Classically the adult hypothalamus is divided into four regions along the rostro-caudal (anterior-posterior) axis: the pre-optic, anterior, tuberal and mammillary regions, each with its resident nuclei, which are arranged in a patchwork manner. In addition, the tuberal hypothalamus contains a specialised region, the subventricular zone, that harbours radial glial-like cells, termed tanycytes. Tanycytes form part of a 2-way circuit that links the peripheral body and the brain. Through their direct and/or indirect connections to the median eminence and cerebrospinal fluid, tanycytes can sample the blood environment and cerebrospinal fluid for parameters such as glucose concentration, and respond by modulating feeding behaviour through leptin and/or glucose concentration via insulin (Barahona et al., 2018; Benford et al., 2017). In this way they help to maintain homeostasis and promote growth during the lifecourse of vertebrates. Some of these processes are orchestrated through hormones released from the pituitary gland. The pituitary gland contains two distinct structures of different origin, the adenohypophysis, derived from oral ectoderm, and the neurohypophysis, derived from neural ectoderm. The adenohypophysis develops from the hypophyseal placode, anterior to the neural ectoderm. During development this placode thickens and through folding of the neural ectoderm comes into contact with the ventral side of the neural ectoderm. Following this there is reciprocal

signalling between the hypophyseal placode and the developing hypothalamus, with signalling from each structure required for the proper patterning of the other. This leads to the outgrowth of the hypophyseal placode to become Rathke's Pouch, an elongated structure that eventually buds off from the oral ectoderm to give rise to the adenohypophysis (Asa and Ezzat 2004; Carreno et al. 2017; Ericson et al. 1998; Takuma et al. 1998; Treier and Rosenfeld 1996; Treier et al. 2001; 1998). Additionally, subsets of tanycytes act as resident stem and progenitor cells, and are capable of giving rise to a limited number of cell types even in the adult hypothalamus (Rizzoti and Lovell-Badge, 2017; Robins et al., 2013; Yoo and Blackshaw et al., 2018).

Study of the hypothalamus has been fraught with challenges: its structural and functional complexity, and the vast numbers of poorly-characterised neurons of wide-ranging function sets it apart from other areas of the CNS, such as the cerebral cortex and spinal cord, where neurons of more restricted function are found in a columnar organisation. Understanding normal hypothalamic neurons and glial cells in more detail is important: changes that occur in hypothalamic cells result in the diseases and differences that we see in the population. One approach to better characterising and understanding hypothalamic neurons is a developmental approach.

1.1.2. Development of the Hypothalamus

Despite its indispensable function, the development of the hypothalamus remains enigmatic. Its neurons and glia develop over a protracted period during embryogenesis and

foetal life, and, as described above, the developed hypothalamus is morphologically complex and contains many neuronal subsets that populate nuclei, with mixed neural cell types clustered in a small area. Early postnatal life is also characterised by widespread cell proliferation in the hypothalamus. There is a lack of mechanistic understanding about hypothalamic development. In particular, although we know something about how early hypothalamic progenitors are induced and how these are directed to differentiate, we understand very little about the earliest phases of hypothalamic development. Nonetheless, over the years, different models have been proposed.

The most widely-accepted model of hypothalamic development is termed the prosomeric model. This, and other previous models, are all based on the assumption that adult hypothalamic nuclei and their resident neurons differentiate from spatially-distinct progenitor subsets that grow isotropically (Puelles and Rubenstein, 2015). The prosomeric model, for instance, separates progenitor cells into an alar and basal domain, based on their position relative to Sonic Hedgehog (SHH) gene expression, with alar rostral to and basal caudal to and including *SHH+* cells, and expression of a handful of transcription factors. This model divides the four hypothalamic regions into two groups: the pre-optic and anterior regions are alar and the tuberal and mammillary regions are basal.

However, importantly, previous models do not take into account the possibility that progenitor cells are born over extensive periods of time, and may migrate or grow away from their site of origin. A recent model, developed by a previous PhD student in the Placzek lab, termed the Anisotropic Growth Model now suggests that the arrangement of

hypothalamic neurons and nuclei occurs due to the anisotropic growth of progenitor cells in time and space (Fu et al., 2017). This model has been developed through a focus on the earliest population of hypothalamic progenitors using the chick model organism. Anisotropic growth is when growth is not equal in all directions, and in developmental biology is important for processes such as the differential cell behaviours required for axis extension during primitive streak formation in the chick embryo and in growth of the fly wing imaginal disc, where marked clones strongly elongate along the proximo-distal axis of the adult wing (González-Gaitán, Capdevila, and García-Bellido 1994; Rozbicki et al., 2015).

1.2. Insight into Hypothalamic Development

1.2.1. Role of the PM in hypothalamic progenitor induction

The Anisotropic Growth Model of hypothalamic development was developed through studies that mapped the location of hypothalamic progenitor cells from early stages. Over the years there has been considerable dispute about the location of hypothalamic progenitor cells within the neural plate/early neural tube and the tissues that mediate their induction. Fate mapping studies using chick-quail chimaeras suggested that anterior and tuberal hypothalamic progenitors lie above surface ectoderm cells that will give rise to Rathke's pouch, the precursor to the anterior pituitary gland (Couly and Le Douarin, 1987), and that mammillary hypothalamic progenitors lie above prechordal mesoderm (PM) (García-Calero et al., 2008). The more recent study in the Placzek lab (Fu et al., 2017), using

DiI/DiO (lipophilic dye retained in cell walls over the course of multiple divisions) to target

small groups of progenitor cells, disputes this, and suggests instead that all basal

hypothalamic progenitor cells lie above the prechordal mesoderm (PM) and prechordal

mesendoderm (PME, the anterior-most part of the PM that is fused with endoderm) (Fu et

al., 2017). This in turn suggests that signals from the PME/PM tissue may induce

hypothalamic progenitors, an idea first suggested through descriptive studies a century ago

(Adelmann, 1922).

There is much evidence, particularly in chick, that the PME/PM induces hypothalamic

progenitor identity in overlying neural tissue. Heterotopic grafts in vivo showed that the

PM/PME is capable of inducing presumptive hypothalamic tissue from uncommitted

ectoderm, as shown by expression of *NKX2.1*, a marker of hypothalamic progenitors (Pera

and Kessel, 1997). Tissue recombination studies ex vivo showed that the PM induces

hypothalamic cells, including a set of cells in the anterior ventral forebrain midline, known as

Rostral Diencephalic Ventral Midline (RDVM) cells, characterised through their expression of

SHH and BMP7 (Dale et al., 1997, 1999) and wider sets of basal hypothalamic cells, defined

through expression of Nkx2.1 and Six3 (Ohyama et al., 2005). Conversely, when the PM is

ablated physically, prior to the appearance of hypothalamic progenitors, hypothalamic cells

are not induced, as judged by the lack of expression of SHH and *NKX2.1*, and a reduction in

diencephalic height (Patten et al., 2003; Pera and Kessel, 1997). Additionally, such chicks

develop cyclopia (Pera and Kessel, 1997), a phenotype characterised by loss of the ventral

midline, loss of more general basal tissue, and failure of the developing cerebral vesicles to

separate.

Genetic manipulation of the PM in mouse and zebrafish models also show the PM's necessity in ventral forebrain induction; these models either completely or partially fail to induce *Shh* in ventral diencephalic cells (Aoto et al., 2009; Chiang et al., 1996; Filosa et al., 1997; Harrelson et al., 2012; Sagai et al., 2019; Schier et al., 1997) and mice develop with cyclopia and holoprosencephaly.

A combination of descriptive work and fate-mapping shows that the PM/PME lies directly beneath prospective hypothalamic progenitor cells for an extended period of time: in chicks, from Hamburger-Hamilton (HH) 5 to 10 (head process stage to 10 somites). In this thesis I will use somite number when available and appropriate, that is between HH7 and HH13+, 1 to 20 somites, in the chick embryo beyond this stage somites become difficult to count with certainty as anterior somites have begun to dissociate. Over this time, the signalling properties of the PM/PME change, and current models suggest a 3-step signalling model for the induction of basal hypothalamic progenitors (hereafter referred to as prospective basal hypothalamic progenitor cells: pBHyp cells) (Fig. 1.1).
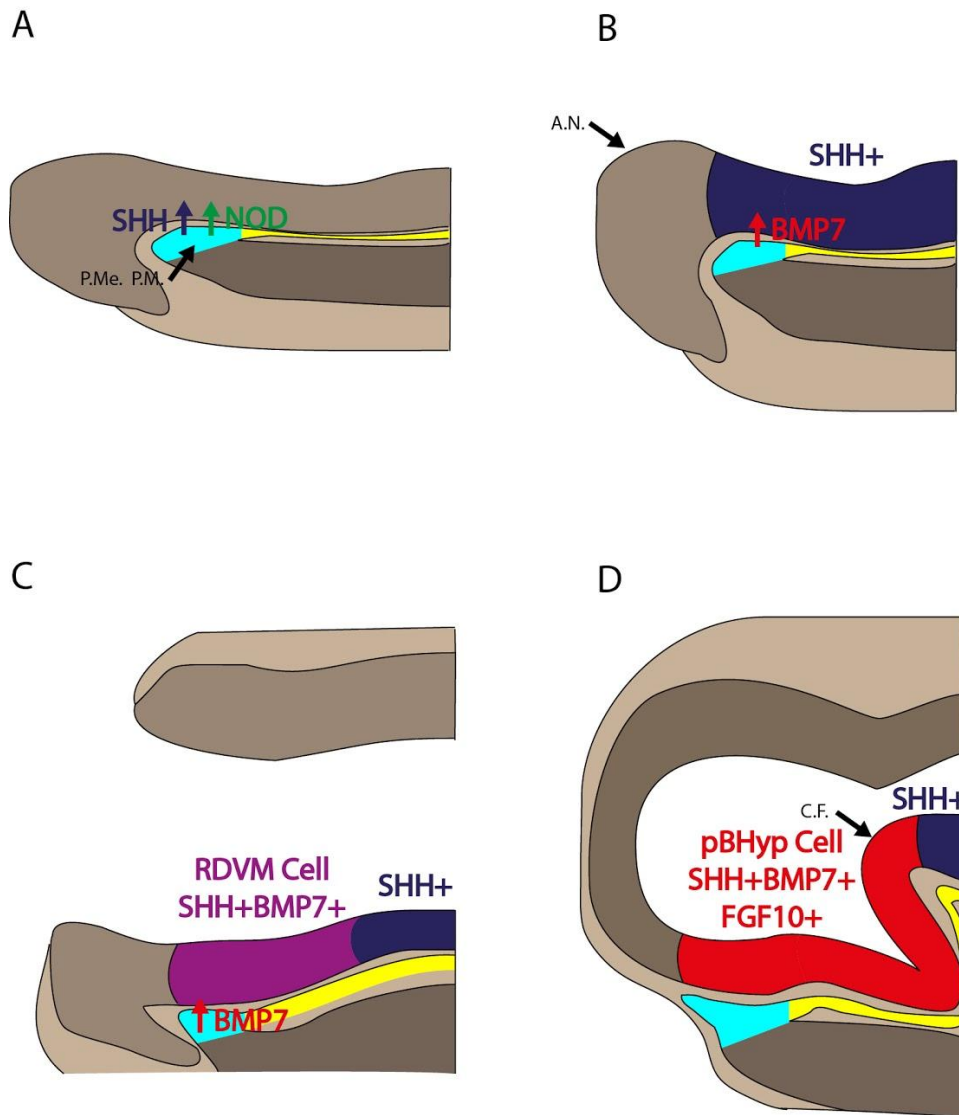
Figure 1.1: 3 Step Signalling from the PM/PME. A) At HH5 SHH and Nodal from the PM/PME cooperate to induce its SHH expression in overlying ventral midline cells. B) By 1 somite there is a change in PM/PME signalling so that it now expresses BMP7 which induces RVDM character in the overlying neuroectoderm (C). D) Continued BMP signalling then induces *FGF10+* pBHyp character at 10 somites (Vesque et al, 2000, Patten et al, 2003, Ellis et al, 2015).

At HH5, PM/PME cells express Shh and Nodal (Aoto et al., 2009; Dale et al., 1997, 1999; Epstein et al., 1999; Patten et al., 2003), but around HH5+-7, PM/PME cells begin to upregulate BMP7 (Dale et al., 1997, 1999; Ellis et al., 2015; Vesque et al., 2000). Tissue

recombination studies ex vivo, and manipulation of the PM and PM-derived signals in vivo, support the idea that RDVM induction is mediated by the sequential expression and signalling of SHH and BMP7 in/from the PM (Dale et al., 1999; Fu et al., 2017). Thus, SHH from the PM acts with Nodal to induce SHH in RDVM cells (Chiang et al., 1996; Placzek and Briscoe, 2005). Then, once BMP7 is upregulated in the PM, it co-operates with SHH to mediate the PM's ability to induce RDVM cells: thus, in vitro the application of anti-BMP7 antibodies to neural midline explants prevents the appearance of BMP7 (an RDVM marker) and instead, markers of a more posterior ventral midline population (the floor plate) are detected (Dale et al., 1997, 1999). Conversely, the PM's inductive capability can be mimicked by the application of SHH and BMP7 to naïve neural explants (Dale et al., 1997). Work following on from this showed that ventral midline cells exposed to SHH and BMP7, but not SHH alone, in ex vivo culture upregulate BMP7 (Dale et al., 1997).

Studies in chick and mouse show that RDVM cells act as a signalling centre through their ability to express Shh. Explants studies ex vivo and genetic studies in vivo suggest that Shh deriving from RDVM cells acts as a classic morphogen to pattern adjacent cells along the dorso-ventral axis, similar to its activity in the posterior neural tube (Shimogori et al., 2010; Szabó et al., 2009). However, over the years, evidence has accumulated to show that in addition, RDVM cells themselves differentiate further, giving rise, at around 10 somites, to a population of cells that are characterised through expression of FGF10: these are pBHyp cells. Fate mapping studies in our lab have shown that pBHyp cells are a highly proliferative progenitor population that gives rise to anterior, tuberal and mammillary progenitors of the basal hypothalamus ((Fu et al., 2017); see section 1.2.2 below). Two lines of evidence

suggest that RDVM cells will differentiate to pBHyp cells. First, RDVM and pBHyp cells appear to occupy the same relative position over the period of 1 to 10 somites. Thus, the PM lies beneath RDVM cells at 1 to 7 somites and beneath pBHyp cells at 10 somites. Moreover, fate mapping studies indicate that RDVM cells lie immediately caudal to the telencephalon at 1 to 7 somites (Dale et al., 1999), while double in situ hybridisation of *FGF10* and *FOXG1* (the latter a telencephalic marker), show that at 10 somites, pBHyp cells lie immediately caudal to the telencephalon (Fu et al., 2017). Thus, RDVM and pBHyp cells appear to have a common anterior boundary at the telencephalon. Second, explant studies suggest that PM-derived BMP7 induces BMP7 in RDVM cells at 4 somites, but that prolonged BMP signalling then goes on to alter the properties of RDVM cells, so that they upregulate *FGF10*, and progress to pBHyp cells at 10 somites (Dale et al., 1999; Fu et al., 2019, 2017; Manning et al., 2006).

In summary, these studies indicate that hypothalamic development is induced by prolonged and changing signalling from the PM/PME. First, the PM/PME induces *Shh+BMP7+* RDVM cells, a transient state that is defined at 4 to 7 somites. Then, continued BMP signalling causes RDVM cells to make the transition to pBHyp cells at 10 somites by upregulating *FGF10* (Fig.1.1).

1.2.2. Sequential anisotropic growth of hypothalamic progenitor populations from pBHyp cells

During the transition from RDVM cells to pBHyp cells this population undergoes a proliferative arrest and then becomes highly proliferative, as shown by incorporation of BrDU during DNA replication (Manning et al., 2006). DiI/DiO lineage tracing studies have shown that after 10 somites a subset of pBHyp cells grow anisotropically and are displaced/migrate anteriorly to give rise to *FGF10-/FOXG1-* anterior progenitors (pAnt), including SHH+ and ISL1+ cells (Fig.1.2. white and green regions), between HH10-HH15 (Fu et al., 2017). pAnt cells are therefore displaced anterior to the PM (García-Calero et al., 2008; Pearson and Placzek, 2013). The anterior anisotropic generation of pAnt cells, and therefore the growth of the pAnt region, is followed by the anisotropic growth of a progenitor population that is displaced/migrates posteriorly to give rise to *FGF10-/EMX2+* Mammillary progenitors (pMam) after HH15 (Fig.1.2. blue region) (Fu et al., 2017). Finally, as pAnt and pMam populations arise, the pBHyp population itself undergoes a poorly-understood differentiation step: some cells are retained as cells that continue to co-express SHH and FGF10; a more posterior population, however, maintains FGF10 and BMP7, upregulates Tbx2 and downregulates SHH. I refer to the former population as pBHyp cells and the latter as ventro-tuberal progenitors (pVT): see Fig. 1.2 and Fig. 1.3). Centrally-retained *FGF10+* pVT cells will give rise to the infundibulum, future posterior pituitary, via ventrally directed anisotropic growth (Pearson et al., 2011). Current work suggests that both pVT and pMam regions are generated from a *SHH+/FGF10+* pBHyp population, but it is not clear whether pMam regions are generated directly from pBHyp cells or indirectly via pVT cells (Placzek et al, unpublished).
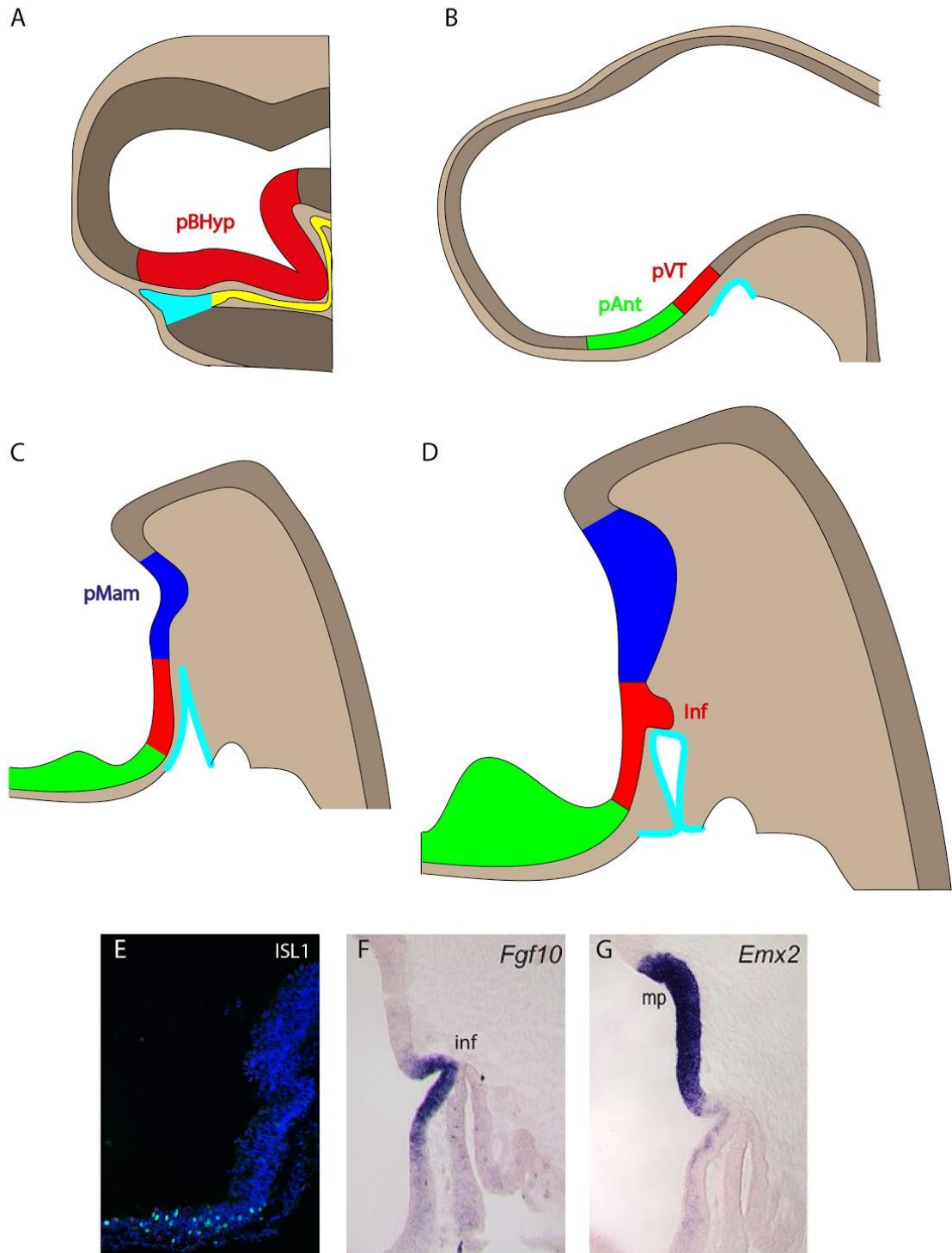
Figure 1.2: Sequential anisotropic growth gives rise to the basal hypothalamus. A-B) *FGF10+* pBHyp cells (red region) first give rise to pAnt (green, ISL+/SHH+, shown in E), after this point centrally retained *FGF10+SHH-* cells are referred to as pVT cells, although there may remain a *FGF10+SHH+* pBHyp population also retained. C) At around HH15 growth of the pAnt region slows and pMam cells (blue, *EMX2+,*SHH+, shown in G) begin to be generated posteriorly from pVT cells. D) Sequential proliferative growth steps between 10 somites and HH25 have now generated pAnt and pMam regions while retaining *FGF10+* population(s), pVT cells (shown in F), centrally (Fu et al, 2017). At around HH25 these centrally retained

pVT/pBHyp cells then give rise to the infundibulum through further anisotropic growth directed ventrally (D, F).

1.2.3. Molecular mechanisms that drive differentiation of distinct basal hypothalamic progenitor populations

The question remains of the molecular mechanisms that direct this anisotropic growth and differentiation? To date we know something about the emergence of SHH+ pAnt cells. SHH is expressed in pAnt cells as they grow and differentiate from pBHyp cells. As pAnt cells are displaced anteriorly over time, they downregulate SHH and upregulate p57 (Fig. 1.2, 1.3 and 1.4).

Figure 1.3: Diagram illustrating anisotropic growth. Groups of progenitors are represented by coloured balls, with time progressing from top to bottom and anterior to the left and posterior to the right. The initial pBHyp population first gives rise to pAnt cells, followed by pVT cells, while being centrally retained. pAnt cells then give rise to committed *p57+* Ant cells. In the diagram, pVT cells generate *FGF10-/BMP7+* pMam cells.
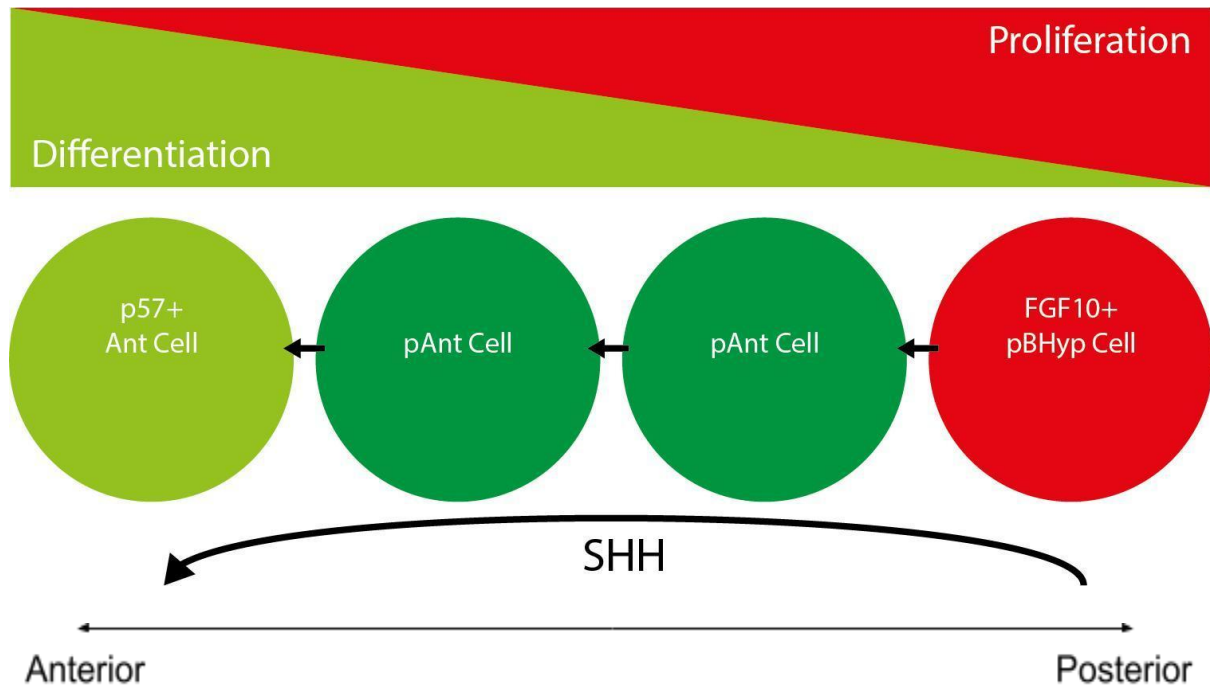
Figure 1.4: SHH is required for the generation of pAnt and committed Ant cells. Groups of progenitors are represented by coloured balls with anterior to the left and posterior to the right. In the absence of SHH signalling, SHH+ pAnt cells fail to develop and committed *p57+* anterior cells are absent, suggesting that SHH signalling is required for the progression from pBHyp to pAnt and ultimately committed anterior cell (Fu et al, 2017).

Exposure of embryos to cyclopamine, an inhibitor of SHH signalling, prevents pAnt cells from forming, in both chick and zebrafish (Fu et al., 2017; Muthu et al., 2016). Likewise, when SHH is deleted from the hypothalamus in mouse there is an anterior expansion of the pVT markers *Bmp4, Fgf10,* and *Tbx3,* and a loss of differentiating anterior and 'tuberal' neuronal cell types (Carreno et al., 2017; Corman et al., 2018; Orquera et al., 2016; Zhao et al., 2012). (It is important to note that the Anisotropic growth model suggests that both differentiated anterior and tuberal neurons/nuclei originate from 'pAnt' cells). This suggests that SHH is

required to direct pAnt cells that will then undergo neurogenesis and differentiate to neurons that occupy both basal anterior and basal tuberal nuclei.

Additionally, we know something about the emergence of pVT cells. This progenitor population maintains expression of BMP7 and FGF10 but downregulates SHH (Fig. 1.2 and 1.3). Studies in both chick and mouse have shown the mechanism of Shh downregulation in pVT cells, showing that it is mediated by the transcriptional repressors, *TBX2/TBX3* in response to BMP signalling. Expression of Shh in RDVM/pBHyp cells is driven through a particular enhancer, termed Shh brain enhancer 2 (SBE2) and the transcription factor SOX2 binds to SBE2 to drive Shh expression (Zhao et al., 2012). TBX3 has been shown to downregulate SHH by preventing SOX2 from interacting with SBE2 (Trowe et al., 2013). BMP2 and BMP7 have been shown to be able to induce TBX2 in a concentration dependant manner (Manning et al., 2006). As yet, however, it is unclear how BMP2/7 induces Tbx2/Tbx3: BMP can signal via a canonical pSMAD1/5/8 pathway (Ohyama et al., 2008) or a non-canonical p38 MAPK pathway (Ohyama et al, in preparation) in the hypothalamus. There is some evidence from another system, the developing heart, this could be directed by the canonical pathway, where pSMAD5 is capable of activating *Tbx2* transcription (Singh Reena et al., 2009). Further, *Tbx2* does appear to have SMAD binding sites 5' to the coding sequence that recapitulate most *Tbx2* expression in LacZ assays in mouse and when deleted abolish reporter expression in mouse (Shirai et al., 2009). However the hypothalamus of these animals was not studied so it is unknown if these regulatory elements also control hypothalamic *Tbx2* expression.

In summary, analyses of pAnt and pVT cells indicate that the former require SHH signalling and the latter BMP signalling, the Arcuate, ventromedial and dorsomedial nuclei derive from pAnt SHH expressing/responsive cells. A key aim of my thesis will be to ask whether different levels of BMP signalling are present within pBHyp cells, leading to the differential emergence of pAnt and pVT/pMam cells. However, before expanding on the Aims, I will first introduce the BMP signalling pathway.

1.3. BMP signalling

1.3.1. Canonical BMP signalling

BMPs received their name for their ability to induce osteogenic differentiation in the presence of decalcified bone (Urist, 1965). Study of individual BMPs came later, along with knowledge of their canonical signalling pathway. BMP ligands form dimers that signal through the assembly of heterotetrameric receptor complexes. These are typically thought to be formed of two homodimer receptors, one from the type 1 category and the other from type 2, both of which are extracellular receptors with a signal membrane pass and a serine/threonine kinase intracellular domain, ligand binding brings constituently active type 2 receptors into close enough proximity to transphosphorylate type 1 receptors (Heldin et al., 1997). There are three type 1 and three constituently active type 2 receptors that have been shown to bind BMPs (Dijke et al., 1996). This can be prevented by the binding of endogenous extracellular BMP inhibitors that prevent interaction with receptors (Walsh et

al., 2010). Which receptors are recruited and in what order depends on which are being expressed by the target cell and constituents of the signalling ligand dimer. BMP7 firsts interacts with type 2 receptors that then recruit type 1 receptors (Yamashita et al., 1995). In the case of BMP2 the order is reversed and type 1 receptors are initially bound to, resulting in the recruitment of type 2 receptors (Koenig et al., 1994). For both orders this results in the transphosphorylation of the type 1 receptors by type 2 receptors which can then transduce signalling downstream. In the case of BMPs type 1 receptor phosphorylation results in phosphorylation of receptor regulated SMADs 1, 5 and 8 (R-SMADs) (Hoodless et al., 1996). Type 1 BMP receptor BMPR1A is essential for regulating feeding by mediating the response to low leptin levels by promoting feeding behaviour (Gautron and Elmquist, 2011; Peng et al., 2012; Zhang et al., 1994). In canonical signalling R-SMAD phosphorylation leads to the formation of a trimeric SMAD complex with co-SMAD SMAD4, which is essential for embryonic development (Sirard et al., 1998). The complex is then translocated to the nucleus where, in the presence of co-activators/co-repressors and DNA-binding co-factors, they can modulate transcription (M. Kawabata et al., 1998, 1998). Co-repressors encompass inhibitory SMADs (I-SMADs) SMAD6 and SMAD7, which can compete for receptors, promote receptor degradation via ubiquitination, dephosphorylation of the receptor, and interfere with DNA binding of SMAD complexes (Ebisawa et al., 2001; Hayashi et al., 1997; Shi et al., 2004; Zhang et al., 2007). There is also the integration of other signalling pathways to modulate BMP signalling. For example, at the R-SMAD level pSMAD1 can be further phosphorylated after translocation to the nucleus by Erk MAPK and GSK3 which promotes it's ubiquitination and degradation (Fuentealba et al., 2007; Kretzschmar et al., 1997).

1.3.2. Non-canonical BMP signalling

BMPs have also been shown to function independently of SMAD complexes. BMP4 in Xenopus is capable of activating MAPK family member TAK1 through BMP type 1 and 2 receptors to cooperate in the induction of ventral tissue within the embryo (Shibuya et al., 1998; Yamaguchi et al., 1999, 1995). In addition to this the p38 MAPK pathway has been shown to be required for BMP2 induced neural differentiation in rat PC12 cells (Iwasaki et al., 1999). How these different actions are achieved through the same receptors is a major gap in the knowledge of non-canonical BMP signalling. However, it has been proposed that this could be explained via different signalling from preformed signalling complexes (canonical) versus BMP ligand induced complexes (non-canonical) (Hassel et al., 2003).

1.3.3. The inhibitory relationship between BMP and SHH signalling

SHH has long been understood to induce ventral cell types in the spinal cord (Marti et al., 1995): loss of *Shh* leads to an absence of these cells (Chiang et al., 1996). Similarly, BMP signalling is required for establishment of dorsal and intermediate neurons in the spinal cord (Nguyen et al., 2000). These two signalling pathways are required for the proper establishment of distinct cell types at discrete locations along the dorso-ventral axis of the spinal cord (Patten and Placzek, 2002). This is achieved via the induction of multiple cross-inhibitory transcription factors that specify the domains along the dorso-ventral axis of the spinal cord (Briscoe et al., 2000). This is in part regulated by Gli3, a repressor of SHH signalling; constitutively active mutations act to increase repression of SHH and show a

ventral expansion of dorsal cell types with BMP signalling capable of inducing expression of Gli3 (Meyer and Roelink, 2003). The same effect can be shown with constitutively active BMP receptor 1b, which when expressed in the chick spinal cord causes ventral shift of the MSX1/2 boundary with DBX2 (Timmer et al., 2002). Conversely, ectopic expression of the BMP inhibitor Follistatin results in a dorsal shift in progenitor cell types, reflective of increased BMP inhibition leading to lower BMP signalling received by target cells and therefore misspecification as more ventral cell types, such as the dorsal shift of the Isl1/2 (ventral) Lim1/2 (dorsal) boundary (Liem et al., 2000). In summary, these studies show the inhibitory relationship between SHH and BMP signalling in the spinal cord is required for the proper establishment of transcription factor boundaries. There is also evidence from the developing brain that BMP2, but not BMP7, can inhibit SHH induced progenitor proliferation (Rios et al., 2004). So although they are temporarily co-expressed in the pBHyp cells they appear to resolve and this opens the possibility of a SHH high, BMP low to SHH low, BMP high gradient within the developing hypothalamus. This could result in differential proliferation rates and elaborate pattern within pBHyp cells.

1.4. Thesis aims

As detailed above the hypothalamus is a critical region for survival and mutations that affect its development can have a wide range of severities. Understanding of its development has been furthered over the years since its first description in the 1890's. However there is still uncertainty about the range of and the requirement for BMP signalling in the development

of the hypothalamus. To this end in this thesis I set out to use the chick embryo as a model system to investigate these questions.

The aims of this thesis are:

1. To gain a thorough understanding of the relationship between BMP family members and development of the hypothalamus

2. Assess the requirement for BMP signalling in the specification of pBHyp cells

3. Investigate the relationship between BMP family members and emerging Anterior Progenitors

4. Deduce what function continued BMP expression serves after the specification of pBHyp cells

This work is important for our understanding of the development of the hypothalamus, the progression of RVDM cells to pBHyp cells and then pAnt or pVT cells, how *BMP2* and *BMP7*, and their inhibitors, relate to RVDM, pBHyp and pAnt or pVT cells. This could give insight into how individual BMPs relate to pBHyp induction, as well as how BMP signalling directs hypothalamic development and cell specification. It may also shed light on how developmental processes that could one day be co opted to help treat disease thought to originate within the adult and/or developing hypothalamus.

Chapter 2:

Materials and Methods

2.1. Chick Husbandry

Fertilised Bovan medium brown chicken eggs (Henry Stewart & Co, Norfolk, UK) were incubated at 37°C humidified incubators and staged according to Hamburger Hamilton criteria (Hamburger and Hamilton, 1951). All experiments involving live embryos were performed in accordance with University of Sheffield regulatory standards.

2.2. In Ovo Manipulations

Embryos were accessed via removal of a small section of shell above the air sack, followed by removal of the inner shell membrane. A small incision was then made in the vitelline membrane. Embryos were visualized using blue food dye (Dr. Oetker, discontinued) diluted 1:5 in Leibovitz's L-15 medium (Thermo Fisher, 11415056) injected into the yolk sac.

Affi gel beads (BIO-RAD, 153-7301, lot: 64032298) were soaked in either: 200µg/µl Recombinant human Noggin (NOG) (R&D Systems, 6057-NG, Lot TNT1614111) and recombinant mouse Chordin (RD systems, 758-CN-050) or recombinant human BMP7 (RD Systems, PHC9544, Lot 831547A), with 0.1% bovine serum albumin in phosphate-buffered

saline (PBS, Sigma, P4417) overnight at 4°C before insertion into the prosencephalic

ventricle, above the prechordal mesendoderm/prechordal mesoderm.

2.3. Ex Ovo Manipulations

For explant culture embryos were dissected out into ice-cold L-15 medium. Embryos were

then cut into 150μm fillets by a tissue chopper (The Mickle laboratory engineering Co. Lts.,

McIlwain Tissue chopper). Fillets were selected based on morphology then incubated in

12U/ml Dispase (Roche, 04942086001) in L-15 for 5-10 minutes before dissection of the

desired region. Concurrently collagen beds were prepared as described (Placzek and Dale,

1999). Briefly, 90μl of collagen collected from rat tails was mixed with 10μl of 10x DMEM

(Sigma, D2429) and 3μl 0.8M $NaHCO_3$ (Fisher Chemical, 514240/53), vortexed to mix until

the solution turned light pink, 25μl was then pipetted into the bottom of a 4 well plate

(Thermo Scientific, 176740), spread to form a disc and allowed to set at room temperature

for 30 minutes. Explants were then placed on the collagen bed, excess media was removed,

then a second layer of collagen was added on top of the explant before allowing 30 minutes

for setting. Explants were cultured at 37°C 5% CO_2 in OPTI-MEM (Fisher Scientific,10149832)

containing 4% foetal calf serum (Biosera, FB-1550/50), 100U/ml Pen/Strep (Fisher Scientific,

11548876), 2mM L-Glutamine (ThermoFisher, 35050061) for 20 hours with either

Dorsomorphin (5mM stock, Sigma, P5499-5MG) in DMSO or rhBMP7 (RD Systems, PHC9544,

Lot 831547A) or in control conditions before fixation.

2.4. Histological techniques

Embryos were collected at desired stages and dissected in L-15 then fixed in 4% paraformaldehyde (PFA, Sigma-Aldrich, P6148-5009) in 0.12M phosphate buffer at 4°C for 2 hours. Dissections were performed with No. 5 forceps (Dumont, 11251-20) and spring scissors (Vannas, 15018-10).

For slide mounted section analysis embryos were washed in PBS then cryoprotected in 30% (w/v) sucrose (Sigma, S0389) in 0.1M phosphate buffer at 4°C overnight. Embryos were then mounted in optimal cutting temperature solution (OCT; VWR, 361603E) with the desired orientation and frozen on dry ice. Sections were taken at 15μm thickness on a cryostat (Bright instruments, OTF), collected onto superfrost slides (Thermo Fisher, 10149870), air dried for no more than 1 hour before rehydration in PBS of slide for immunofluorescence or stored at -20°C before in situ hybridisation.

2.5. In Situ Hybridisation

Competent bacterial cells (Sigma, CMC0001-4X40UL) were transformed with plasmids using a heat shock method (Froger and Hall, 2007) then plated out onto selective plates and grown overnight at 37°C. A single colony was then selected, grown overnight in selective media then plasmids were extracted using a modified MiniPrep protocol called MiraPrep (Pronobis et al., 2016) using miniprep kit (QIA prep Spin MIniprep, 154047007), and RNase (ThermoFisher, #EN053), with ethanol precipitation.

2.5.1. Riboprobe synthesis

DNA template plasmids were linearised prior to transcription. 20μg of plasmid DNA was linearised in 100μl reactions following manufacturer's instructions. NEB and Promega restriction enzymes were used. The resulting linear DNA was phenol-chloroform extracted and then ethanol precipitated. Precipitated DNA was resuspended in 20μl double distilled (dd) H_2O.

Antisense digoxigenin (DIG)-labelled and fluorescein (FITC)-labelled riboprobes were synthesised by in vitro transcription. Reactions contained 1μg template DNA, 4μl 5x transcription buffer (Promega, P118B, New England Biolabs (NEB), B90126), 2μl 10x DIG or FITC RNA labelling mix (Roche, 26591020, 118522120), 20U Murine RNase inhibitor (NEB, M03145), 20U appropriate RNA polymerase T3, SP6, or T7 (Promega, P207B, P108B, NEB M03785), then made up to 20μl with DEPC-treated H_2O. Reactions were incubated in a 37°C water bath while transcribing. RNA was then purified using a column based binding method (Probe Quant G-50 MicroColumns, 28903408). Purified RNA was resuspended in 50% Formamide (AppliChem, A2156) in DEPC-treated H_2O.

Table 2.1 Riboprobe templates used in this study for in situ hybridisation

Probe Name	Restriction Enzyme	RNA Polymerase	Source
BMP2	HindIII	T3	Gift from Paul Brickell
BMP4	XbaI	T3	Gift from Paul Brickell
BMP7	XhoI	T3	Gift from Brian Houston
NOG	Xh01	T3	Clonned from Williamson Library
CHRD	EcoRI	SP6	Gift from Kevin Lee
FGF10	Xho1	SP6	Gift from Malcolm Logan
FOXG1	XbaI	T7	Gift from Lena Gunhaga
RAX	BamHI	T7	Gift from Hideyo Ohuchi
p57	BamHI	T7	Gift from Matt Towers
ASCL1	EcoR1	SP6	Gift From Valerie Dupe
TBX2	Sal1	T7	Gift from Cliff Tabin

2.5.2. In Situ Hybridisation

For in situ hybridisation analysis slide mounted section were treated with 4% PFA for 10 minutes at room temperature, washed with PBS, actylated with 1.12% Triethanolamine (Biochemika, 90279), 0.25% Acetic anhydride (Sigma-Aldrich, A6404) for 10 minutes at room temperature and washed with PBS.

Samples were incubated in prehybridisation solution (see below) for 4 hours at 68°C. Samples were then incubated in hybridisation solution (prehybridisation solution, DIG- or FITC-labelled riboprobe diluted between 1:200-1:1000 based on gel electrophoresis analysis of transcription reaction) overnight at 68°C. Stringency washes comprised of 50%

formamide, 5x saline-sodium citrate buffer (SSC), 1% sodium dodecyl sulphate (SDS) for 1 hour followed by 50% formamide (Sigma, 47671), 2x saline-sodium citrate buffer (SSC), 1% Tween-20 for 1 hour both at 68°C. Samples were then washed thoroughly with TBST (1x Tris-buffered saline, 1% Tween-20), blocked in 10% heat inactivated goat serum (HINGS) in TBST for 2 hours at rt, cooled to 4°C for 15 minutes, then incubated with anti-DIG- or anti-FITC-alkaline phosphatase (AP) antibody conjugates (1:2000 in in situ blocking solution; Roche, 11093274910, 11426338910) overnight at 4°C rocking. Samples were then washes thoroughly in TBST, equilibrated in NTMT (0.1m NaCl, 0.1m pH9.5 Tris, 50mM $MgCl_2$, 1% Tween-20) and then moved into staining solution (NTMT, 0.45mg/ml 4-nirto blue tetrazolium chloride, Roche, 11383213001, 0.175mg/ml 5-bromo-4-chloro-3-imdolyl phosphate, Roche, 11383221001) in the dark at rt. Once staining has reached desired extent samples were washed in PBS to prevent further reaction. Slide mounted sectioned were then coverslipped with glycergel (Dako, C056330-2). Experiments involving control and treatment tissue were developed for the same period of time in pairs.

Prehybridisation solution was made up as follows:

50% Formamide, 5x SSC, pH 7.0, 2% (w/v) Blocking powder (Roche, 11096176001), 0.1% Triton X-100, 0.5% CHAPS, 1mg/ml Yeast RNA, 5mM EDTA, 50μg/ml Heparin.

2.5.3. Fluorescent In Situ Hybridisation

Single fluorescent in situ hybridisation was adapted from the chromogenic protocol (Fig. 2.5.2.), using the TSA Plus Cyanine 3/Fluorscein System (PerkinElmer, NEL753001KT). Post stringency washes samples were washed with TNT (0.1M pH7.5 Tris-Hcl, 0.15M NaCl, 0.5%

Tween-20). Samples were then blocked (0.5% blocking powder, Roche, 11207733910, TNT) for 2 hours at room temperautre, cooled to 4°C for 15 minutes, then incubated overnight at 4°C with anti-DIG or FITC-horseradish peroxidase (POD) antibody conjugate (1:500 in blocking solution). Following thorough TNT washes samples were stained by 5-10 minutes incubaton in FITC-Tyramide (1:50 in 1x Plus amplification diluent from TSA kit), at room temperature in the dark. Samples were then thoroughly washed in TNT, slide mounted sectioned were coverslipped with Fluoroshield containing DAPI (SigmaAldrich, F6057-20ML), and stored at 4°C in the dark prior to imaging.

2.6. Immunofluorescence

Following rehydration slide mounted sections were blocked over night at 4°C in PBS containing 1% HINGS (Heat inactivated goat serum, Simga-Aldrich, g6767), and 0.1% Triton-X100 (Sigma, 79284-500ML). Samples were then incubated for 1 to 5 nights with primary antibody/antibodies in appropriate blocking solution, whole mount samples rocking. Samples were then thoroughly rinsed with PBTr (PBS, 0.5% Triton-X100) then incubated with appropriate secondary antibodies/antibody in blocking solution for 1 to 3 nights at 4°C. Samples were then thoroughly washed with PBTr and slide mounted sections were coverslipped with DAPI containing Fluoroshield.

Table 2.2. Primary antibodies used in this study

Primary antibody	Species	Dilution	Source
pSMAD1/5/8 (D5B10)	Rabbit IgG	1:500	Cell Signalling Technology,
SHH (68.5 e1)	Mouge IgG	1:50	Made in house

pH3	Rabbit IgG	1:1000	Upstate
ISL1 (4D5.61)	Mouse IgG	1:50	DSHB

Table 2.3. Secondary antibodies used in this study

Secondary antibody	Dilution	Source
Alexa Fluor 488	1:500	Molecular Probes
Alexa Fluor 594	1:500	Molecular Probes

2.7. Image Capture and manipulation

2.7.1. Imaging whole mount embryos and explants

Whole mount embryos and explants were imaged using a Leica MZ10F stereomicroscope with Leica LAS X software.

2.7.2. Imaging embryonic sections

Embryonic sections with chromogenic staining were imaged using an Olympus BX60 compound light microscope. Fluorescently labelled embryonic sections were imaged using a Zeiss AxioImager.Z1 fluorescent compound microscope using an Apotome.2 and Zeiss ZEN 2 software.

2.7.3. Image manipulation and measurements

Image manipulations, including merging of channels, were performed using Adobe

photoshop. Measurements of expression regions, expression domains, and cell counts were

measured using FIJI (Fiji is just ImageJ, v1.51q).

Chapter 3:

Active BMP signalling prefigures and predicts pBHyp cells

3.1. Introduction

As discussed in the Introduction, over the years there has been considerable dispute about the location of hypothalamic progenitor cells within the neural plate/early neural tube, and dispute as to the source of signals that induce hypothalamic progenitor cells. Fate mapping studies using chick-quail chimaeras have suggested that the hypothalamic anlage is adjacent to, and contacted by surface ectoderm cells that will give rise to Rathke's pouch, the precursor to the anterior pituitary gland (Couly and Le Douarin, 1987). However, many other studies dispute this, and suggest instead that hypothalamic progenitor cells lie adjacent to the prechordal mesendoderm (PME)/prechordal mesoderm (PM), which induces hypothalamic identity in overlying neural tissue. Descriptive studies a century ago first suggested that the PME/PM lies close to the hypothalamus and may be important for its development (Adelmann, 1922). More recently, the PM has been shown to induce a set of cells in the anterior ventral forebrain midline, known as Rostral Diencephalic Ventral Midline (RDVM) cells, characterised through their expression of SHH and BMP7 (Dale et al., 1999). RDVM cells are induced by the PM/PME around 4 to 7 somites, and numerous studies show that the PM, and the induced RDVM cells, are vital for hypothalamic development. Heterotopic grafts showed that the PM is capable of inducing hypothalamic tissue from

uncommitted ectoderm, as shown by expression of *NKX2.1*, a marker of ventral

hypothalamic progenitors (Pera and Kessel, 1997). This is corroborated by the ability of the

PM to induce RDVM and hypothalamic gene expression profiles, including SHH, BMP7 and

NKX2.1 in neural plate explants in vitro (Dale et al., 1997, 1999). Conversely, when the PM is

ablated physically at HH5 ventral forebrain midline cells are not induced, as judged by the

lack of expression of Shh, *NKX2.1*, cyclopia and a reduction in diencephalic height (Patten et

al., 2003; Pera and Kessel, 1997). Genetic manipulation of the prechordal mesoderm in

mouse models also show the PM's necessity in ventral forebrain induction; these models

either completely or partially fail to induce *SHH* in ventral diencephalic cells and mice

develop with cyclopia and holoprosencephaly (Filosa et al., 1997; Harrelson et al., 2012).

Importantly, a recent fate-mapping study shows the lineage-relationship of RDVM cells and

later hypothalamic cells. This study showed that RDVM cells differentiate to pBHyp cells at

10 somites (Fu et al., 2019, 2017). pBHyp cells are themselves a highly proliferative

progenitor population that gives rise to much of the basal hypothalamus (Fu et al., 2017).

The PM underlies cells as they make the transition from RDVM to pBHyp cells (Dale et al.,

1999; Fu et al., 2017). These experiments provide strong support that hypothalamic

progenitors are underlain by PME/PM, but the critical question is what signals from the PM

induce RDVM cells and pBHyp cells?

RDVM induction is mediated by the sequential expression and signalling of Shh and BMP7

in/from the PM (Dale et al., 1999; Fu et al., 2017). Many previous studies have revealed that

Shh from the PM, where pro-Nodal maintains SHH via inhibiting BMP signalling, acts with

Nodal to induce Shh in RDVM cells (Chiang et al., 1996; Ellis et al., 2015, Placzek and Briscoe,

2005). However, soon after expressing Shh pro-Nodal is endogenously downregulated in the PM, resulting in BMP7 is upregulation which in turn downregulates SHH (Dale et al., 1997, 1999; Ellis et al., 2015; Vesque et al., 2000). A number of studies indicate that BMP7 then co-operates with Shh to mediate the PM's ability to induce RDVM cells, that in turn differentiate to pBHyp and basal hypothalamic cells. First, hypothalamic markers can be inhibited in vitro by the application of anti-SHH or anti-BMP7 antibodies to PM explants, both of which prevent *NKX2.1* expression in neural explants and instead induce markers of more posterior ventral midline population, Foxa2. Second, the PM's inductive capability can be mimicked by the application of SHH and BMP7 to similar explants (Dale et al., 1997). Work following on from this showed that once ventral midline cells stably express *SHH* in ex vivo culture, application of BMP7 leads to the upregulation of both *BMP7* itself, and *FGF10*, the latter a marker of pBHyp cells (Dale et al., 1997; Fu et al., 2017; Manning et al., 2006). These studies suggest, therefore, that in vivo, expression of BMP7, *FGF10,* and the progression of RDVM to pBHyp cells is controlled by sustained BMP signalling from the PM/PME. However, as yet not study has directly analysed whether the canonical BMP signalling pathway is activated as RDVM or pBHyp cells are induced in vivo, and if so, whether activation occurs uniformly throughout RDVM cells (defined through *SHH/BMP7* expression) and pBHyp cells (defined through *FGF1*0 expression).

RDVM cells appear to sit immediately caudal to the telencephalon based on fate mapping (Dale et al., 1999). pBHyp cells are characterised by expression of *FGF10* and FGF10 has been shown via double in situ hybridisation with *FOXG1*, a telencephalic marker, to abut the telencephalon (Fu et al., 2017). This suggests that RDVM give rise to pBHyp cells at ~10

somites. To establish if RDVM cells do abut the telencephalon it is necessary show

complementary marker expression profiles with telencephalic markers. Beyond this if RDVM

cells do give rise to pBHyp cells then one would expect RDVM markers to prefigure pBHyp

markers such as *FGF10*. However, no study has directly compared RDVM and pBHyp position

and marker expression or found a specific marker of RDVM cells. Are members of the BMP

family, including its signal transducers and inhibitors, able to predict the extent of the pBHyp

cell population? Indeed, it would appear to be the case that timely BMP exposure is vitally

important for hypothalamic specification and regionalisation, but thorough analysis of likely

active BMPs along the AP axis has yet to be done. Critical to the question of activity is the

presence of endogenous inhibitors. The BMP subfamily inhibitors included in this chapter

are Chordin and Noggin. These have been selected as they are known to be expressed in or

around RDVM cells during their induction and transition to pBHyp cells (Bachiller et al.,

2000; Vesque et al., 2000).

In this chapter I hypothesised that the canonical BMP signalling pathway is active in RDVM

cells and increases as RDVM cells progress to pBHyp cells. My null hypothesis is that BMP

signalling will be uniform along the AP axis of RDVM and pBHyp cells.

To address this hypothesis my aims were to:

1. Characterise the expression domains of *BMPs* and *BMP* inhibitors in RDVM and

   pBHyp cells, relative to known morphological landmarks

2. Clarify the relationship between expression domains of BMPs and BMP inhibitors

   with the extent of canonical BMP signalling, assessed through pSMAD1/5/8

   expression

3. Determine whether canonical BMP signalling is confined to RDVM and pBHyp cells, and excluded from telencephalic progenitors.

4. Finally, I examined the spatial relationship of pSMAD1/5/8 expression relative to the PME/PM and the surface ectoderm.

3.2. Results

Sagittal sections allow for the reliable definition of morphological features between 4 and 10 somites

Previous studies have analysed expression of BMP7 and the BMP inhibitor, Chordin, over HH6-10, but have done so in transverse sections or wholemounts (Dale et al., 1999; Lyons et al., 1995; Vesque et al., 2000). A recent study shows that sagittal sections are a powerful way of characterising pBHyp cells, as they can be identified on the basis of their position relative to the underlying PM (Fu et al., 2017). I therefore first analysed expression of BMPs in sagittal sections at 4 to 10 somites, i.e. the time when RDVM and pBHyp cells are induced, to determine the anteroposterior (AP) location of gene expression. I studied expression of BMP2 and BMP7, as previous studies had already indicated these to be expressed in the ventral forebrain midline (Chapman et al., 2002; Dale et al., 1999; Lyons et al., 1995; Manning et al., 2006). I began by establishing morphological structures that could be confidently and consistently identified in sagittal sections.

My results show that the midline can be identified based upon the morphology of the neural tube during neurulation. At the 4 somite stage (4s) neurulation is underway but the anterior

and anterodorsal neural tube remain open, therefore in anterior midline sections location

shown by the dotted line in (Fig.3.1.A), only ventral midline tissue is present (Fig.3.1.A'). The

neuroectoderm at 4s has few morphologically identifiable structures, the anterior neuropore

(AN) is one, an opening at the anterior extreme of the invaginating neural tube. I will be

using AN to reference to the anterior-most point of the neuroectoderm. I will then define

gene localisation relative to the AN. Located immediately ventral to the neuroectoderm is

the axial mesoderm, made up of the prechordal mesoderm (PM), and, in anterior-most

positions, the prechordal mesendoderm (PME) a fusion of PM and pharyngeal endoderm

cells (Adelmann, 1922; Dale et al., 1999) (Fig.3.1.A' arrowheads) Fate-mapping and marker

expression have shown that at this stage, RVDM cells overlie the PM/PME (Dale et al., 1999).

My analyses reveal that the PM and PME have small, rounded nuclei in comparison to the

elongated nuclei of the neuroectoderm (Fig.3.1.A'). The posterior limit of the PM is not

possible to define on the basis of morphology alone in sagittal sections as it thing then

connects to the notochord. Taken together this means at 4s I can define regions of

neuroectoderm by their position relative to the AN and the PM/PME cells (Fig.3.1.A'').

RVDM cells at this point are above the PM/PME, however in sagittal section they are not

morphologically definable.

The morphology of the developing neural tube changes rapidly and by the 7 somite stage

(7s), around 4.5 hours later, significant changes have occurred in the anterior neural tube.

Continuing neurulation means dorsal neuroectoderm is now present above the ventral

midline, however the AN continues to be open at the rostral extent of the neural tube

(Fig.3.1.B). Sagittal sections reveal that the ventral neuroectoderm begins to bend and

generate the cephalic flexure (CF) (Fig.3.1.B'). This structure gives the approximate caudal limit to RDVM/future pBHyp cells (Dale et al., 1999; Fu et al., 2017). Using the rostral most PME, the AN and the CF, the position and AP extent of RDVM cells can be approximated to lie 75μm-215μm from the AN at 7s, in agreement with a previous study (Dale et al., 1999).

4.5 hours further, at the 10 somite stage (10s), the morphology of the neural tube has changed markedly once again. The AN is now almost closed and can no longer be seen on some midline sections. I will now refer to the anterior extent of the neuroectoderm (AEN) as opposed to the AN (Fig.3.1.C-C'). The PM/PME and CF are morphologically defined landmarks that give an approximate localisation of pBHyp cells. Strikingly, pBHyp cells now form a characteristic 'dimple' (MP, unpublished), visible in sagittal sections as a groove (red arrowheads).

These studies show that there are morphological features definable in sagittal sections that can be used to estimate the approximate localisation of RDVM cells at 4s and 7s and pBHyp cells at 10s. By combining these observations with gene expression data I can define the localisation of *BMP2* and *BMP7* in the context of what is already known about the development of RVDM/pBHyp cells along the AP axis.
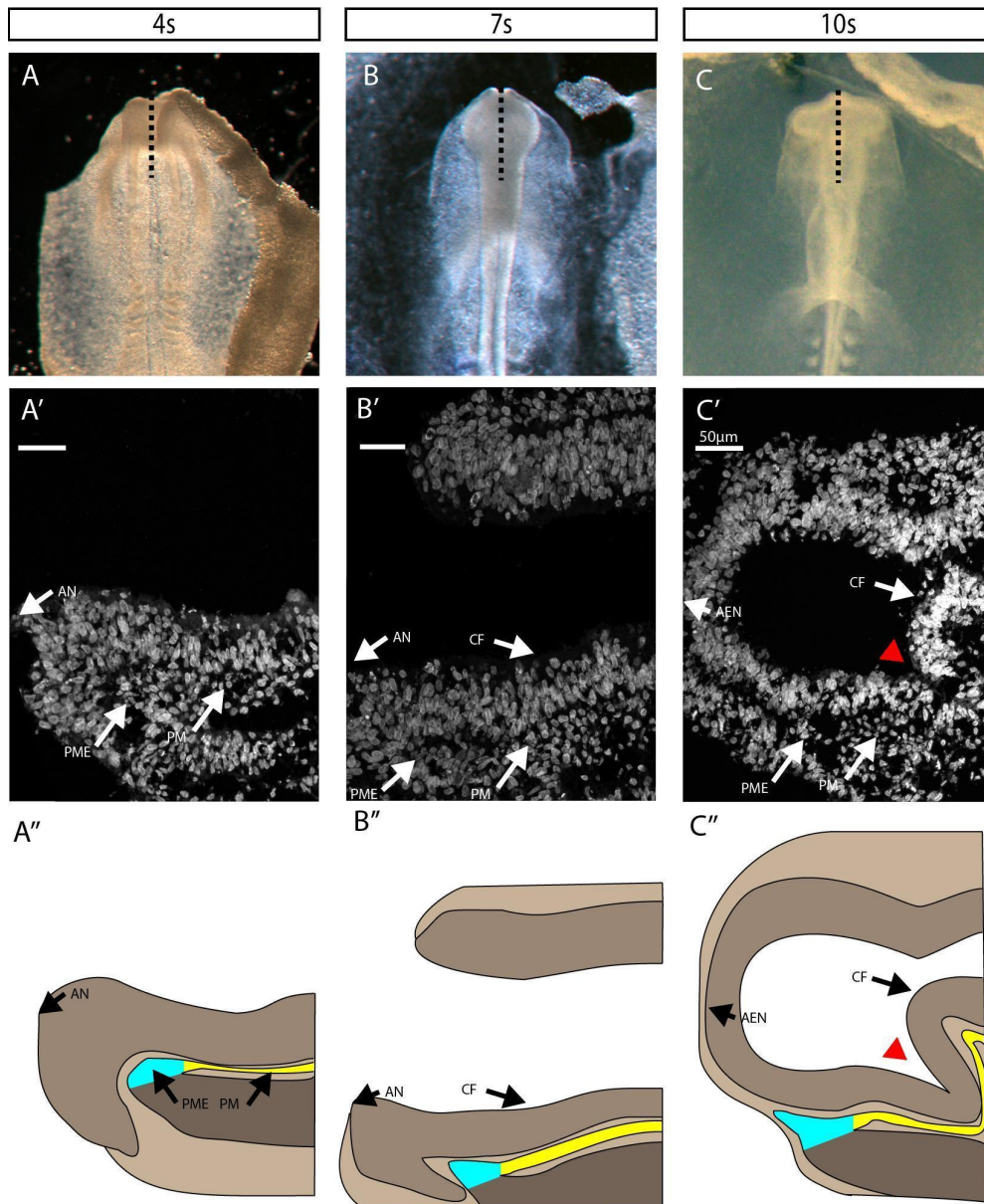
Figure 3.1: Morphology of the neuroectoderm changes dramatically between 4 and 10s. A,B,C) Wholemount view of embryos, line indicates the position of the sagittal section shown in (A',B',C'), represented schematically in (A'',B'',C''). A-A'') . At the 4s stage the anterior neuropore (A.N.) is open to such an extent that no dorsal tissue overlies the anteroventral neural tube at the level of the prechordal mesendoderm/prechordal mesoderm (PME/PM) (blue/yellow, A''). B-B'') By 7s (~4.5hrs after 4s) neurulation has continued. The Cephalic Flexure (C.F.) appears. C-C'') By 10s (~4.5hrs after 7s) the A.N. is mostly closed, the C.F. has further curved in the ventral neuroectoderm overlying the PM making it very apparent. A characteristic groove is obvious in the pBHyp domain, called the dimple (red arrowhead).

BMP2 and *BMP7* are expressed within the anterior ventral neural tube from 4s in the absence of inhibitors *NOG* and *CHRD*

Having defined a method for localising gene expression I began to analyse expression patterns. First by conducting in situ hybridisation experiments for genes known to be expressed in the PM/RDVM cells, and that are known to play important roles in hypothalamic induction and specification (Dale et al., 1999; Davis and Camper, 2007; Manning et al., 2006; Ohyama et al., 2005; Peng et al., 2012). *BMP7* is known to be expressed in the PM from HH5+, then expressed in RDVM cells from 1 somite (Dale et al., 1999; Vesque et al., 2000). BMP2, likewise, has been detected in anterior midline structures from HH5-10 (Chapman et al., 2002; Lyons et al., 1995). These studies however used transverse sections (meaning gene expression localisation along the AP axis was reconstructed from multiple sections) or wholemount views. By analysing sagittal sections I shall better interrogate localisation of gene expression on the AP axis and define position within PM/PME and RDVM/pBHyp cells. At the same time, I analysed expression of the BMP inhibitors, Chordin and Noggin, to provide a first indication of when and where BMP signalling might be stimulated.

At 4s, my study (Fig.3.1) and a fate-mapping study (Dale et al., 1999) show that RDVM cells extend ~75-200 micron from the AN. *BMP2* and *BMP7* are both detected in this domain. The anterior limit of each is difficult to define, but each appears to be upregulated ~100μm from the AN (Fig.3.2.A; B), potentially marking anterior-most RDVM cells. However, at this stage, the canonical BMP inhibitor, *CHRD* is likewise detected in RDVM cells, although

potentially is limited to more posterior RDVM domain (Fig.3.2.C). The BMP inhibitor *NOG* is

expressed only in the notochord (Fig.3.2.D). This data is summarised in (Fig.3.2.E). The

presence of weak *BMP2/BMP7* transcripts in the absence of *CHRD/NOG* opens the

possibility that BMPs may be active in anterior-most RDVM cells at 4s.

At 7s, RDVM cells likewise extend ~75-200 micron from the AN. *BMP2* and *BMP7* may

together define RDVM cells at this stage (Fig.3.2.F, G) although *BMP7* expression extends

posteriorly in the ventral midline. They are beginning to resolve however, with expression of

BMP2 stronger anteriorly and *BMP7* stronger posteriorly. Whereas *CHRD* at 4s has a similar

border in both the axial mesoderm and the neuroectoderm this is not true at 7s, *CHRD* has

an anterior limit closer to the AN in the neuroectoderm than the axial mesoderm (Fig3.2.H).

NOG is still only expressed in the notochord (Fig3.2.I). This data is summarised in (Fig3.2.J).

The presence of *BMP2/BMP7* transcripts in the absence of *CHRD/NOG* suggests that BMPs

may be active throughout RDVM cells at 7s.

At 10s, the distinctive groove makes the position of pBHyp cells more easy to define. *BMP2*

appears to be largely confined to anterior pBHyp cells (ie anterior to the groove) (Fig.3.2.K).

By contrast, *BMP7* is now confined to pBHyp within and posterior to the groove. (Fig.3.2.L).

Low levels of BMP7 are detected in pBHyp cells close to the groove and strong BMP7

expression is detected in posterior-most pBHyp cells; additionally, expression extends

posterior to the CF. At 10s *NOG* is still only expressed in the notochord (Fig3.2.M), *CHRD*

localisation is now further from the AEN with its anterior limit appearing to retreat

(Fig3.2.N). This data is summarised in (Fig3.2.O).

The presence of BMP transcripts and lack of inhibitors confirms the possibility of there being

active BMP signalling as RVDM cells make the transition to pBHyp cells, albeit that

expression is complex and dynamic. Next I set about ascertaining whether this is the case.

	BMP2	*BMP7*	*CHRD*
4s	A n=2/2	B n=2/2	C n=4/4
7s	F n=2/2	G n=2/2	H n=5/5
10s	K n=4/4	L n=6/6	M n=3/3

	NOG	
4s	D n=3/3	E
7s	I n=1/1	J
10s	N n=3/3	O

BMP2

BMP2/7

CHRD+BMP2/7
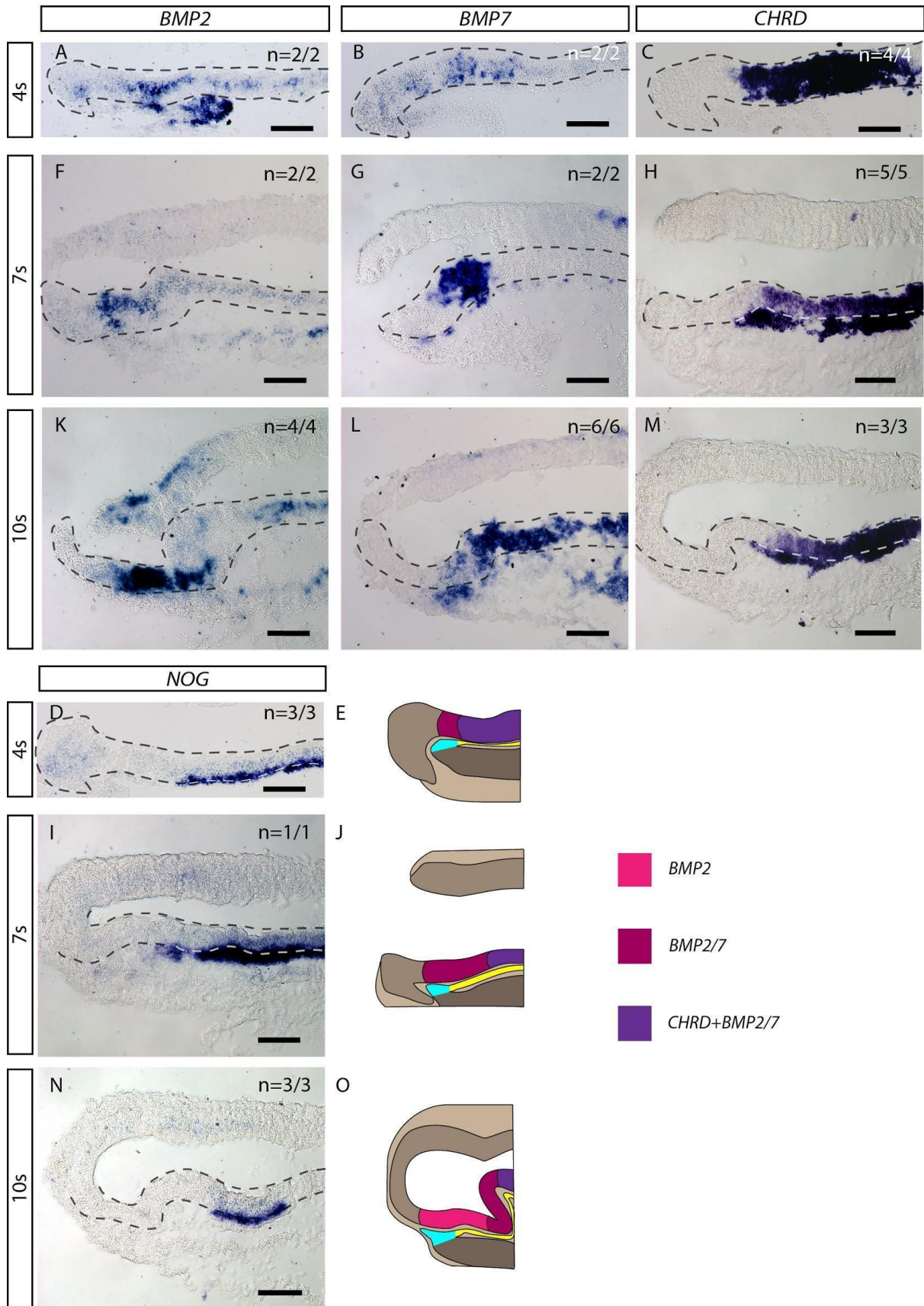
Figure 3.2: *BMP2* and *BMP7*, but not their inhibitors *CHRD* and *NOG* are expressed in RVDM/pBHyp cells. A) At the 4 somite (4s) stage *BMP2* is expressed within the ventral neural tube, with varying staining intensities along the anteroposterior (AP) axis. B) *BMP7* is expressed in the ventral neural tube at 4s, patches of staining are present along the AP axis. C) *CHRD* is expressed at 4s in the ventral neural tube and notochord, showing weakest intensity staining anteriorly. D) At 4s *NOG* is expressed in the notochord but not in the overlying neuroectoderm. E) Schematic summarising (A-D). F) *BMP2* continues to be expressed in the ventral neural tube at 7s, showing high staining intensity anteriorly. G) *BMP7* continues to be expressed in the ventral neural tube at 7s, with high intensity staining weakening anteriorly. Note expression can also be seen in the underlying prechordal mesoderm and notochord. H) *CHRD* shows reduced staining intensity in the anterior most region of its ventral neuroectoderm expression at 7s. I) *NOG* continues to be expressed only in the notochord at 7s. J) Schematic summarising (F-I). K) *BMP2* continues to be expressed in the ventral neural tube and shows high staining intensity anteriorly at 10s. L) *BMP7* shows high intensity staining in the ventral neural tube at 10s, again with weaker expression anteriorly. M) At 10s *CHRD* shows a similar expression pattern as in (G) with high intensity staining becoming weaker anteriorly. N) *NOG* continues to only be expressed in the notochord at 10s. O) Schematic summarising (J-M).

pSMAD1/5/8 is present in RVDM and pBHyp cells from 4s, but not at uniform levels

pSMAD1/5/8 is the canonical intracellular signal transducers for BMP2 and BMP7. To

ascertain how BMP transcription patterns translate to active BMP signalling within RVDM

cells I have used an antibody specific to the phosphorylated form of SMAD1/5/8, indicative

of active signalling. By combining this with previously-published expression patterns I can

deduce how the interplay between BMPs and their inhibitors impacts on pSMAD1/5/8

localization.

At 3s pSMAD1/5/8 is localized only to PM/PME cells and is not detected in overlying neuroectoderm cells (Fig.3.3.A-A'''). By 4s however pSMAD1/5/8 is detected in RDVM cells, but appears confined to those above the PME (Fig.3.3.B-B'''). By 7s pSMAD1/5/8 is detected over a longer A-P extent, and is detected in cells above the PME and PM (Fig.3.3.C-C'''). However, expression is not uniform and is now only weakly detected above PME cells, the anterior most RDVM cells (Fig.3.3.C-C'''). A similar profile is detected at 9s, when RDVM cells are progressing to pBHyp cells: expression is detected throughout RDVM/pBHyp, but strongest expression is confined to cells that lie anterior to the groove.

Overall, a tentative conclusion is that pSMAD1/5/8 is detected in RDVM and developing pBHyp cells, but is dynamic, and is restricted to RDVM cells that lie adjacent to those expressing the highest levels of *BMP2/7* in the absence of inhibitors. My null hypothesis (BMP signalling uniform through RDVM cells) is incorrect. Potentially, instead, BMPs signal in a paracrine manner within RDVM cells.
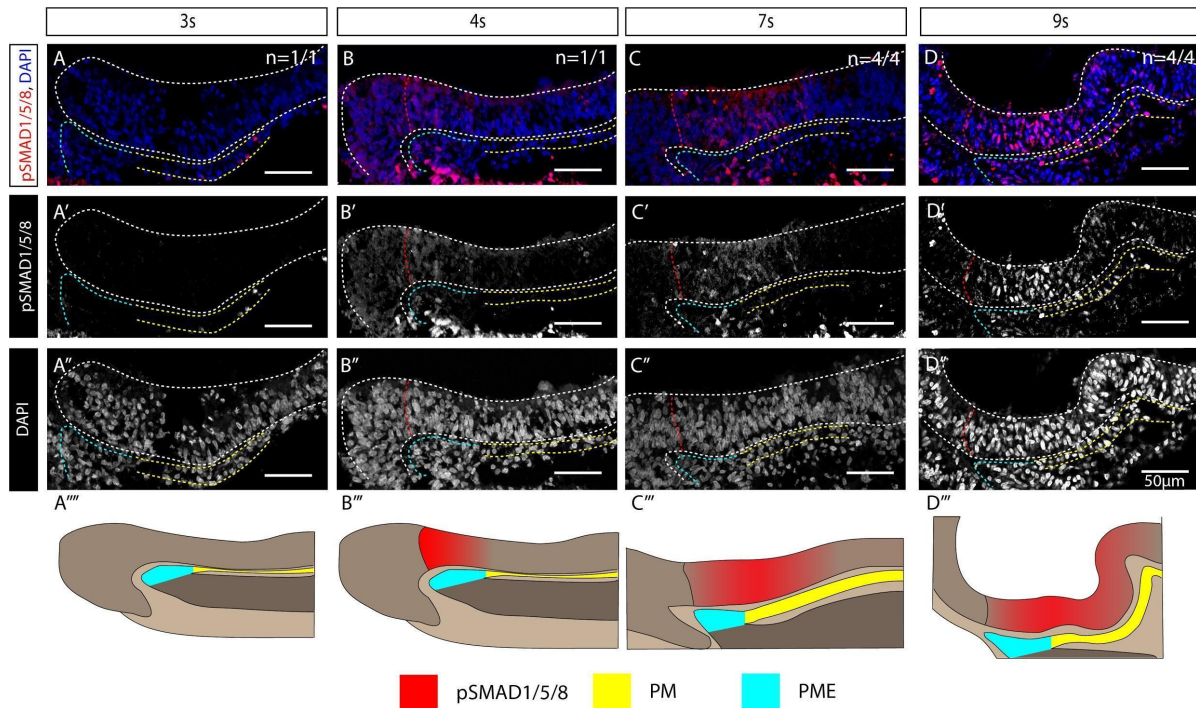
Figure 3.3: pSMAD1/5/8 is present from 4s in the ventral neural tube and shows differential levels from 7s. A) At 3s no pSMAD1/5/8 is present in the ventral neural tube however it is located in prechordal mesendoderm cells (yellow) underlying the neural tube (A-A'''). B) At 4s pSMAD1/5/8 is present in the ventral neural tube (red) and the underlying PME and PM cells (blue and yellow) (B-B'''), at this stage pSMAD1/5/8 appears to be in a high low pattern anterior to posterior. C) At 7s pSMAD1/5/8 continues to be localised to the ventral neural tube and underlying axial mesoderm cells (C-C'''), however a low high low pattern now appears to be present in the expression within RVDM cells. D) By 9s a clear low high low pattern is visible, with the highest levels detected in the region above the PME/PM boundary (D-D'''). A-A''',D-D''') This broken down into immunofluorescence, pSMAD1/5/8, DAPI and a schematic, respectively.

pSMAD1/5/8 and *FOXG1* show complementary expression during pBHyp induction

To confirm that pSMAD1/5/8-expressing cells represent 'anterior' RVDM/pBHyp cells I next compared the localisation of pSMAD1/5/8 with the telencephalic progenitor marker *FOXG1*. Previous work has indicated that pBHyp cells abut *FOXG1*-expressing telencephalic progenitors (Fu et al., 2017). I therefore chose to examine the relationship between the

expression domains of *FOXG1* and pSMAD1/5/8 using in situ hybridisation and immunofluorescence, respectively. If pSMAD1/5/8 demarcates anterior RDVM/pBHyp cells, it should show complementary expression to *FOXG1*.

At 9s and 10s as RDVM cells progress to pBHyp cells, pSMAD1/5/8 and *FOXG1* show complementary expression profiles. Similar to the 7s embryo (Fig. 3.3.C-D), expression of pSMAD1/5/8 is not uniform within RDVM cells. RDVM/pBHyp cells that abut the telencephalon express pSMAD1/5/8 only weakly. Strong expression is detected in RDVM cells anterior to the groove and weak expression is detected in RDVM/pBHyp cells posterior to the groove (Fig.3.4.A^I-A^V;Fig.3.4.B^I-B^V). This relationship is summarised in (Fig.3.4.A^{VI}, B^{VI}).

These data show that during pBHyp cell induction pSMAD1/5/8 is localised to RVDM cells but not telencephalic progenitors. This data shows that active BMP signalling, assessed by pSMAD1/5/8 localisation, is not detected uniformly within RDVM/prospective pBHyp cells. Instead, highest levels are detected in RDVM cells that lie anterior to a developing groove, with lower fluorescence in cells bordering the prospective telencephalon. Next I chose to assess the relationship between pBHyp cells and pSMAD1/5/8.
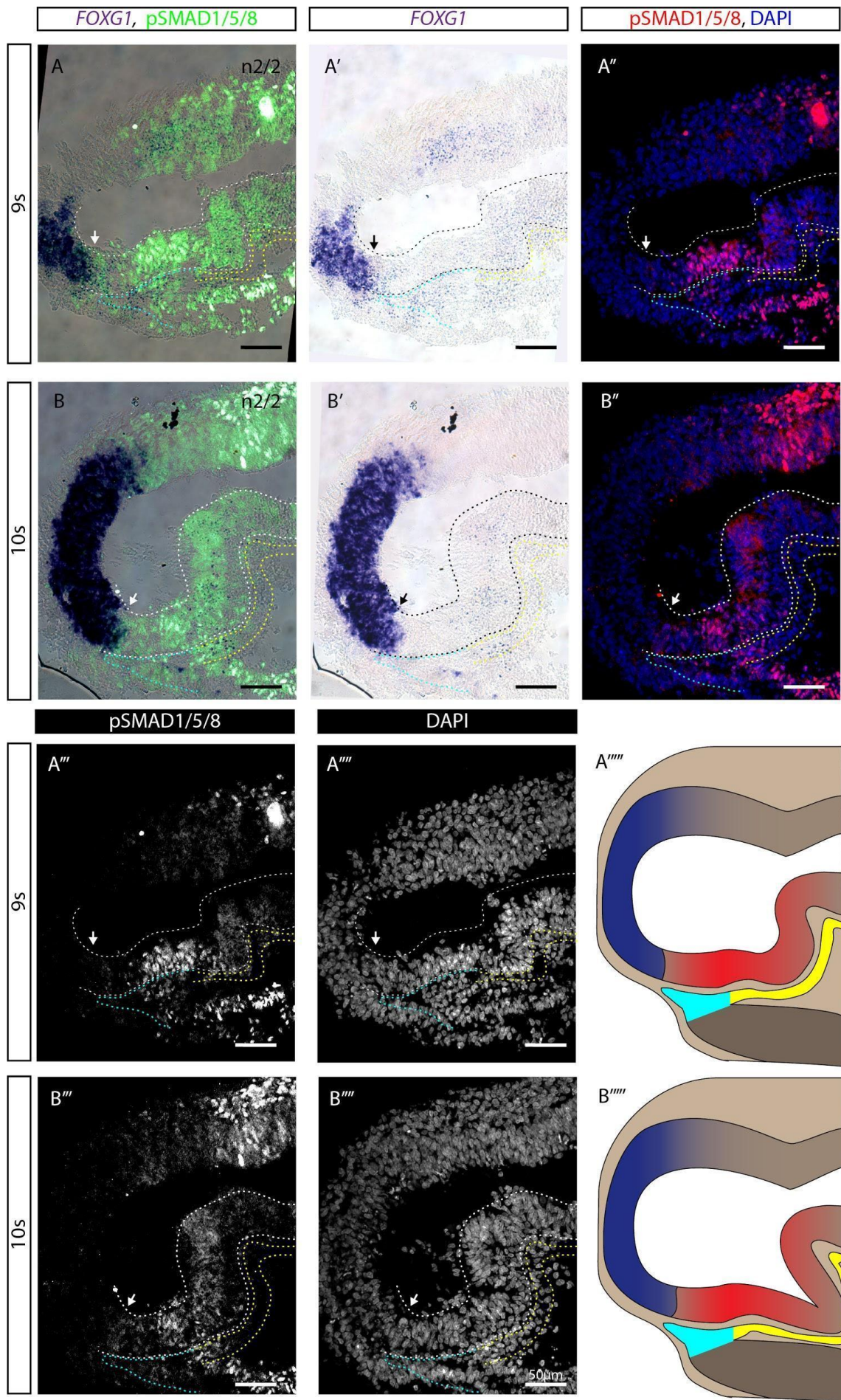
Figure 3.4: pSMAD and FOXG1 show complementary expression during pBHyp induction. A,B) At 9s and 10s, (A) and (B), *FOXG1* in situ shows complementary expression with pSMAD1/5/8 immunofluorescence at its anterior limit (arrow), ~75µm and ~85µm from the AEN, respectively. A'-A''''',B'-B''''') This broken down into chromogenic in situ, immunofluorescence, pSMAD1/5/8, DAPI and a schematic, respectively.

pSMAD1/5/8 prefigures and predicts *FGF10* expression

pBHyp cells appear to develop from RDVM cells at 10 somites and are characterised by their upregulation of *FGF10* (Fu et al., 2017). Previous work has shown that *FGF10* and *FOXG1* are complementary at 10 somites, ie that pBHyp cells abut telencephalic progenitors (Fu et al., 2017). I have shown (Fig.3.4) that pSMAD1/5/8 has a complementary expression pattern with *FOXG1*, a marker of the telencephalon. This raises the possibility that pSMAD1/5/8 signalling prefigures and predicts *FGF10* expression. Next I therefore investigated how pSMAD1/5/8 correlates with the pBHyp marker, *FGF10*.

FGF10 is not expressed within RVDM cells at 7s (Fig.3.5.A), at a time when pSMAD1/5/8 is present within RVDM cells (Fig.3.5.B). However by 10 somites, I detect *FGF10* (Fig.3.5.C). My analyses confirm the previous study (Fu et al., 2017) that suggests that at 10 somites , *FGF10* defines pBHyp cells*:* thus, I detect expression in cells above the PME/PM, and anterior to the CF. Co-analysis of *FGF10* expression and pSMAD1/5/8 localisation in the same sample shows their expression domain is between ~77µm and ~200µm from the AEN (Fig.3.5.C^i-C'''). The two markers show very closely related expression regions. This analysis makes a case for an in vivo relationship between active BMP signalling and *FGF10* induction, and suggests that

pSMAD1/5/8 localisation in RDVM cells prefigures and predicts *FGF10* positive pBHyp cells

Finally, my work demonstrates, for the first time, that *FGF10* is not uniformly expressed in pBHyp cells: expression levels go from low to high to low (going from ant-post: Fig.3.6.C), closely mimicking the levels of pSMAD1/5/8 (Fig.3.5 and Fig.3.6.C").

FGF10, *FOXG1*	pSMAD1/5/8

7s

A n=1/1

B n=4/4

50µm

FGF10	pSMAD1/5/8

10s

C n=3/3

C' n=3/3

FGF10, pSMAD1/5/8	C'''

10s

C'' n=3/3

50µm
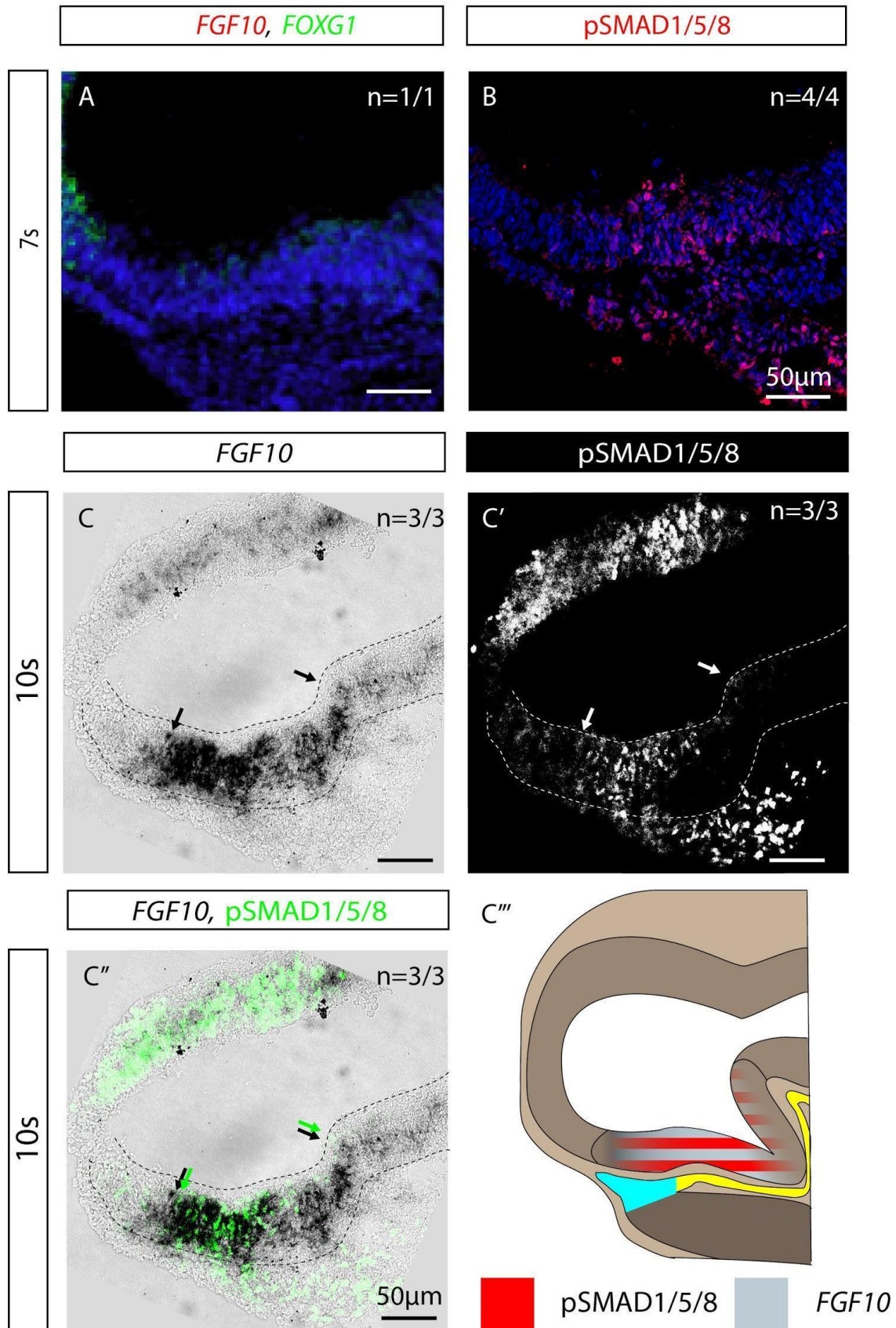
	pSMAD1/5/8		*FGF10*

Figure 3.5: pSMAD1/5/8 predicts and prefigures *FGF10* expression. A) *FGF10* is not expressed at 7s in the ventral neural tube, B) pSMAD1/5/8 is expressed in the ventral neural tube at 7s, with an anterior limit ~70μm from the A.N. and a posterior limit ~190μm from the A.N. C-C'') Both *FGF10* and pSMAD1/5/8 are expressed in the ventral neural tube with similar anterior and posterior limits, anteriorly ~77μm from the AEN and posteriorly ~200μm from the AEN. C''') Schematic summarizing (C-C'').

The telencephalic-hypothalamic progenitor boundary marks the point of contact of PME and surface ectoderm

My observations strongly suggest that pSMAD1/5/8 marks prospective hypothalamic progenitors, and provides the earliest known specific marker for this population. Because pSMAD1/5/8 is detected through immunohistochemistry, it provides the opportunity to more easily examine the position of RDVM/pBHyp cells relative to adjacent tissue.

I therefore analysed pSMAD1/5/8 expression relative to that of LHX3, a marker of the surface ectoderm, including surface ectoderm that will involute to form Rathke's pouch. Co-analysis of pSMAD1/5/8 and LHX3 at 10 somites shows the position of pSMAD1/5/8-expressing cells above the PME/PM (Fig.3.6). Intriguingly, the anterior boundary of RDVM/pBHyp cells correlates with the point at which the LHX3-expressing surface ectoderm moves ventrally, beneath the PME/PM (Fig.3.6). Therefore, the telencephalic-hypothalamic progenitor boundary (*FOXG1*/pSMAD1/5/8) marks the point of contact of PME and surface ectoderm. This shows that pBHyp cells are in contact with the future anterior pituitary from an early stage, as suggested by earlier fate mapping work (fu et al., 2017).
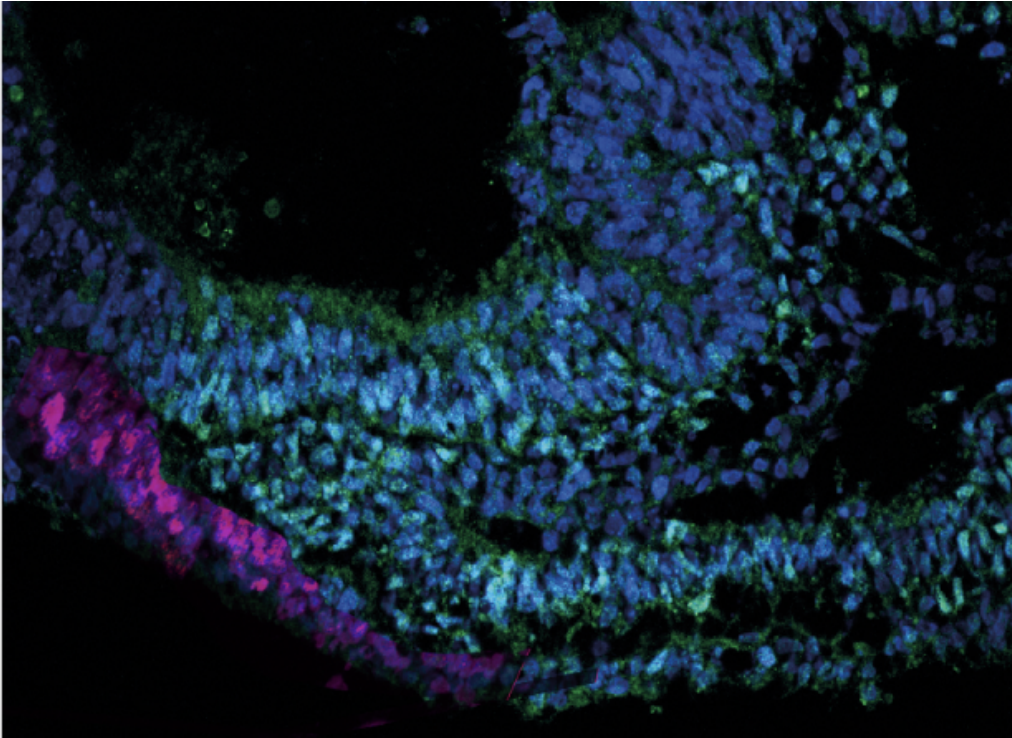
Figure 3.6: pBHyp cells make contact with surface ectoderm at 10s. pSMAD1/5/8 (green) shows that pBHyp make contact with LHX3 (magenta) positive surface ectoderm where surface ectoderm moves under the PM/PME.

Summary Schematic of In Situ and Immunofluorescence data presented in this chapter

Figure 3.6 summarises the expression profiling. From 4s pSMAD1/5/8 is localized to a subset

of RVDM cells, appearing to have a limit anterior to *BMP2* expression and a posterior limit

within the *CHRD* expressing region of ventral midline cells (Fig.3.6.A). At 7s however,

pSMAD1/5/8 is located further from the AN, posterior to the *BMP2* expression. (Fig.3.6.B).

Also, *BMP2* is expressed more anteriorly than *BMP7* from 7s onward (Fig.3.6.A-C). By 10s

FGF10 is induced and shows a similar expression region to pSMAD1/5/8, anteriorly abutting

the *FOXG1+* telencephalon, and posteriorly stopping at the cephalic flexure (Fig.3.6.C). At all

times pSMAD1/5/8 is closely adjacent to areas that express *BMP2* and *BMP7*.

A

B

C

FOXG1   BMP2   BMP2/7   pSMAD1/5/8

FGF10   BMP7   SHH   CHRD+BMP7
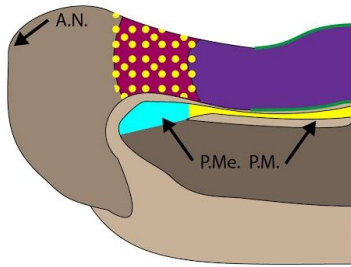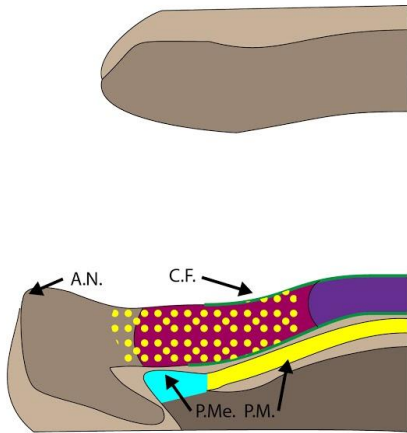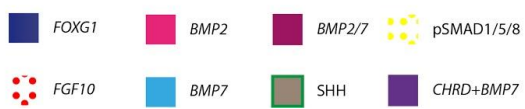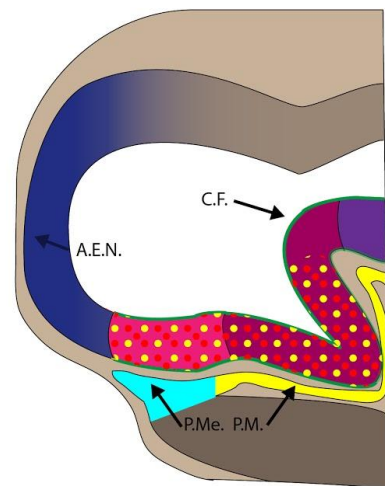
Figure 3.7: Summary schematic of RVDM/pBHyp cell development from 4s to 10s. Please see key for colour/gene relations. A) At 4 somite BMP7 from the PM/PME induces BMP2 and BMP7 expression in overlying ventral midline cells, pSMAD1/5/8 is confined to a region anterior to *CHRD* expression. B) By 7 somites as *CHRD* is downregulated/displaced pSMAD1/5/8 extends posteriorly. C) Continued BMP signalling then induces *FGF10+* pBHyp character at 10 somites. AN anterior neuropore, AEN anterior extent of neuroectoderm, CF cephalic flexure, PME prechordal mesendoderm, PM prechordal mesoderm.

3.3. Discussion

In this chapter I have performed an in-depth analysis, using sagittal and serial adjacent sections, of BMP family members and their inhibitors along the anterior posterior axis, focusing on RDVM and pBHyp cells. My results show, in particular, that the canonical BMP signalling pathway is active in RDVM cells, and that pSMAD1/5/8 prefigures and predicts the pBHyp domain. Thus, pSMAD1/5/8 is the earliest-known marker for RDVM cells that will progress to pBHyp cells and my studies add weight to the suggestion that pBHyp cells are diencephalic cells that immediately abut telencephalic progenitors. Intriguingly, my results show that pSMAD1/5/8 and *FGF10* are not uniform: each is expressed in a low-high-low manner along the A-P extent of RDVM and pBHyp cells. My data provides a resolution to long-standing disputes as to the relative position of prospective hypothalamic cells to adjacent tissues. I show that RDVM/pBHyp cells are largely underlain by the PME/PM, but that these abut surface ectoderm cells: thus the surface ectoderm/PME boundary likely demarcates the anterior-most RDVM/pBHyp cells. Close proximity between Rathke's Pouch and the infundibulum is required for their proper patterning at later stages (Ericson et al., 1998).

3.3.1. BMPs and BMP signalling is highly dynamic in the early-forming hypothalamus

My studies show that BMPs are expressed dynamically as RDVM/pBHyp cells form, and raise many questions. First, as shown by their increasing distance from the AN/AEN, *BMP2* and *BMP7* expressing regions are progressively displaced/regress from the AN during the course of 4s to 10s (Fig3.2.2). This could be due to more anterior (telencephalic) cells proliferating and displacing BMP expressing cells posteriorly. Another possibility is a regression of BMP expression domains relative to the AN/AEN, that is to say cells at the anterior limit of *BMP2/BMP7* expression downregulate these BMPs in response to the presence/lack of some unknown signal. Lineage tracing via labelling of these cells at 4s based on distance from the AN, targeting regions known to be expressing *BMP2/BMP7,* and later analysing which regions labelled cells gave rise to could ascertain if these cells continue to express *BMP2/BMP7* and are displaced by more anterior proliferation or if they down regulate *BMP2/BMP7* during the course of their development.

Second, although expression of *BMP2* and *BMP7* appears similar at 4s, by 10s, *BMP2* is expressed in a more rostral region that *BMP7*. How this occurs is not clear, nor is it clear what the later impact might be on RDVM or pBHyp cells. However, *BMP7* is capable of inducing its own expression in the PM and RVDM cells (Dale et al., 1997; Vesque et al., 2000), whereas BMP2 is expressed only in the neuroectoderm. This difference in expression pattern could be the result of different modes of induction or varying competency in RVDM

cells to express BMPs. Further testing, possibly including explant studies of HH5 neuroectoderm, would be needed to test whether BMP7 could induce *BMP2* ex vivo. High concentration SHH has been shown to be able to induce *NKX2.1* in neuroectoderm explants, but not in the presence of anti-BMP7 IgG (Dale et al., 1997). This suggests that high levels of SHH signalling may be capable of inducing BMP7 expression in neuroectoderm. Studies in mouse have shown that in the developing anterior pituitary SHH is capable of inducing BMP2 expression (Treier et al., 2001). SHH and BMP7 have been shown to be sufficient to induce *NKX2.1* expression in mouse embryonic stem cell derived neural progenitor cells (Ohyama et al., 2005). All these data together show the importance of BMP signalling in the specification of pBHyp, a question that remains is the role *BMP2* expression plays. Previous work has shown BMP2/BMP7 heterodimers show greatly increased in vitro alkaline phosphatase induction capability compared to either homodimer, and this holds true for in vivo bone forming assays (Israel et al., 1996). Work in zebrafish has shown that BMP2/BMP7 heterodimers and not a combination of both homodimers possess enough receptor affinity to overcome extracellular repression in vivo to elicit the signalling response required form dorsoventral patterning in the zebrafish embryo (Little and Mullins, 2009). Perhaps this is also the case during in vivo chick BMP signalling in RVDM cells, I have reported here an area that expresses *BMP2* but appears to show no pSMAD1/5/8 localisation, as well as a region expressing *CHRD* and shows pSMAD1/5/8 localisation. Testing this possibility would require an in vivo knockdown of BMP2 or BMP7, through as system such as electroporation of a siRNA construct designed to reduced gene translation, followed by addition of BMP2/BMP7 heterodimer to test whether they are necessary and sufficient to induced pBHyp character. Timely inhibition and inhibitory release is key to the proper functioning of BMPs during development and adult function, this is in part achieved by extracellular inhibitors such as

Chordin, which restricts BMP signalling in the PM/PME and ventral neuroectoderm (Dale et al., 1999; Patten and Placzek, 2002).

3.3.2. Active BMP signalling is restricted by BMP inhibitor Chordin and prefigures and predicts pBHyp

My results, together with an earlier study (Dale et al., 1999) show a downregulation of Chordin/displacement of Chordin expressing cells in the RVDM region from anterior to posterior. Here I suggest that this downregulation enables BMPs to signal, and to promote SMAD1/5/8 phosphorylation. The observation that pSMAD1/5/8 is expressed at high levels in cells adjacent to *BMP2/7*-expressing domains suggests that BMP signalling promotes pSMAD1/5/8 in a paracrine manner. However, the low level of pSMAD1/5/8 and BMPs gives credence to the idea that pSMAD1/5/8 is required for the induction of BMPs in RVDM cells, as in the dorsal spinal cord (Lee and Jessell, 1999).

In summary, the data in this chapter shows a close correlation of pSMAD1/5/8 with *FGF10*, the marker of pBHyp cells at 10s. Further, previous work has shown that BMP7 is necessary and sufficient to induce *FGF10* in HH6 neural explants ex vivo (Manning et al., 2006), suggesting that paracrine BMP7 is required for progression to a pBHyp identity. An unknown question is whether the RDVM-intrinsic expression of pSMAD1/5/8 is enough to direct the upregulation of *FGF10* in RDVM cells, or whether continued signalling from the PM or RDVM cells is required? In other words, has BMP signalling at 4 somites set up the conditions necessary for *FGF10* expression at 10 somties or is continued BMP signalling required for

FGF10 upregulation? In the next chapter, these are the questions I will be attempting to

address via an ex vivo culture system.

Chapter 4:

FGF10 expression is regulated by BMP type 1 receptor signalling during ex vivo culture

4.1. Introduction

Ex vivo explant culture allows for populations of cells to be removed from their in vivo environment and continue development in the absence of other tissues and signals. Additionally it allows for cell populations to be exposed to particular signals, or signal inhibitors, to ascertain their impact. This technique has proven invaluable in deciphering the extrinsic factors that contribute to induction and patterning of neural tissues, and in understanding when intrinsic factors begin to allow cells to commit to particular fates. Work in this area has been used to show the complex signalling events that pattern ventral diencephalic tissue and the developing hypothalamus (Dale et al., 1999; Ericson et al., 1998).

Such ex vivo explant studies were critical in implicating SHH and BMP7 as the factors originating from the PM that induce hypothalamic character (see previous Chapter). Initial studies showed that BMP7 is able to co-operate with SHH to induce expression of *NKX2.1*, a

hypothalamic marker, in HH5/6 neuroectoderm explants (Dale et al., 1997). Following this observation, it was shown that BMP7 is capable of inducing genes associated with the tuberal and mammillary hypothalamus, *FGF10* and *EMX2* respectively, in HH5/6 neuroectoderm explants (Manning et al., 2006). In this study *SHH*-expressing cells taken from the anterior ventral midline (fated to become RDVM/pBHyp cells), were continuously exposed to BMP7: they upregulated *FGF10,* then *EMX2,* after culture times appropriate to those seen for in vivo expression of *FGF10* and *EMX2*. This suggests that sustained culture of HH5/6 neuroectoderm with BMP7 supports the induction of RDVM cells, the progression of RVDM cells to pBHyp and then to more committed pMam cells. An outstanding question is whether such pBHyp explants required the continual exposure to BMP7, or whether they could differentiate in an intrinsic manner. The expression of *BMP2/7* and the lack of inhibitors as shown in Chapter 3 indicates that they might be able to differentiate intrinsically; however, these expression profiles do not mean, a priori, that pBHyp explants will express pSMAD1/5/8. First it must be shown that endogenous BMP expression is capable of maintaining active BMP signalling.

To summarise: the studies above suggest that BMP signalling plays important roles in the specification and/or survival of ventral diencephalic cells. However, as I showed in Chapter 3, BMPs and BMP signalling become endogenous to RDVM cells at 4 somites. As yet, no study has looked at whether RDVM-endogenous *BMP7* expression at 4 somites is sufficient to induce SMAD1/5/8 phosphorylation. Further the necessity for BMP signalling in the progression of RVDM cells to pBHyp has not yet been tested.

If *BMP7* expression in RVDM cells at 1 somite is all that is required in order to progress to pBHyp identity (i.e. cells that express *FGF10*), then after this point BMP signalling could be inhibited with no effect on *FGF10* expression. The alternate possibility is that there is a requirement for sustained BMP signalling activation for *FGF10* upregulation: either explanation is possible based on previous work explanting HH5/6 neuroectoderm and continually exposing it to BMP7 (Manning et al, 2006). In order to begin to pick apart whether endogenous BMP7 expression in RVDM cells is sufficient to autonomously govern progression to pBHyp fate RVDM cells must be explanted (Fig.4.1). A second key question, prompted by my studies showing pSMAD1/5/8 expression, is whether ongoing pSMAD1/5/8 is required for FGF10 expression.
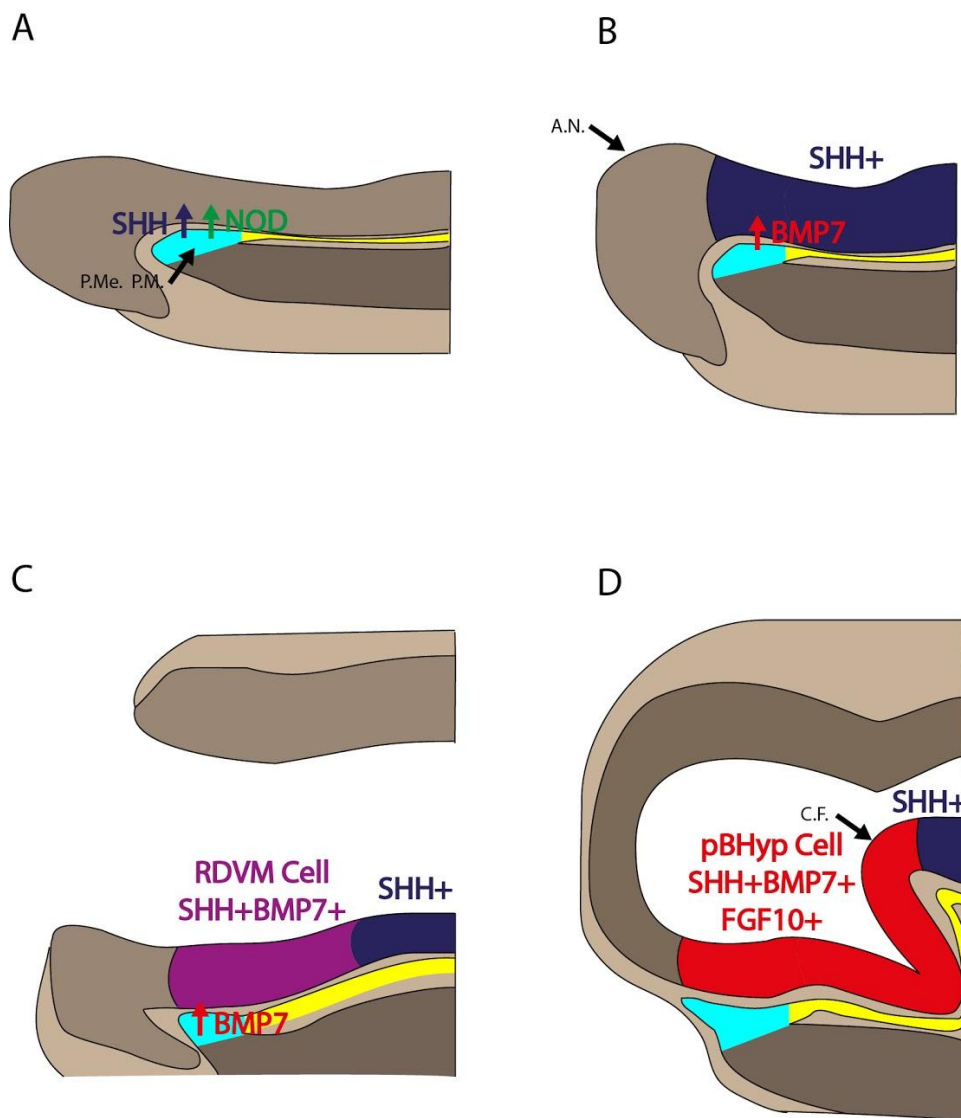
Figure 4.1: 3 Step Signalling from the PM/PME. A) At HH5 SHH and nodal from the PM/PME cooperate to induce its SHH expression in overlying ventral midline cells. B) By 1 somite there is a change in PM/PME signalling so that it now expresses BMP7 which induces RVDM character in the overlying neuroectoderm (C). D) Continued BMP signalling then induces *FGF10+* pBHyp character at 10 somites (Vesque et al, 2000, Patten et al, 2003, Ellis et al, 2015).

In this chapter I set out to ask if there is a requirement for continued BMP7 exposure, and

pSMAD1/5/8 signalling in order for 4 somites RDVM cells to upregulate FGF10? Is exogenous

BMP7 from the axial mesoderm required to specify pBHyp cells? To answer these questions I

will be investigating the role of BMP7 and BMP signalling in the induction of *FGF10* during the progression of RVDM cells to pBHyp cells. I will be doing this using an ex vivo explant culture system to assess the necessity of exogenous BMP7 and endogenous BMP signalling for *FGF10* upregulation. The aims of this chapter are to establish if:

- Endogenous *BMP2/7* expression is enough to maintain pSMAD1/5/8 phosphorylation in vitro.

- Endogenous BMP signalling is capable of inducing *FGF10* expression in vitro.

- Exogenous BMP7 affects *FGF10* expression.

- There is a requirement for continued pSMAD1/5/8 signalling in the upregulation of *FGF10*.

These are important questions as they will shed light on the continued *BMP7* expression in the axial mesoderm and its function, as well as the role of endogenous BMP expression in progression of RDVM cells to pBHyp cells.

4.2. Results

Defining an explant protocol to assay *FGF10* expression

In order to define the requirement for exogenous BMP7 or endogenous BMP signalling on *FGF10* upregulation in RDVM cells in vitro I have defined a protocol using neuroectoderm

explants taken at 4s and cultured (a) alone (b) exposed to human BMP7 (hBMP7); or (c) exposed to Dorsomorphin (Dors), a potent inhibitor of type I BMP receptors and therefore an inhibitor of pSMAD1/5/8 (Yu et al., 2008).

I will summarise the protocol briefly here: a detailed description can be found in Chapter 2. Embryos were staged in ovo, 4s embryos were selected, dissected in ice cold L15 (Fig.4.2.A), filleted using a tissue chopper (Fig.4.2.B), treated with dispase, the neuroectoderm isolated (Fig.4.2.C), embedded in collagen gel (Fig.4.2.D), and finally immersed in supplemented OPTI-MEM followed by incubation at 37°C with 5% CO_2 for 20 hours before fixation and analysis.

This experiment allows testing of how different areas of the neuroectoderm develop in vitro, deprived of exogenous signalling from structures such as the axial mesoderm. It also provides a system in which exogenous activators or inhibitors can be added in isolation to test their function or that of the related signalling pathway.
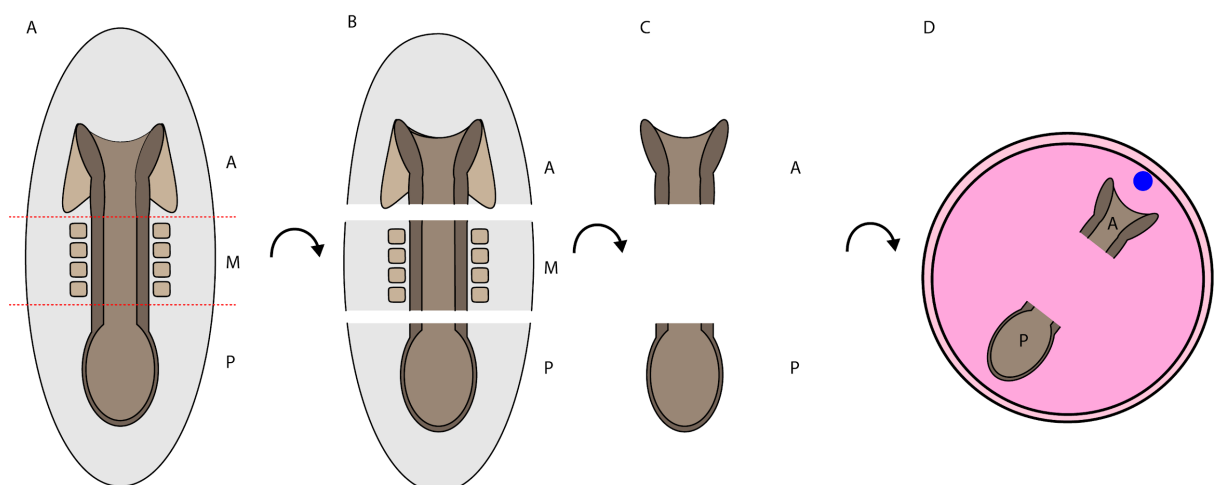
Figure 4.2: Schematic showing explant protocol. A) 4s embryos were selected and immediately moved onto L15 on ice. B) Embryos were then sliced by tissue chopper and treated with Dispase to facilitate neuroectoderm isolation. C) Following Dispase treatment all surrounding tissue was removed, leaving only neuroectoderm. D) These explants were then embedded in collagen, immersed in media and incubated to desired extent.

hBMP7 Treatment Curve Analysis

Previous work has shown that exposure of HH5/6 neuroectoderm explants to hBMP7 induces *FGF10* expression, implicating sustained BMP7 exposure to pBHyp induction (Manning et al., 2006). To build on these experiments, I tested whether BMP7 is likely to promote the transition from RVDM cells to pBHyp cells via induction of pSMAD1/5/8. To do so I tested a range of concentrations of hBMP7 and examined whether each resulted in an increase of pSMAD1/5/8 fluorescence intensity, while maintaining explant survival. I used 4s medial neuroectoderm explants as they are known to express *CHRD*, an inhibitor of BMP signalling, and show no SMAD1/5/8 phosphorylation. They can therefore be used to test the ability of hBMP7 to overcome endogenous inhibition and induce SMAD1/5/8 phosphorylation.

Dissection was similar to that outlined in (Fig.4.2), and medial fillets were selected for testing (Fig.4.3.A-D). Explants were then cultured in the following range ofhBMP7 concentrations: 200ng/ml, 500ng/ml, 750ng/ml, and 1µg/ml. My results (Fig.4.3.E-I) show that hBMP7 treatment above 200ng/ml greatly increased the percentage area of

pSMAD1/5/8 +ve expression (Fig.4.3.J). 500ng/ml was selected as explants showed both greatly increased pSMAD1/5/8 +ve area but also maintained a healthy, neural explant shape.

This establishes that hBMP7 promotes the phosphorylation of SMAD1/5/8 in neural progenitor cells in a concentration dependent manner. In order to determine the requirement of BMP signalling it will also be necessary to employ a knockdown system also, and for this I will use Dorsomorphin.

A

B

C

D

hBMP7 treated

pSMAD1/5/8, DAPI

'DAPI/''pSMAD1/5/8

E Control

F 200ng/ml

G 500ng/ml

750ng/ml

I 1µg/ml

J
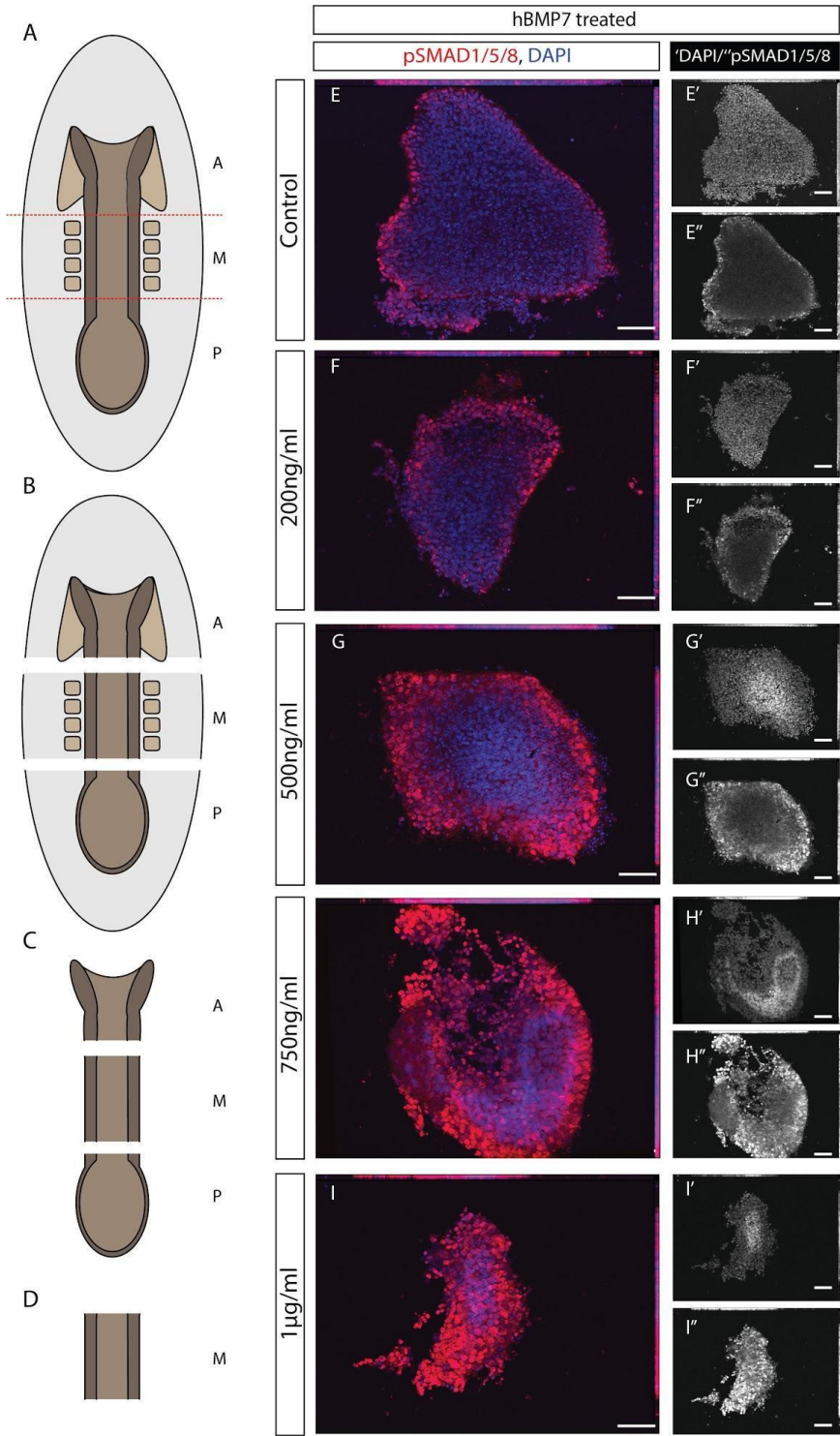
hBMP7 treatment increased pSMAD1/5/8 +ve coverage compared to control
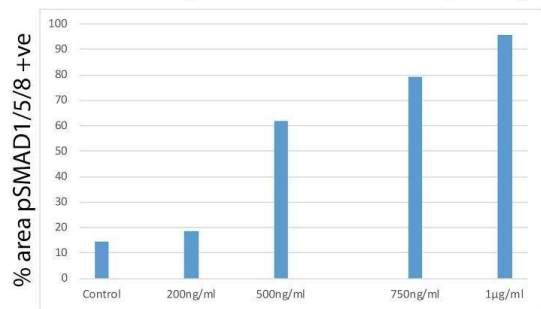
Figure 4.3: hBMP7 greatly increases pSMAD1/5/8 +ve area in neural explants. A) 4s embryos were selected and immediately moved onto L15 on ice. B) Embryos were then sliced by tissue chopper and treated with Dispase to facilitate neuroectoderm isolation. C) Following Dispase treatment all surrounding tissue was removed, leaving only neuroectoderm. D) Medial explants were then isolated from other neuroectoderm based on morphology. These explants were then embedded in collagen, immersed in media and incubated to desired extent. E-E'') pSMAD1/5/8 immunofluorescence in controls, E'-E'' show DAPI and pSMAD1/5/8 channels, respectively. F-F'') pSMAD1/5/8 immunofluorescence in 200ng/ml hBMP7 treated explants, F'-F'' show DAPI and pSMAD1/5/8 channels, respectively. G-G'') pSMAD1/5/8 immunofluorescence in 500ng/ml hBMP7 treated explants, G'-G'' show DAPI and pSMAD1/5/8 channels, respectively. H-H'') pSMAD1/5/8 immunofluorescence in 750ng/ml hBMP7 treated explants, H'-H'' show DAPI and pSMAD1/5/8 channels, respectively. I-I'') pSMAD1/5/8 immunofluorescence in 1μg/ml hBMP7 treated explants, I'-I'' show DAPI and pSMAD1/5/8 channels, respectively. J) hBMP7 treatment greatly increased the proportion of the explant that is pSMAD1/5/8 +ve in a concentration dependent manner, 2 explants per group were analysed. All explants culture for 20 hours.

Dorsomorphin decreases pSMAD1/5/8 percentage coverage

Dorsomorphin has been shown to inhibit the effect of BMP2 and BMP7 but not other TGFβ family member signalling in zebrafish (Yu et al., 2008). It achieves this via binding type I BMP receptors in an ATP mimetic mode, therefore preventing ATP binding and phosphorylation of downstream SMAD1/5/8 (Chaikuad et al., 2012). However, it must be noted, as mentioned earlier (see Introduction section 1.3.2.), that the BMP type 1 receptor can also participate in non-canonical BMP signalling.

Using Dorsomorphin to inhibit BMP signalling ex vivo I first tested a range of concentrations to determine that which maximised pSMAD1/5/8 knockdown (KD) while protecting the viability of the explants. I used 10 somites pBHyp explants for these experiments, as at 10

somites pBHyp cells robustly express *BMP2, BMP7* and pSMAD1/5/8 (Chapter 3)*.* Embryos were staged, filleted, dispased and the pBHyp cells isolated on the basis of morphology and relative position of the PM (Fig.4.4.A-D).

Explants were treated with a range of Dorsomorphin concentrations, 1µM, 2µM, 5µM, and 10µM and after 20hrs culture, analysed for expression of pSMAD1/5/8 and explant integrity. All explants exposed to 10µM showed dissociated cells that appeared to be dying, whereas explants exposed to lower concentrations appeared healthy. Both 2 and 5mM exposure showed similar phenotypes. 2µM was selected as the minimum on the basis of a robust KD of pSMAD1/5/8 and high survival rate of explants (Fig.4.4.J).

Together these experiments show that exposure of pBHyp explants to 2µM Dors robustly eliminates pSMAD1/5/8. I therefore used this and hBMP7 to ascertain the requirement for BMP signalling in *FGF10* induction in RDVM cells.

A

B

C

D

pSMAD1/5/8, DAPI

'DAPI/''pSMAD1/5/8

E   Control   E'   E''

F   1µM   F'   F''

G   2µM   G'   G''

H   5µM   H'   H''

I   10µM   I'   I''
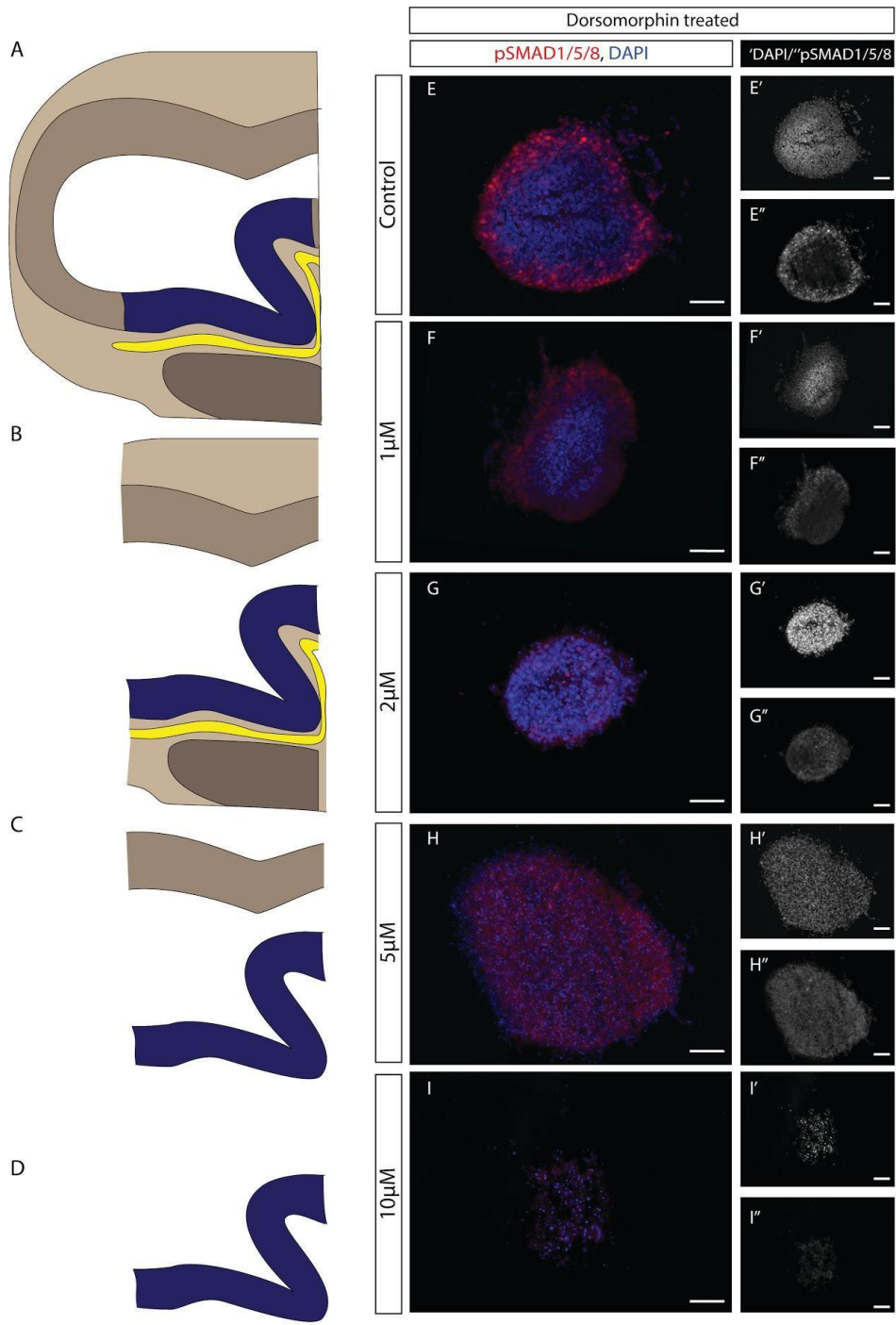
J

Control explants show higher pSMAD1/5/8+ coverage than all treatment levels

% area pSMAD1/5/8 +ve

Con   1µM   2µM   5µM   10µM
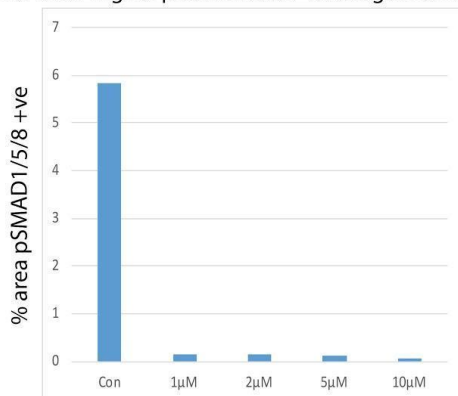
Figure 4.4: Dorsomorphin treatment of 2μM provides a robust pSMAD1/5/8 knock down and explant viability compared to controls and stronger treatments. A) 10s embryos were selected and immediately moved onto L15 on ice. B) Embryos were then sliced by tissue chopper and treated with Dispase to facilitate neuroectoderm isolation. C) Following Dispase treatment all surrounding tissue was removed, leaving only neuroectoderm. D) pBHyp were then isolated from the wider neuroectoderm based on morphology. These explants were then embedded in collagen, immersed in media and incubated for 20hrs. E-E'') pSMAD1/5/8 immunofluorescence in controls, E'-E'' show DAPI and pSMAD1/5/8 channels, respectively. F-F'') pSMAD1/5/8 immunofluorescence in 1μM Dorsomorphin treated explants, F'-F'' show DAPI and pSMAD1/5/8 channels, respectively. G-G'') pSMAD1/5/8 immunofluorescence in 2μM Dorsomorphin treated explants, G'-G'' show DAPI and pSMAD1/5/8 channels, respectively. H-H'') pSMAD1/5/8 immunofluorescence in 5μM Dorsomorphin treated explants, H'-H'' show DAPI and pSMAD1/5/8 channels, respectively. I-I'') pSMAD1/5/8 immunofluorescence in 10μM Dorsomorphin treated explants, I'-I'' show DAPI and pSMAD1/5/8 channels, respectively. J) Dors treatment greatly reduced the area of the explant that is pSMAD1/5/8 +ve above threshold level. All explants cultured for 20hrs.

Anterior explants autonomously upregulated *FGF10* in vitro compared to posterior explants, explants exposed to hBMP7 upregulate *FGF10* more strongly compared to control explants and explants exposed Dorsomorphin fail to properly upregulate *FGF10*

I next asked whether endogenous BMP signalling is capable of acting in an

RDVM-autonomous manner to direct 4s explants to upregulate *FGF10.* In vivo, *BMP2, BMP7*

and pSMAD1/5/8 are expressed in RVDM cells but not in posterior neuroectoderm regions

(Dale et al., 1999; Streit et al., 1998; and Chapter 3), and *FGF10* is upregulated in RDVM cells

but is not upregulated in the posterior neuroectoderm (Fu et al., 2017; Ohuchi et al., 2000).

In order to test the sufficiency of endogenous BMP2/BMP7 in upregulation of *FGF10* in

RVDM cells, 4s neuroectoderm from anterior and posterior regions were explanted (following the protocol outlined in Fig.4.2), with posterior regions serving as a control to ensure in vitro conditions did not lead to *FGF10* upregulation in and of itself. Explants were cultured for 20hrs (to the equivalent of 10 to 13 somites), and then examined for expression of *FGF10*.

As shown in (Fig.4.5.A-B), anterior explants showed a stronger *FGF10* staining, a proxy measure for expression levels, than posterior explants.

In summary, as shown in Chapter 3, at 4s, RDVM cells express *BMP2* and *BMP7* and SMAD1/5/8 phosphorylation in RDVM cells is first detected at 4s. My studies show that these cells, when explanted and allowed to develop, then go on to upregulate *FGF10*. This provides an indication that endogenous BMP signalling is sufficient for the later expression of *FGF10*. The question remains of whether exogenous BMP7 may continue to influence this process or whether 4s RDVM cells simply require time to upregulate *FGF10*.

I therefore next extended my studies, explanting tissue from 4s (HH8) embryos and exposing them to exogenous hBMP7, I hypothesised that exogenous BMP7 might lead to higher levels of *FGF10* expression.

Anterior explants exposed to hBMP7 showed increased *FGF10* staining, indicating higher levels of *FGF10* transcription (Fig.4.5.A, C). This result suggests that in vitro BMP7 from an exogenous source, similar to the PM in vivo, continues to play a role in the progression of RVDM cells to pBHyp following its own induction in RVDM cells. This and previous work has shown that BMP7 is key to the induction of RVDM cells and their progression to pBHyp cells.

If BMP7 is the factor that specifies these identities then it should be able to induce *FGF10* expression in neuroectoderm distant from the hypothalamic primordia. I next asked if hBMP7 is sufficient to induce *FGF10* in regions that in vivo do not express it?

Posterior regions of the neural tube do not express *FGF10* in vivo (Ohuchi et al., 2000). To test whether BMP7 is alone capable of inducing *FGF10* posterior regions of neuroectoderm were explanted, exposed to hBMP7 and cultured for 20hrs, until the equivalent of 10 somites.

Posterior explants exposed to hBMP7 showed increased *FGF10* staining, indicating higher levels of *FGF10* transcription (Fig.4.5.B, D). This result shows that hBMP7 alone is capable of inducing *FGF10* expression in posterior neuroectoderm, suggesting BMP7 is sufficient to induce pBHyp cells from RDVM cells.

These experiments confirm and extend previous observations to show the importance of BMP7 in the progression of RDVM to pBHyp cells, and show that RDVM-endogenous *BMP7* expression at 4s is sufficient to induce *FGF10* expression as well as the ability of BMP7 to induce *FGF10* expression in regions that would not express it in vivo. However, they suggest that highest levels of *FGF10* expression will occur due to ongoing signalling from an extrinsic source - most likely the prechordal mesoderm. Given my previous observations (Chapter 3) that pSMAD1/5/8 is expressed in RDVM cells from 4 somites, I next asked if continued BMP signalling is required for the progression of RVDM cells to pBHyp cells

As mentioned above Dorsomorphin is a potent inhibitor of canonical BMP signalling via binding of type I BMP receptors. This prevents SMAD1/5/8 phosphorylation and therefore transcriptional regulation of downstream targets. If *FGF10* is a target of pSMAD1/5/8 transcriptional activation then treatment with Dorsomorphin should reduce transcription levels and therefore staining.

To test if anterior explants are reliant on type 1 BMP receptor signalling for *FGF10* induction they were cultured in the presence of Dorsomorphin for 20rs until the equivalent of HH10. Dorsomorphin treatment reduced *FGF10* staining of explants, indicating a lower level of *FGF10* expression, relative to control explants that were unexposed (Fig.4.5.A, E). This result suggests that type 1 BMP receptor signalling is necessary for *FGF10* induction/maintenance in RVDM explants.

Control Anterior

A 2/3

Control Posterior

B 3/3

BMP Anterior

C 4/4

BMP Posterior

D 4/4

Dors Anterior

E 1/3

FGF10

200µm
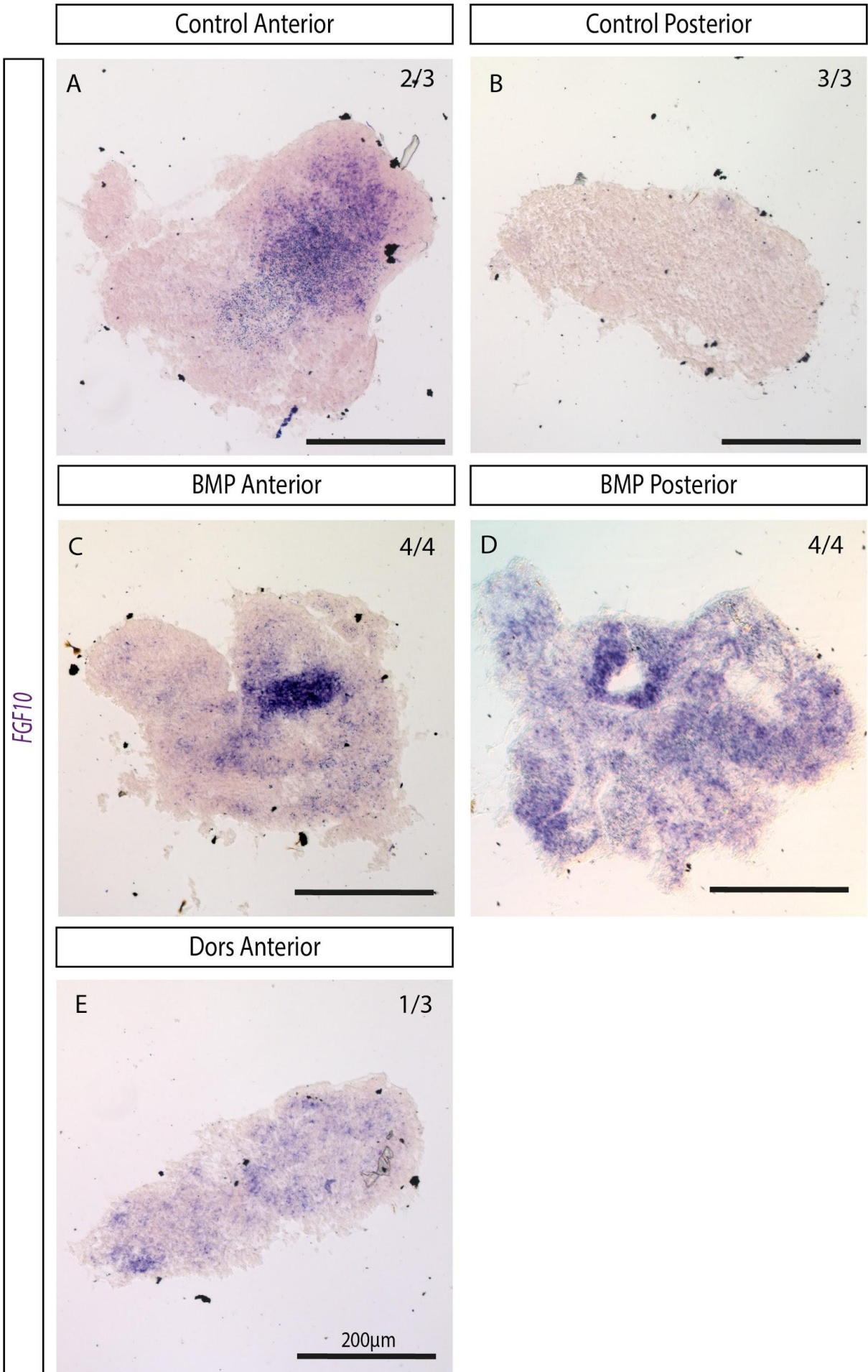
Figure 4.5: Anterior explants autonomously upregulated *FGF10* in vitro compared to posterior explants, explants exposed to hBMP7 upregulate *FGF10* more strongly compared to control explants and explants exposed Dorsomorphin fail to properly upregulate *FGF10*. A) Anterior control explants upregulte *FGF10* in vitro n=2/3. B) Posterior explants fail to upregulate *FGF10* n=3/3. C) Anterior explants exposed to hBMP7 upregulate *FGF10* more stongly compared to anterior control explants n=4/4. D) Posterior explants exposed to hBMP7 upregulate *FGF10* more strongly than control posterior explants n=4/4. E) Most anterior explants exposed to Dorsomorphin show less *FGF10* expression than control anterior explants, n=1/3 upregulated *FGF10*.

4.3. Discussion

My results in this chapter show that endogenous BMP expression, detected in RVDM cells from 4s, is capable of upregulating *FGF10* in an ex vivo culture system. They also show that BMP signalling is necessary for *FGF10* upregulation. Finally, they demonstrate that exogenous hBMP7 is capable of increasing the OD of *FGF10* staining in anterior and posterior explants.

These results taken together suggest a model in which PM-derived BMP7 initially induces its own expression in RVDM cells; BMP7 from RDVM cells then acts together with BMP7 from the PM to induce highest levels of *FGF10*. I find that pSMAD1/5/8 and *FGF10* are sensitive to the levels of BMP: higher levels of BMP induce more pSMAD1/5/8 and higher levels of *FGF10* expression. In Chapter 3, I showed that pSMAD1/5/8 and *FGF10* are not expressed uniformly along the A-P extent of pBHyp cells, but are detected at highest levels in the centre of the pBHyp domain. Why might the central part of the pBHyp domain encounter highest levels of BMP signalling?

Previous studies have shown that the PM defines the extent and limits of pBHyp cells:

FGF10 expressing pBHyp cells are detected as a fan-shaped population, that are immediately

dorsal to the fan-shaped PM (Fu et al., 2017). However, as shown in previous studies

(Adelman, 1922) and my own work in Chapter 3, at its anterior end, the PM merges with the

underlying gut tube, and here, opposes the surface ectoderm. I suggest that there is a

gradient of expression of BMP in RDVM cells and the PM/PME, with the highest levels

posteriorly. The posterior RDVM and PM/PME regions is anterior to *CHRD+* ventral midline

cells and NOG+ notochord, respectively, and this BMP signalling inhibition results in the

highest levels of pSMAD1/5/8 in the central part of the RDVM/pBHyp domain, further from

the source of extracellular BMP inhibitors. I suggest that these high levels then act on cells to

induce highest levels of *FGF10* (Fig.3.6). Double or triple fluorescent in situ hybridisation and

optical clearly could allow a thorough investigation of the spatial relationship between

FGF10, *BMP2*, and *BMP7* as well as inhibitors of BMP signalling such as *CHRD* to test this

model and begin to shed light on the in vivo requirement of different BMPs and signalling

sources in the fine control of *FGF10* expression in pBHyp induction. Analysis of CHRD protein

distribution compared to pSMAD1/5/8 would also add weight to CHRD being the posterior

limiting factor in pBHyp induction. Adding weight to this possibility is the observation that

pBHyp cells cultured ex vivo with CHRD fail to upregulate NKX2.1 and instead express FOXA2,

a marker of the floor plate posterior to pBHyp cells, (Manning et al., 2006).

One additional future experiment would be to examine the effect of Dorsomorphin in vivo

requirement, to ask whether BMP signalling is required for *FGF10* induction in vivo. However

there are issues with using Dorsomorphin as an inhibitor in vivo that pose less of an issue ex

vivo. Dorsomorphin has been shown to have several off-target effects, including inhibition of

Vascular Endothelial Growth Factor (VEGF) and AMP-activated protein kinase (AMPK)

signalling (Hao et al., 2010; Zhou et al., 2001), which could lead to unknown outcomes. An

alternate approach would be to use a more selective pharmacological BMP type 1 receptor

inhibitor such as LDN-193189 (Cuny et al., 2008) or an endogenous inhibitor such as CHRD.

These however would not test the requirement for canonical BMP signalling. To do this one

would have to either knock out R-SMADs simultaneously in RDVM cells which, if R-SMADs

are necessary, would lead to a failure to induce *FGF10*. The converse experiment would be

electroporating in a constituently active R-SMAD/R-SMADs into pre-RDVM cells prior to

BMP7 expression in the PM, explanting the region and electroporated cells should

upregulate *FGF10* if R-SMAD/R-SMADs is/are sufficient. Given the large amount of

modification sites within SMAD linker regions however this is not an ideal solution as

constitutively active SMADs would have to been shown to be able to interact with co-factors

in a similar manner to wild type proteins.

The upregulation of FGF10 in BMP-expressing RDVM cells (ie the progression of RDVM to

pBHyp cells) means that cells are exposed to these two signals/signalling pathways. What

might be the consequences? BMP and FGF signalling have a complex relationship, varying

from synergistic to inhibitory (Schliermann and Nickel, 2018). In the mouse telencephalon,

BMP4 and FGF8 antagonise each other during the formation of the border between

telencephalic dorsal midline and cerebral cortex (Srinivasan et al., 2014). In zebrafish

posterior neural identity is protected from constitutively active BMP signalling by intracellular inhibition of BMP signalling which is mediated by FGF3 (Koshida et al., 2002).

Explanted rat cortical progenitor cells can be delayed in their development by BMP4 and this effect can be inhibited by FGF2 (Lillien and Raphael, 2000).

Intriguingly, there is emerging evidence that FGF and BMP signalling can co-operate to regulate stem-like cells. In undifferentiated rat foetal neural stem cells, BMP signalling induces dormancy and FGF2 is required to maintain stem cell potency (Sun et al., 2011). BMP signalling has been shown to promote self-expanding stem cell divisions in the chick spinal cord (Dréau et al., 2014). Together these findings suggest a model in which FGF signalling is important for the proliferation and/or potency of neural cells and BMP signalling important to prevent their premature exhaustion. Potentially this is the case in the pBHyp domain. If this is the case dual inhibition of FGF and BMP signalling in vivo would be predicted to cause reduced hypothalamic size through growth arrest and precocious terminal differentiation. Deletion models could elucidate the role of BMPs and FGFs in the hypothalamus in vivo.

To-date, however, no study has genetically removed all relevant FGFs and BMPs. In mouse, *Fgf10* has been deleted, and shown to be necessary for the appropriate maintenance of the infundibulum and Rathke's Pouch: excessive apoptosis occurs in these tissues in the mutants (Ohuchi et al., 2000). However, it is likely that the pBHyp domain forms, since it gives rise to the infundibulum (Pearson et al., 2011), most likely because the mouse also expressed *Fgf8*

in the pBHyp region (Ericson et al., 1998). It seems unlikely that double FGF mutants would be viable so perhaps targeted inhibition and explant culture will continue to be the most fruitful means to dissecting the requirement for FGF and BMP signalling in RVDM and pBHyp cell development. Selectively deleting multiple FGF's in the developing hypothalamus could shed light on their role, however there is a delay in systems such as tamoxifen induced Cre recombination that must be appreciated.

In going forwards, therefore, one route would be to ask whether the combined activity of BMP and FGF signalling is establishing an early stem/progenitor niche - a possibility suggested through earlier work (Fu et al., 2019, 2017; Haan et al., 2013; Robins et al., 2013; see Introduction). However, a second route, and the one that I chose to follow, would be to follow-up on my observations that pSMAD1/5/8 and *BMP7* are not uniformly detected along the A-P extent of the pBHyp region, and are detected at low levels in anterior parts of that region. The reason for focusing on this is that previous work in the lab (Fu et al., 2017) has shown that, almost as soon as they can be detected, pBHyp cells begin to proliferate and give rise to progenitors that grow anisotropically and sequentially (Fig.1.3). The first progenitors to grow out of pBHyp cells are 'anterior' progenitors that grow anteriorly, displacing the FGF10 positive pBHyp domain from telencephalic progenitors (Fu et al., 2017; Fu et al., 2019). It has been shown previously that SHH signalling is required to direct the differentiation of anterior hypothalamic progenitors from the pBHyp population (Fu et al., 2017). Importantly, as anterior progenitors form, SHH itself becomes downregulated from central parts of the pBHyp domain. This downregulation is mediated by BMP signalling, via the induction of *TBX2/3* which act as transcriptional repressors of *SHH* (Manning et al., 2006,

Trowe et al., 2013). These studies, together with the model I propose here (Fig.1.3) suggest that a pSMAD1/5/8 or *BMP7* prepattern in pBHyp cells predicts and prefigures the next step in their development - namely the transition of a pBHyp domain where all cells co-express SHH, *FGF10* and pSMAD1/5/8 (at 10 somites), to a domain where SHH is restricted to anterior regions, and downregulated centrally, and conversely, where *BMP7* and pSMAD1/5/8 are detected centrally/posteriorly. In the next chapter I will detail my work on investigating the expression of pSMAD1/5/8, SHH and markers of emerging anterior progenitors over the period 10 to 20 somites.

Chapter 5:

BMP2, *BMP7* and pSMAD1/5/8 are not expressed in emerging anterior progenitors

5.1. Introduction

As described at the end of Chapter 4, studies in chick show that, once induced, pBHyp cells almost immediately begin to differentiate. They do so in a spatially organised manner, generating so-called 'anterior' progenitors - ie progenitors that downregulate *FGF10* and grow anteriorly from *FGF10+* pVT cells that are themselves retained.

Currently, anterior progenitors have not been well-characterised. Studies in chick show that anterior progenitors upregulate SHH and *p57* as they emerge from *FGF10* positive pBHyp cells (Fu et al., 2017). Other studies have shown expression of Notch components in cells that occupy a crescent-shaped domain in a region that may be equivalent to that occupied by pAnt cells (Fu et al., 2017; Ratié et al., 2013), but currently no study has determined whether these are indeed anterior progenitors. Similarly, in mice and zebrafish, progenitors that may be equivalent to anterior progenitors express the paired TF, *Rax* (or its homologue *rx3*) and the HD TF, Islet 1 (Chuang et al., 1999; Corman et al., 2018; Furukawa et al., 1997;

Lee et al., 2016). However, it is not known if *RAX* and Islet 1 are expressed in chick anterior progenitors that emerge from *FGF10+* pBHyp cells.

Here I set out to ask 2 questions:

- Can I better define anterior progenitors, and their spatial relationship with pBHyp cells?
- Is there evidence for a heterogeneity in pBHyp cells, in terms of BMPs or BMP signalling, as anterior progenitors form?

To address these questions I examined sagittal sections of chick embryos over 10 to 20 somites, the time of emergence of anterior progenitors, and at HH15-16 when there are committed anterior cells (Fu et al., 2017).

5.2. Results

During anterior progenitor emergence the neural tube continues to fold

Before analysing expression of particular genes, I analysed the morphology of the neural tube and surrounding structures.

From 14 somites, the primordium of the anterior pituitary, Rathke's Pouch (RP), becomes visible as the ectodermal placode thickens, invaginates and extends posteriorly/dorsally (Fig.5.1.A-C). As this happens, a pouch-like structure, the mammillary pouch (MP) begins to form just posterior to the tip of RP (Fig.5.1.C).
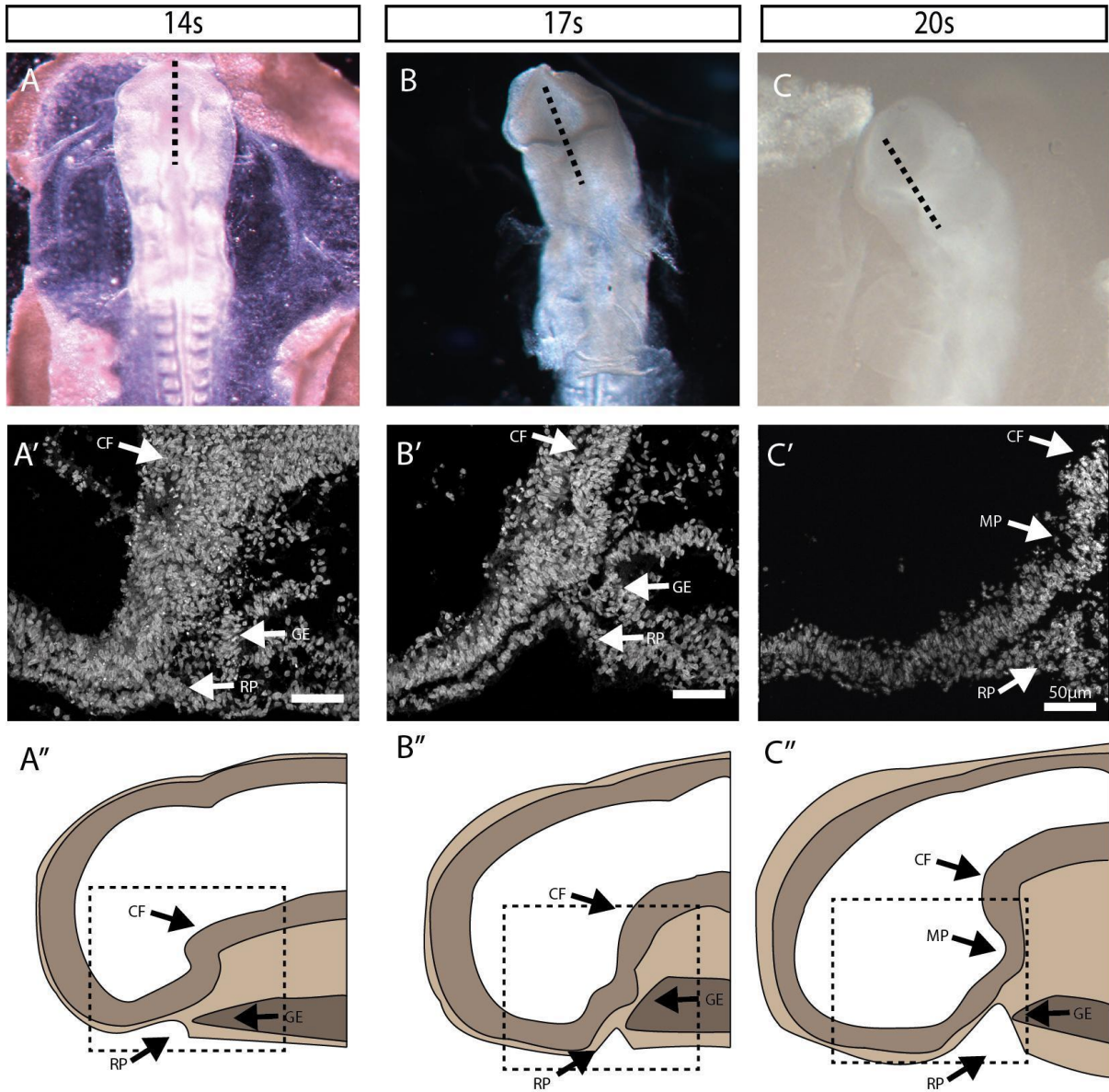
Figure 5.1: Morphology of the neuroectoderm changes somewhat between 14 and 20s. A,B,C) Wholemount view of embryos, line indicates the position of the sagittal section shown in (A',B',C'), represented schematically in (A'',B'',C''). A-A'') . At the 14s stage the rudimentary Rathke's Pouch is thickening (RP, A''). B-B'') By 17s (~4.5hrs after 14s) RP begins to invaginate. The Cephalic Flexure (CF) becomes more prominent. C-C'') By 20s (~4.5hrs after 17s) RP forms a finger like protrusion underneath the ventral tuberal hypothalamus, the CF has further curved in the ventral neuroectoderm making it very apparent. The Mammillary pouch (MP) begins to form as an out pocketing of neuroectoderm. During this period the anterior gut ectoderm (GE) maintains a close relationship to the developing RP. CF, cephalic flexure, GE, gut ectoderm, MP, Mamillary Pouch, RP, Rathke's Pouch.

pSMAD1/5/8 is expressed in the *FGF10+* domain as anterior progenitor cells emerge

As outlined in the Introduction, *FGF10* positive progenitors begin to give rise to anterior and mammillary progenitors over 10 to 20 somites; however, as they do so, an *FGF10* positive progenitor population persists in the ventral tuberal hypothalamus, lying immediately above RP (Fig.5.2.A: from Fu et al., 2017). The posterior extension of RP occurs simultaneous with the emergence of anterior progenitors from *FGF10* positive pBHyp cells (Fu et al., 2017). Therefore, by HH15, *FGF10* positive pBHyp descendants lie above RP (Fig.5.2.A red arrowheads) and emerging anterior hypothalamic progenitors lie anterior to RP (Fig.5.2.A, yellow arrowheads). I next examined the profile of pSMAD1/5/8 at this stage. My analyses reveal that pSMAD1/5/8 is expressed in the *FGF10* positive domain: thus expression is confined to the ventral tuberal hypothalamus that lies immediately above RP (Fig.5.2.B). This raises questions as to the pattern of BMPs themselves over these stages.
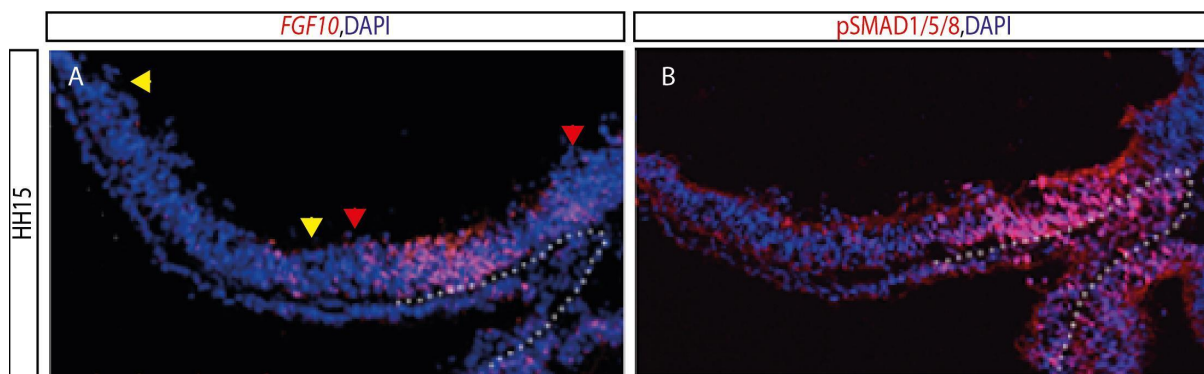
Figure 5.2: pVT cells are *FGF10+* and pSMAD1/5/8+. At HH15 both *FGF10* (A) and pSMAD1/5/8 (B) are localised to pVT (red arrowheads), lying above Rathke's Pouch (Dotted outline), posterior to the pAnt region (yellow arrowheads).

BMP2 and *BMP7* continue to segregate during anterior progenitor emergence

To examine this, I profiled the expression of *BMP2* and *BMP7* as well as the inhibitors *CHRD* and *NOG* over 14s-20s, i.e during anterior progenitor specification.

At 14 somites *BMP2* is expressed in a region overlying the rudimentary Rathke's Pouch, extending posteriorly to the cephalic flexure. This profile suggests that at 14 somites, *BMP2* prefigures the future pSMAD1/5/8+ *FGF10+* ventral tuberal hypothalamus (Fig.5.3.A). Notably, there is a difference in expression along the anterior-posterior axis, with weak *BMP2* expression detected anteriorly, and stronger expression detected posteriorly (Fig.5.3.A). *BMP2* is also detected in the telencephalon, but what is clear is that there is a *BMP2* negative area, between the telencephalic and hypothalamic expression: its position, anterior to RP, suggests that this region is likely to contain emerging anterior progenitors (Fu et al., 2017). Expression of BMP2 is, however, highly dynamic and over 17s-20s, BMP2 appears to be downregulated in the ventral tuberal hypothalamus, and is now detected in cells at the telencephalic-hypothalamic boundary, and the mammillary pouch of the posterior hypothalamus (Fig.5.3.F,K). *BMP7* at 14s is expressed only in a posterior subset of pVT cells, close to the cephalic flexure (Fig.5.3.B), and at 17s-20s, is detected in the posterior mammillary pouch, and in cells posterior to this. This dynamic pattern of expression of *BMP2* and *BMP7* suggests that the functions of BMP2 and BMP7 are not redundant. Over the period 14s-20s neither *CHRD* nor *NOG* is expressed in hypothalamic progenitors (Fig.5.3.C,D,I,J,O,P).

In summary, I draw three conclusions. First, the BMP inhibitors *CHRD* and *NOG* are not expressed in the developing hypothalamus from 10s to 20s, confirming that BMPs themselves are likely to contribute to the pSMAD1/5/8 expression detected (Fig.5.2.B). Second, at 14 somites, BMP2 appears to predict the pSMAD1/5/8+ FGF10+ ventral tuberal hypothalamus. Third, by 20 somites, when pAnt cells are forming, BMPs appear to be expressed distal to the FGF10+ domain: BMP2 anterior-distally and BMP7 posterior-distally.

BMP2 | BMP7 | CHRD

A 3/3 | B 2/2 | C 3/3

F 2/2 | G 2/2 | H 3/3

K 1/1 | L 2/2 | M 2/2

NOG

D 3/3 | E

I 2/2 | J

N 1/1 | O

BMP2

BMP7

BMP2/7

CHRD+BMP7

14s
17s
20s
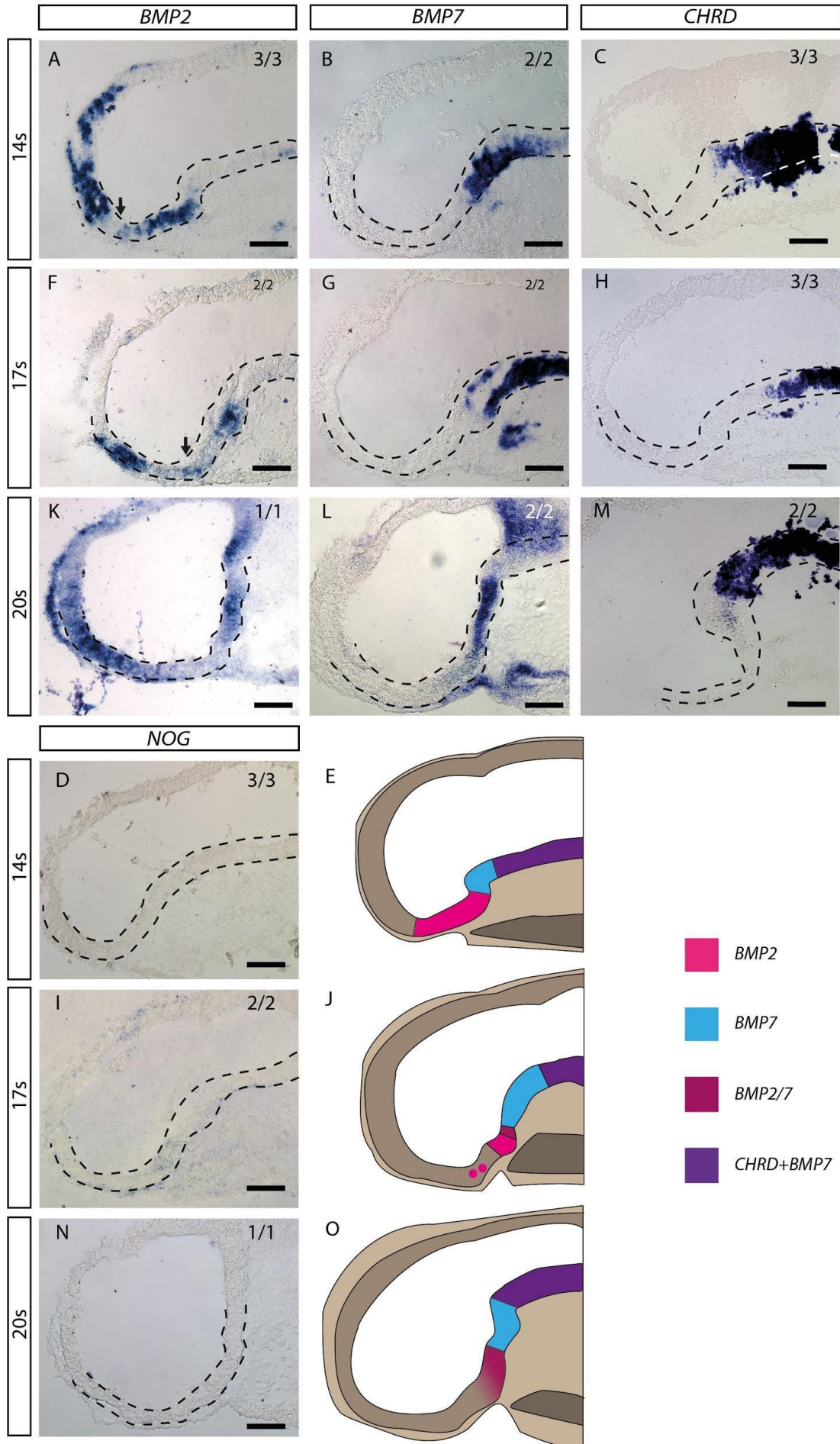
Figure 5.3: *BMP2* and *BMP7* continue to segregate during pAnt emergence. A) *BMP2* is expressed in ventral tuberal hypothalamus at 14s, is not detected in emerging pAnt cells (arrow), and is then detected in the telencephalon. B) At 14s *BMP7* is expressed in the posterior pVT cells and appears not to be coexpressed with *BMP2*. C-D) *CHRD* and *NOG* are not expressed in the developing hypothalamus at 14s. E) Schematic summarising A-D. F) At 17s, *BMP2* expression is detected weakly in pVT cells above RP (arrow) and a large *BMP2* negative region is present between hypothalamic and telencephalic expression. G) Anterior *BMP7* expression partially overlaps with *BMP2* posterior expression. H-I) *CHRD* and *NOG* are not expressed in the developing hypothalamus at 17s. J) Schematic summarising F-I. K) At 20s, *BMP2* expression is detected in the mammillary pouch and telencephalon. L) *BMP7* expression extends from the mammillary pouch, more posteriorly, suggesting coexpression with *BMP2*. M-N) *CHRD* and *NOG* are not expressed in the hypothalamus at 20s. O) Schematic summarising L-O**.**

At pBHyp induction pSMAD1/5/8 is co-expressed with SHH however during anterior progenitor emergence they refine to distinct progenitor subsets

The observation that pSMAD1/5/8 and *FGF10* occupy the same domain of the ventral tuberal hypothalamus led me to hypothesise that pSMAD1/5/8 will not be detected in emerging anterior progenitors. To test this I simultaneously analysed markers of the anterior region and pSMAD1/5/8.

Initially I analysed the relationship between pSMAD1/5/8 and SHH, a signalling factor that is initially expressed throughout pBHyp but quickly becomes confined to anterior and mammillary progenitors during development between 10s and 20s (Manning et al., 2006, Fu et al., 2017). At 10s, SHH is expressed throughout pBHyp cells; additionally, expression extends posteriorly, in floor plate cells (Fig.5.4.A). Double-labelling with pSMAD1/5/8 shows that at 10s, SHH and pSMAD1/5/8 show the same anterior limits. This confirms previous observations (Fig.3.4 and Fu et al., 2017), where double-labelling showed that both

pSMAD1/5/8 and SHH abut *FOXG1+* telencephalic progenitors. However, double-labelling reveals that the overlap is transient, and by 14s SHH is now expressed more anteriorly than pSMAD1/5/8 (Fig.5.4.B). By 17s SHH is beginning to be downregulated in pVT cells lying over Rathke's pouch (Fig.5.4.C; Manning et al., 2006). The SHH-negative territory correlates with pSMAD1/5/8 localisation (Fig.5.4.C). At 20s and continuing to HH16 there is a clear distinction between the anterior SHH-positive region and the ventral tuberal SHH-negative region. Further, a region which is both SHH negative and pSMAD1/5/8 negative appears to be detectable (Fig.5.4.D[IV] between the red and green lines; Fig.5.5).

In summary, my studies show that as pBHyp cells generate anterior progenitors and themselves persist as *FGF10+* pVT cells, pSMAD1/5/8 becomes confined to the *FGF10+* pVT cells while SHH is detected in emerging pAnt cells. Other studies have shown that at 7-20s, there is a small overlap in SHH and *FGF10* expression at the pVT/pAnt boundary (Manning et al., 2006). I do not detect an overlap of SHH and pSMAD1/5/8 at 20s, but instead detect a gap between SHH and pSMAD1/5/8 that persists until HH16. Potentially, therefore, pSMAD1/5/8 is restricted to posterior parts of the *FGF10+* ventral tuberal domain.
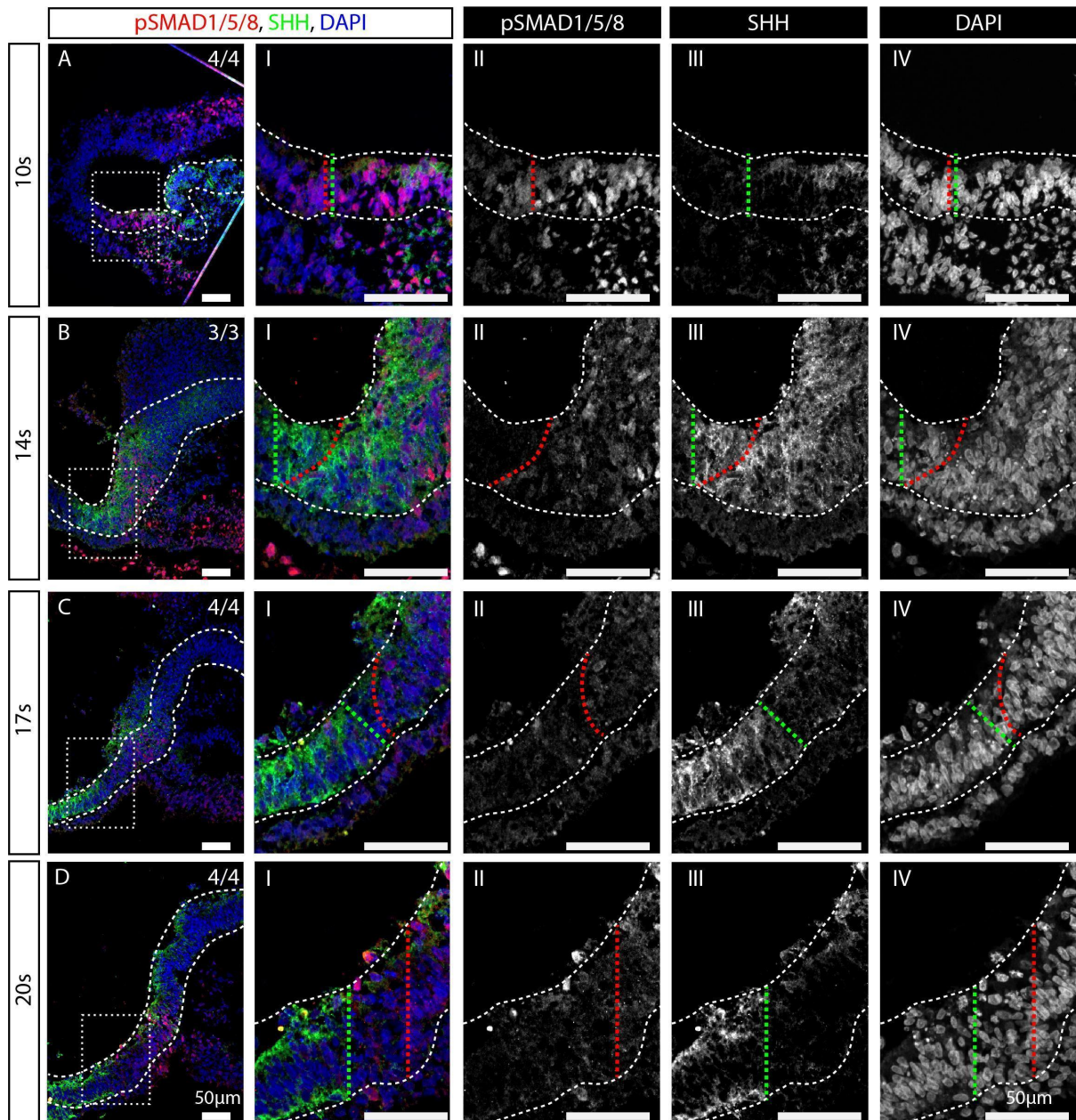
Figure 5.4: SHH is co-expressed with pSMAD1/5/8 at 10s but is downregulated in pSMAD1/5/8+ cells by 20s. A-D) Red line denotes anterior pSMAD boundary. A-B) Green line denotes SHH's anterior limit. C-D) Green line indicates anterior hypothalamic SHH's posterior limit. A) At 10s pSMAD1/5/8 is co-localised with SHH with a similar anterior limit. B) By 14s SHH is expressed in a region anterior to pSMAD1/5/8. C) SHH downregulation begins in the pSMAD1/5/8 domain at 17s. D) By 20s there is clear SHH positive anterior progenitor domain and a SHH negative ventral tuberal progenitor domain. There is now a region which is both SHH negative and pSMAD1/5/8 negative (IV, between the lines).
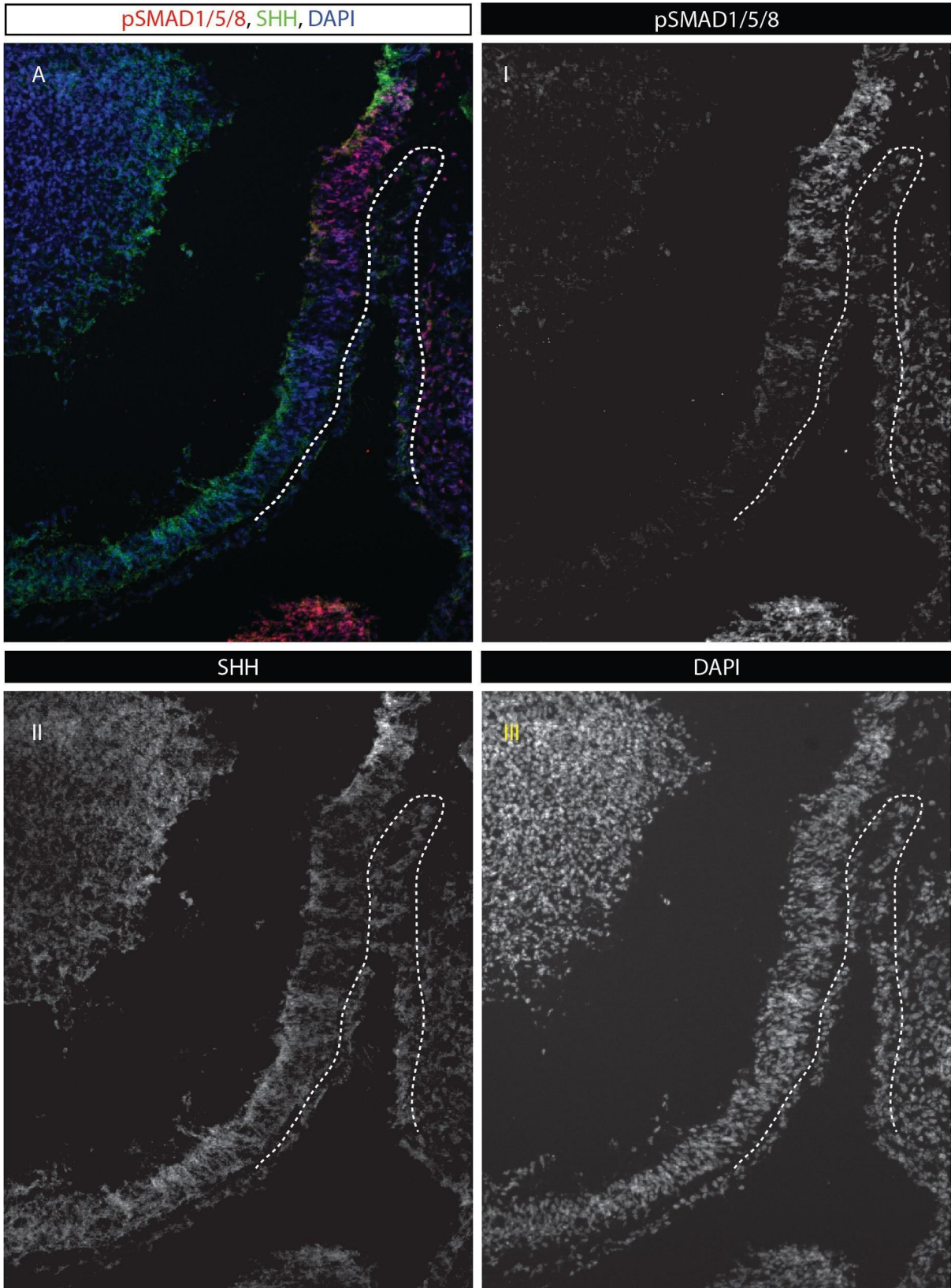
Figure 5.5: At HH16 there is a clear SHH- pSMAD1/5/8- region. Between the SHH+ pAnt region and the pSMAD1/5/8+ pVT region there is a SHH- pSMAD1/5/8- region. A-III) Multichannel view followed by, pSMAD1/5/8, SHH, and DAPI, respectively.

TBX2 is expressed in pBHyp cells and partially overlaps with pSMAD1/5/8

Previous studies have shown that BMP7 mediates the downregulation of SHH in the tuberal region, via *TBX2/Tbx3* (Manning et al., 2006; Trowe et al., 2013). My results clearly implicate pSMAD1/5/8 as the intracellular transducer mediating *TBX*2/*Tbx*3 upregulation and hence SHH downregulation in pVT cells. If this is the case, I hypothesise that pSMAD1/5/8 localisation will predict *TBX2* expression. I tested this by performing in situ hybridisation for *TBX2* followed by immunofluorescence for pSMAD1/5/8.

My results showed a close spatial relationship between pSMAD1/5/8 and *TBX2* at 10s and 14s (Fig.5.6.A-B). However, I failed to detect pSMAD1/5/8 in its normal pattern at 10 somites: there appeared to be a gap in its expression (panel IV). This gap correlated exactly with the *TBX2*-expressing domain. I therefore conclude that the in situ protocol in some way interfered with the immunohistochemical analysis. Thus, I was unable to conclude the precise spatial relationship of pSMAD1/5/8 and *TBX2.* This caveat applies to all other in situ hybridisation followed by immunofluorescence in this chapter.
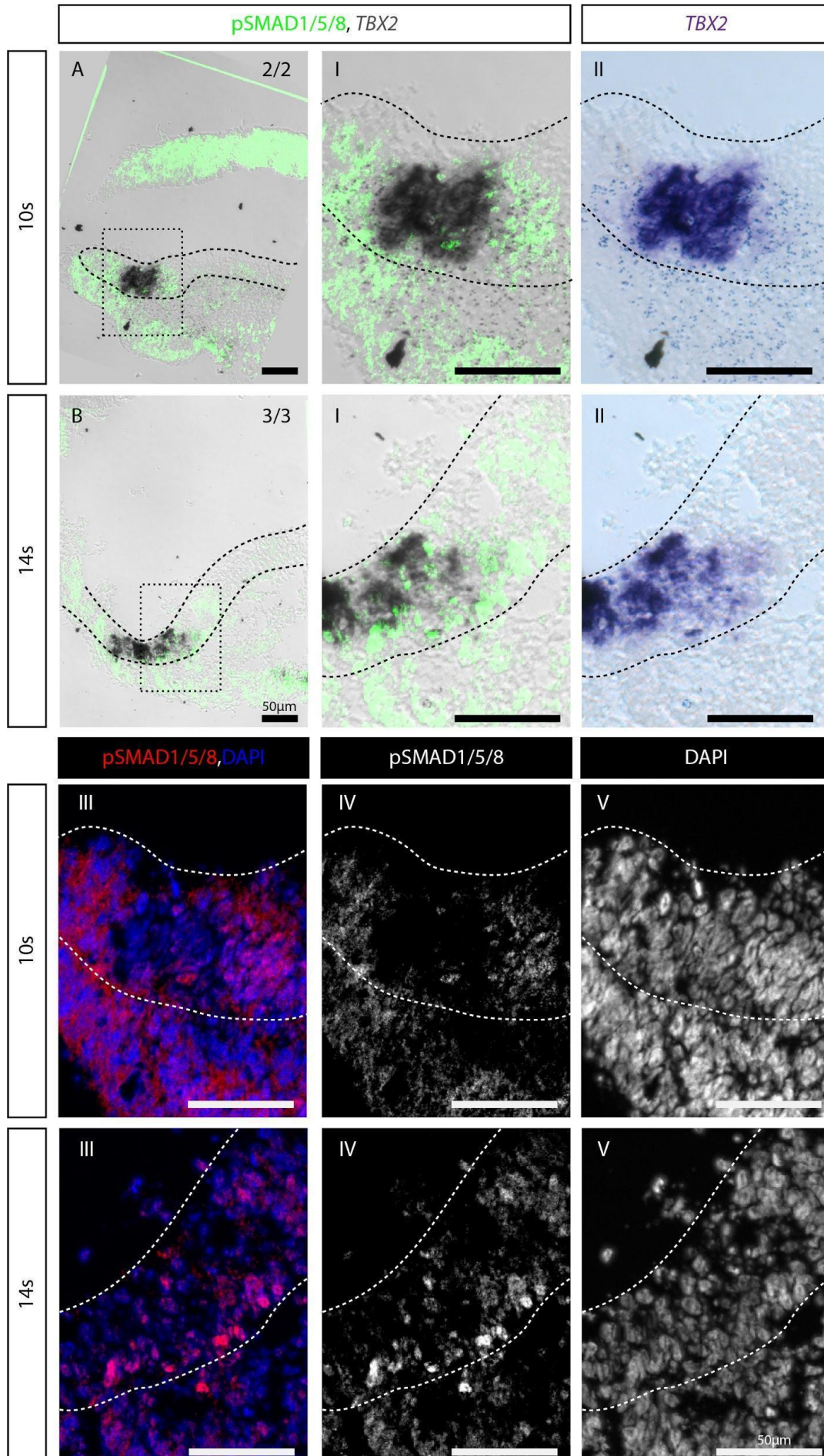
Figure 5.6: *TBX2* is expressed in the pBHyp region, and then in pVT cells. *TBX2* would be expected to overlap with pSMAD1/5/8 at both 10s and 14s. A'-A''''',B'-B''''') High power images of the area boxed, chromogenic in situ, immunofluorescence, pSMAD1/5/8, and DAPI images, respectively.

Hypothalamic progenitor marker *RAX* becomes restricted to anterior ventral tuberal and anterior progenitors

RAX is a transcription factor expressed in the developing eye and forebrain in chick (Ohuchi

et al., 1999). It is widely conserved, and a Rax homologue is expressed in similar regions in

mouse and zebrafish (Chuang et al., 1999; Shimogori et al., 2010). In the hypothalamus

Rax/rx3 has been shown to be necessary for the proper specification of anterior and

'tuberal' hypothalamic cell types (Lu et al., 2013; Muthu et al., 2016). According to the

anisotropic growth model these cell types originate from pAnt cells (Section 1.2.3). However,

as yet no study has profiled the expression of chick *RAX* during the period of pAnt

emergence.

At 10s *RAX* is widely detected. Expression extends from the cephalic flexure, through the

pBHyp domain and into the presumptive telencephalon (Fig.5.7.A). Double labelling of *RAX*

and pSMAD1/5/8 (in situ followed by immuno) shows that *RAX* is expressed more widely

than pSMAD1/5/8 (Fig.5.7.A.I-V). By 14s *RAX* expression is greatly reduced and is now

localised to emerging pAnt and anterior pVT cells. Thus expression is largely detected

anterior to pSMAD1/5/8 labelling, albeit with some overlap (Fig.5.7.B). By HH16,

pSMAD1/5/8 and RAX show a similar posterior boundary in pVT cells, but RAX additionally extends into anterior progenitors (Fig.5.8).

pSMAD1/5/8, *RAX*	*RAX*
A 4/4	I	II
B 3/3	I	II

pSMAD1/5/8,DAPI	pSMAD1/5/8	DAPI
III	IV	V
III	IV	V

10s

14s

10s

14s

50μm

50μm
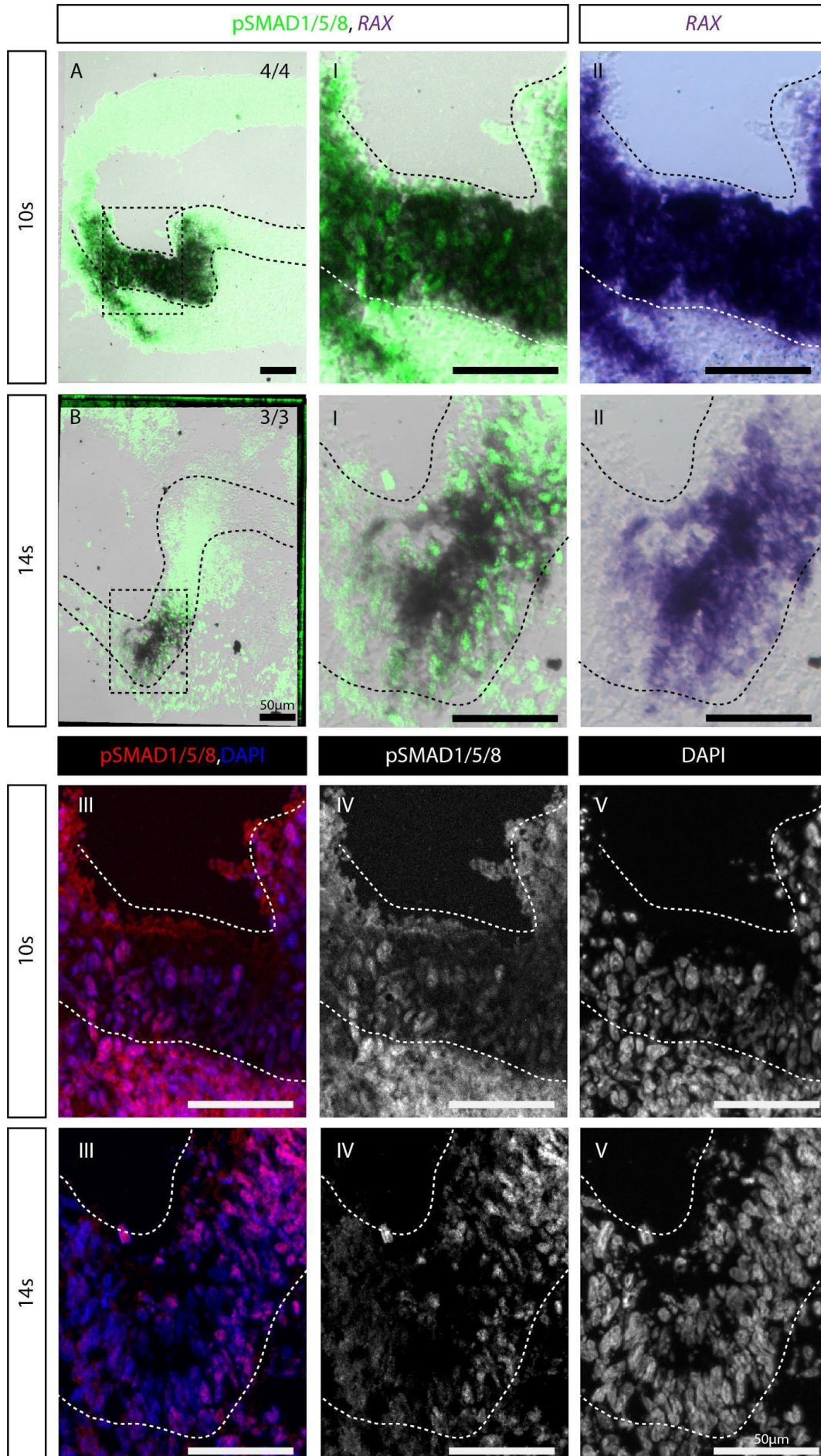
Figure 5.7: *RAX* shows dynamic expression between 10s and 14s. *RAX* expression is dynamic *RAX* is expressed widely at 10s, i.e. overlaps with and extends well beyond the region that expresses pSMAD1/5/8. At 14s, RAX is localised to a region rostral to pSMAD1/5/8 localisation and is weaker in those cells with high pSMAD1/5/8 labelling. A) At 10s *RAX* in situ shows much wider expression than pSMAD1/5/8 immunofluorescence. Those cells that label strongly for pSMAD1/5/8 do appear weaker for *RAX* staining. B) By 14s *RAX* is expressed in cells anterior to strong pSMAD1/5/8 labelling. A'-A''''',B'-B''''') show high-powerimage of the area boxed, chromogenic in situ, immunofluorescence, pSMAD1/5/8, and DAPI images, respectively.
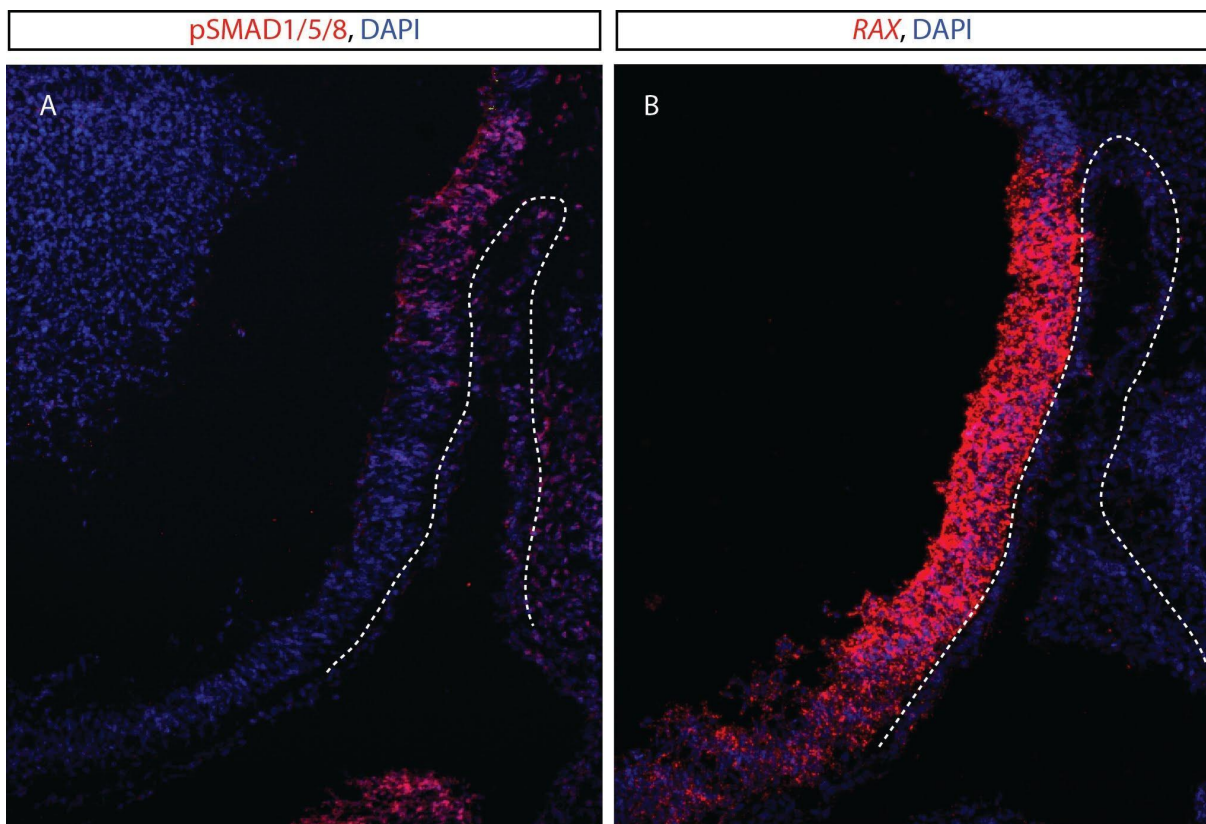
Figure 5.8: At HH16 *RAX* is present within anterior and ventro-tuberal regions, overlapping with pSMAD1/5/8 localisation. A) pSMAD1/5/8 is present within ventro-tuberal cells. B) *RAX* is present within a region overlying Rathke's Pouch and extends anteriorly into posterior anterior hypothalamic progenitors.

ASCL1 appears to mark cells that are differentiating from pBHyp to anterior progenitors

ASCL1 is a proneural transcription factor that is also involved in progenitor proliferation (Castro et al., 2011). Previous studies in the chick have shown that it is detected in a crescent-shape set of cells in the ventral diencephalon at 20 somites (Ware et al., 2014). Anterior progenitors, characterised by their expression of SHH and p57, are detected in a similar crescent-like domain (Fu et al., 2017). Therefore, ASCL1 is potentially a marker of early anterior progenitor cells and may be involved is the progression of pBHyp progenitor cells to a more specified, pAnt neuronal fate. The relationship between pSMAD1/5/8 and *ASCL1* could provide insight into the mechanisms that lead to the specification of anterior progenitors, and I therefore performed double label studies of ASCL1 and pSMAD1/5/8

At 10s *ASCL1* is already detected in the pBHyp domain. Expression is confined to the most anterior parts of the pBHyp domain, ie to regions that express low levels of pSMAD1/5/8: thus *ASCL1* is detected anterior to cells that express high levels of pSMAD1/5/8 localisation (Fig.5.9.A.I-V). This relationship is still obvious at 14s: *ASCL1* is detected in anterior progenitors, overlaps with pSMAD1/5/8 in cells at the junction of pAnt/pVT cells, and is not detected in pVT cells that show high pSMAD1/5/8 labelling (Fig.5.9.B.I-V).

Together, this profile suggests that *ASCL1* is an early marker of progenitor cells that are progressing from a pBHyp identity to a pAnt identity.

pSMAD1/5/8, *ASCL1*

ASCL1

pSMAD1/5/8, DAPI

pSMAD1/5/8

DAPI

10s

14s

10s

14s

A 4/4

B 6/6

I

I

II

II

III

III

IV

IV

V

V

50μm

50μm
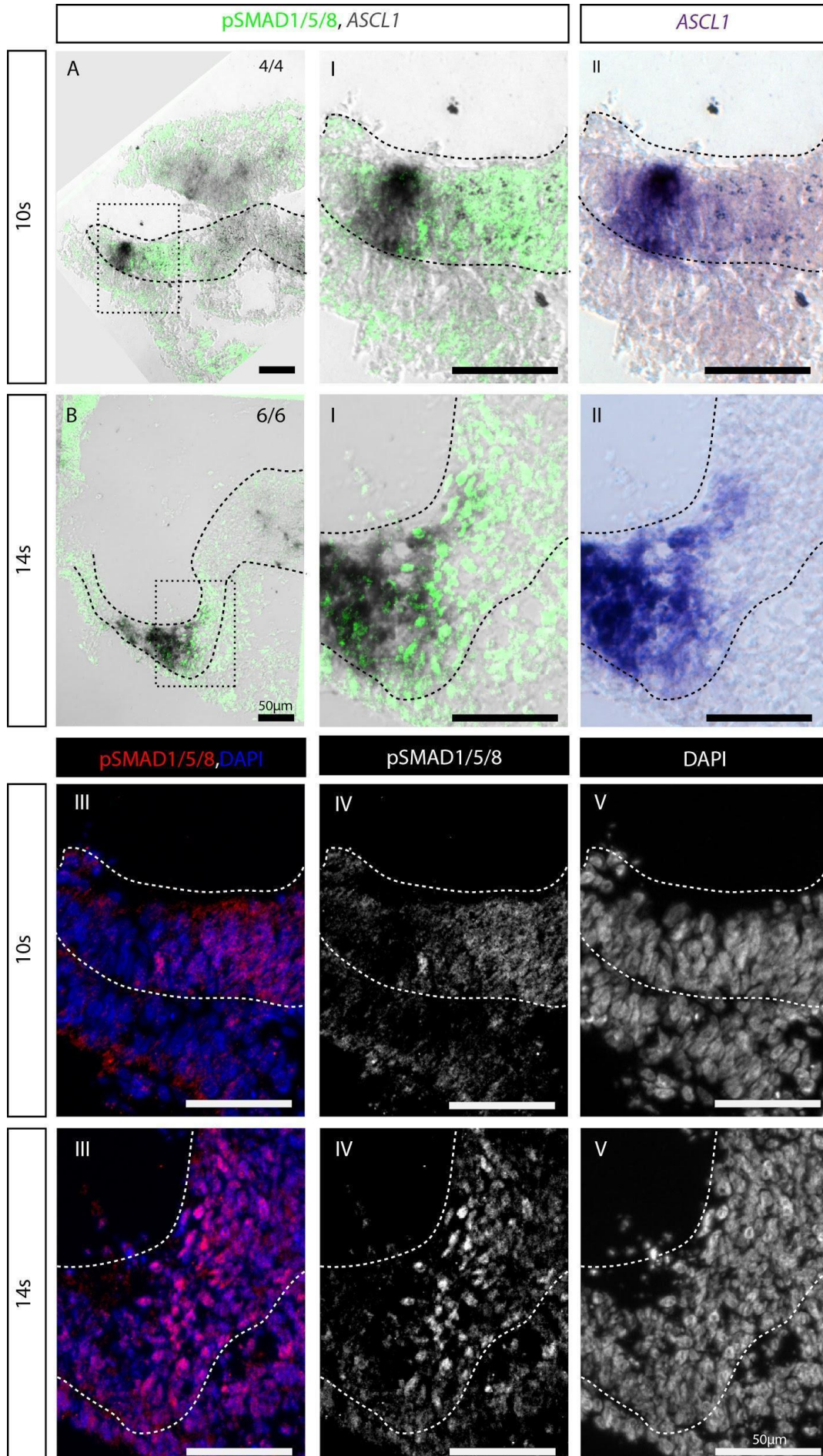
Figure 5.9: *ASCL1* and pSMAD1/5/8 show complementary profiles: *ASCL1* is expressed where there is weak/no pSMAD1/5/8 labelling, and vice-versa. A-B) Show expression at 10s and 14s respectively. A[I]-A[IV], B[I]-B[IV]) show high-power images of the area boxed, chromogenic in situ, immunofluorescence, pSMAD1/5/8, and DAPI images, respectively.

ISL1 marks anterior progenitors

ISL1 has been shown to be essential for the proper specification of neurons of the tuberal hypothalamus, including neuropeptide Y and POMC neurons of the Arcuate nucleus (Nasif et al., 2015). Studies in mouse have shown that ISL1 is widely expressed in the ventral anterior hypothalamus, and is likely to be regulated as anterior progenitor cells emerge (Carreno et al., 2017; Orquera et al., 2016). However, as yet, no study has carefully examined its expression relative to pBHyp and anterior progenitor development. I therefore set out to investigate when and where ISL1 is expressed.

At 10s and 14s ISL1 is not expressed in hypothalamic progenitors (Fig.5.10.A-B). By 17s ISL1+ cells begin to be detected in the neuroectoderm rostral to RP and therefore in the pAnt region (Fig.5.10.C). These cells shown no pSMAD1/5/8 labelling and upregulate ISL1 in a region distant to the pSMAD1/5/8-expressing pVT cells. ISL1+ cell differentiation begins around 17s then proceeds rapidly, so that at 20s there are many more ISL1 +ve cells in the pAnt domain. These cells show a similar distribution to SHH at HH16 (Figure.5.11).

These results show that ISL1 is upregulated in cells occupying the anterior region and that are no longer pSMAD1/5/8 +ve. This suggests that one possibility is that ISL1 is inhibited by BMP signalling, as is perhaps the case in the spinal cord. Another possibility (not mutually

exclusive) is that there is only a requirement for early/intermediate levels of BMP signalling in ISL1 cell specification, and that these cells must then escape BMP signalling to progress down their differentiation pathway.
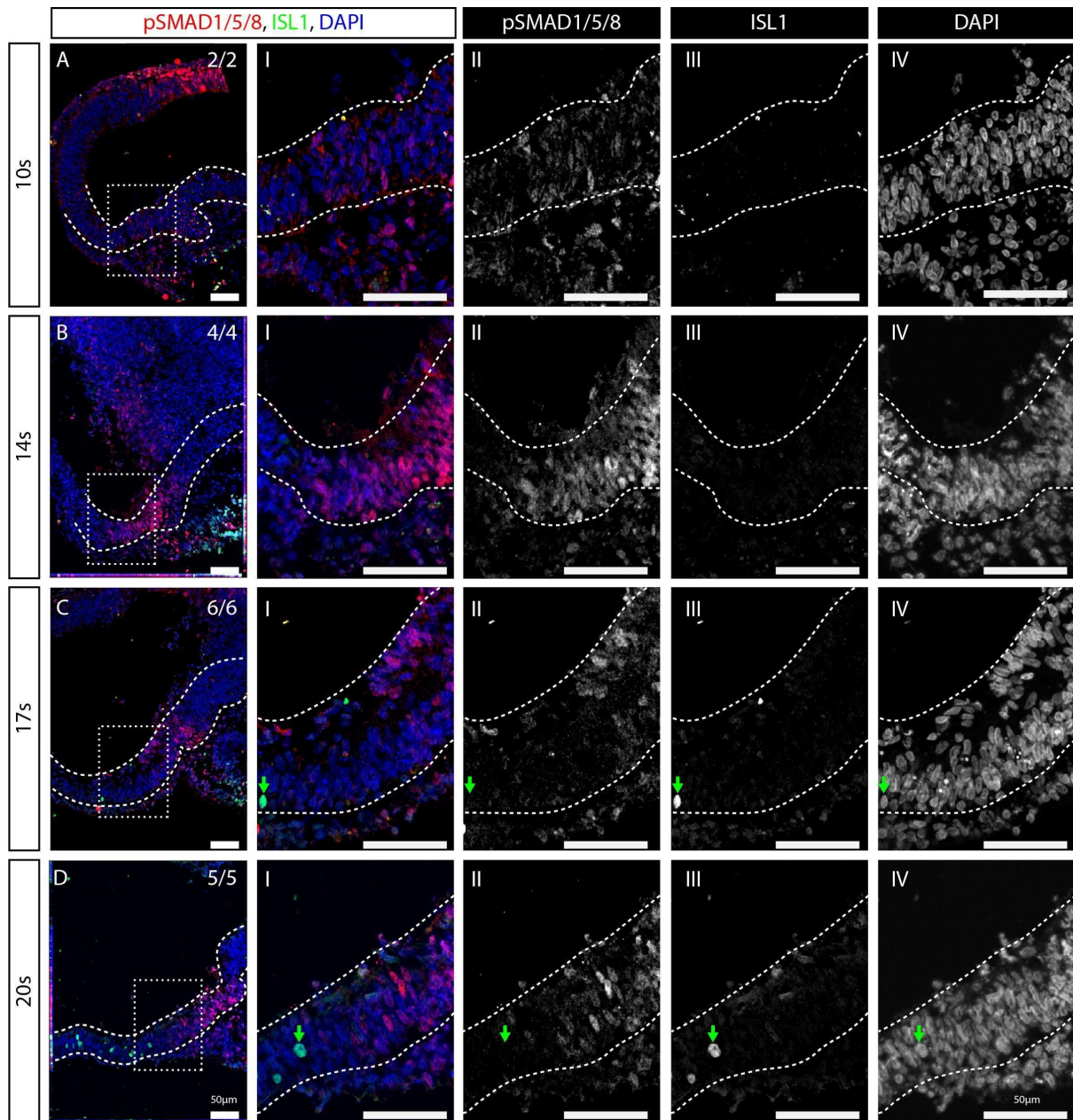
Figure 5.10: ISL1 is upregulated in anterior hypothalamic progenitors that are pSMAD1/5/8 negative. A-B) ISL1 is not expressed in hypothalamic progenitors between 10s and 14s. C) At 17s ISL1 positive cells are localised to the anterior hypothalamus, rostral to R.P. D) ISL1 positive cells populate the growing anterior hypothalamus, and are spatially separate from pSMAD1/5/8 positive progenitors.
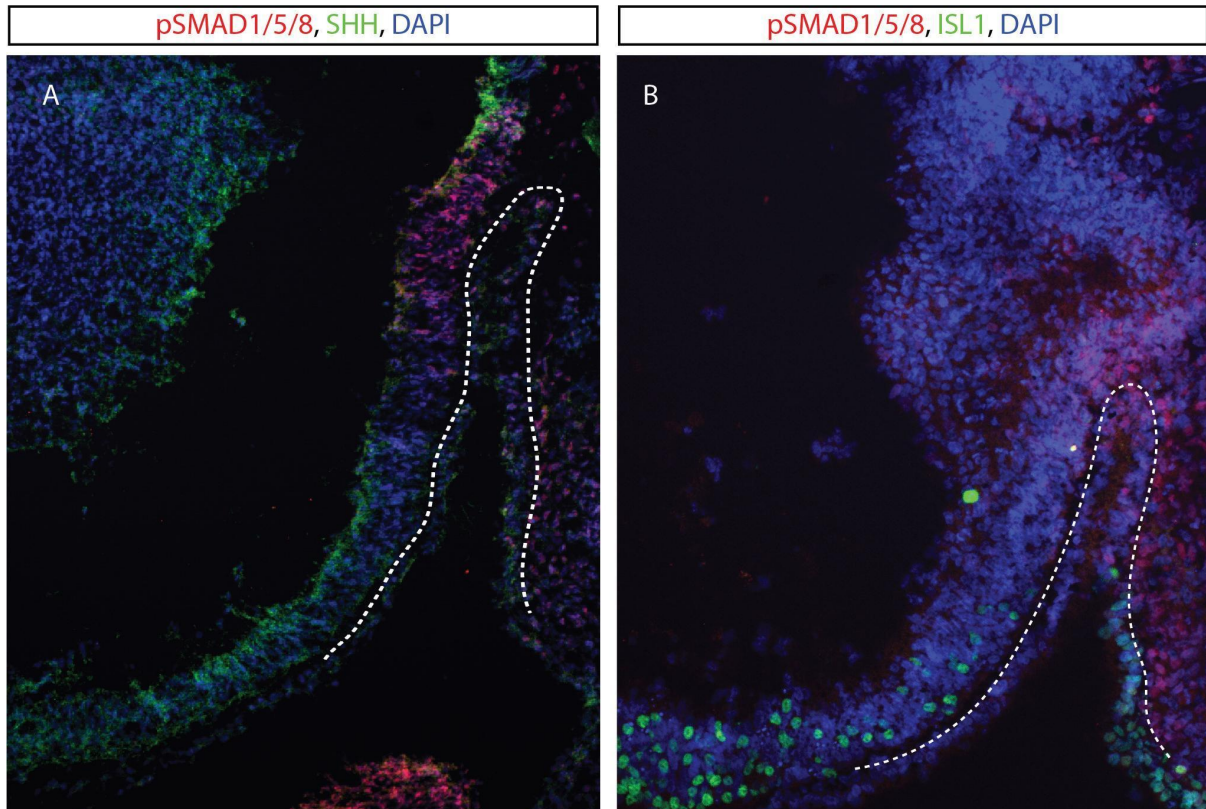
Figure 5.11: At HH16 ISL1+ cells are localised to within the anterior hypothalamic SHH+ region. A-B) SHH (A) and ISL1 (B) is localised to the anterior hypothalamic domain, anterior to the pSMAD1/5/8+ ventro-tuberal domain.

Terminally differentiated progenitors, marked by *p57*, do not co-express pSMAD1/5/8

p57 has been shown to mark the differentiating cells that will give rise to the

suprachiasmatic nucleus and anterior cells of the hypothalamus at 12 somites, based on fate

mapping work (Fu et al., 2017). If it is the case that BMP signalling inhibits anterior

differentiation programmes than there should be no colocalisation of pSMAD1/5/8 with *p57*.

To assess this, I compared the expression of p57 and pSMAD1/5/8.

At 10s no *p57* was detected in pBHyp cells (Fig.5.12.A.I-V). By 14s *p57* +ve cells are detected rostral to the strongly labelled pSMAD1/5/8 positive region (Fig.5.12.B.I-V). There appears to be no colocalisation in the rostral most *p57* positive cells with pSMAD1/5/8, however more caudal *p57* positive cells may show some degree of pSMAD1/5/8 labelling (Fig.5.12.B.I).

These results further suggest there is some degree of separation from pSMAD1/5/8 +ve pBHyp cells and differentiating anterior hypothalamic cells.

pSMAD1/5/8, *p57*		*p57*

10s — A 4/4 | I | II

14s — B 6/6 | I | II (50µm)

pSMAD1/5/8, DAPI	pSMAD1/5/8	DAPI

10s — III | IV | V

14s — III | IV | V (50µm)
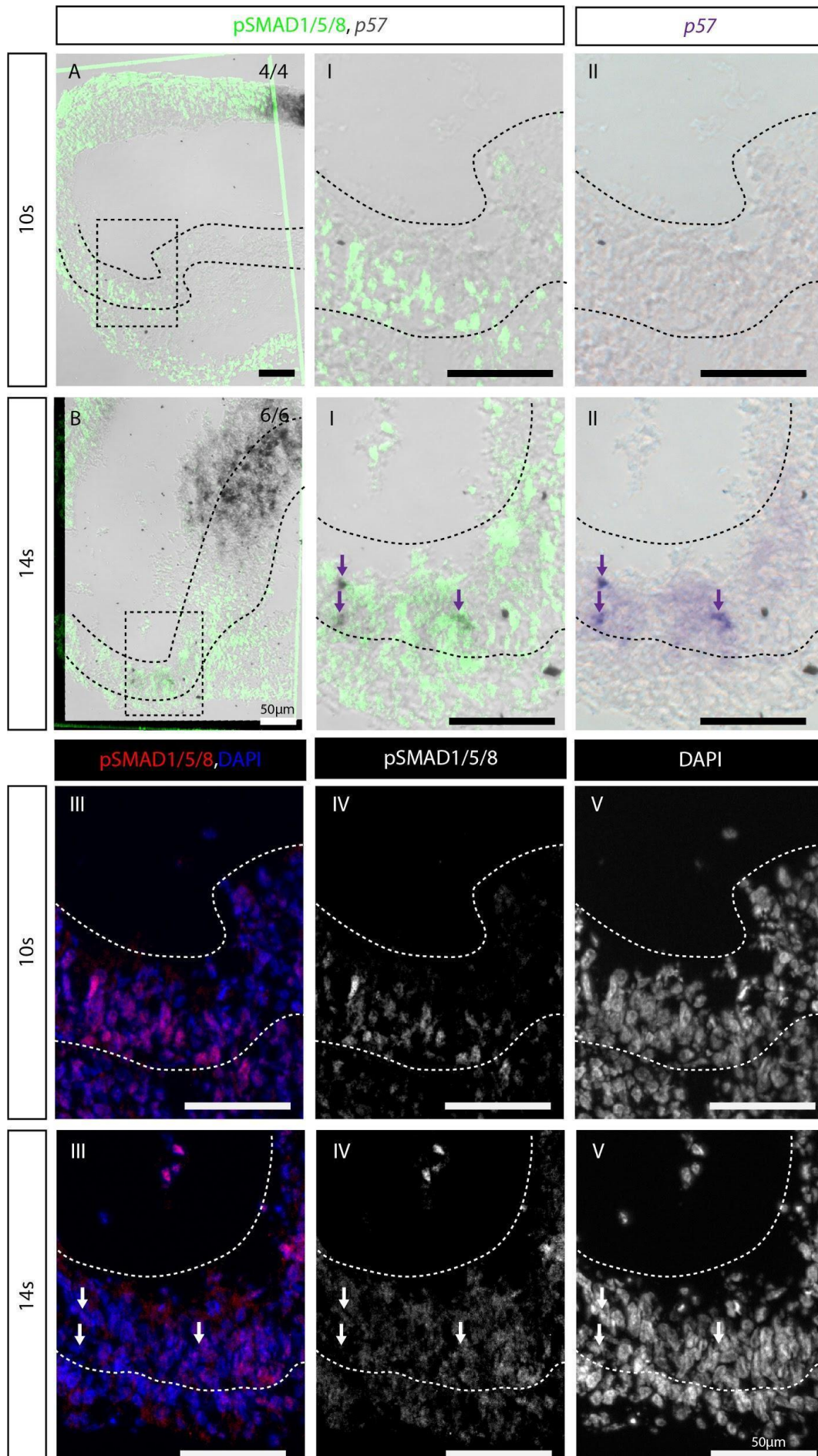
Figure 5.12: pSMAD1/5/8 is excluded from differentiating p57 +ve cells. A) At 10s *p57* is not expressed within pBHyp cells. B) By 14s some *p57* positive cells are present in anterior regions but partially overlapping with pSMAD1/5/8 immunofluorescence at its posterior limit. A'-A''''',B'-B''''') This broken down into a blown up image of the area boxed, chromogenic in situ, immunofluorescence, pSMAD1/5/8, and DAPI images, respectively.

Summary Schematic of the relationship between the BMP family and anterior hypothalamic region emergence

This schematic summarises the expression patterns described in this chapter.

At 10s *RAX* is widely expressed throughout the ventral neuroepithelium (Fig.5.13.A),

whereas pSMAD1/5/8 is confined to pBHyp progenitors in a low high low pattern with the

anterior low region either partially or wholly with *ASCL1*. By 14s anterior progenitors have

emerged and upregulated *p57* and maintained SHH (Fig.5.13.B). There is also a progression

from a pSMAD1/5/8+ *FGF10+* population to upregulation of progressively more specified

identity with upregulation of *RAX* and then *ASCL1.* At 17s there is a downregulation of SHH

in pVT cells (Fig.5.13.C). This is accompanied by a progressive displacement/downregulation

of *BMP2* from anterior progenitors with some cells remaining in the anterior region. By 20s

there is now an anterior region which expresses SHH and ISL1, followed posteriorly by a

SHH- pSMAD1/5/8- region between the anterior and the pSMAD1/5/8+ pVT region

(Fig.5.13.D).

A

B

C

D

	BMP2		BMP2/7		ASCL1		pSMAD1/5/8		ASCL1+TBX2		p57
	BMP7		CHRD+BMP7		TBX2		RAX		SHH		ISL1
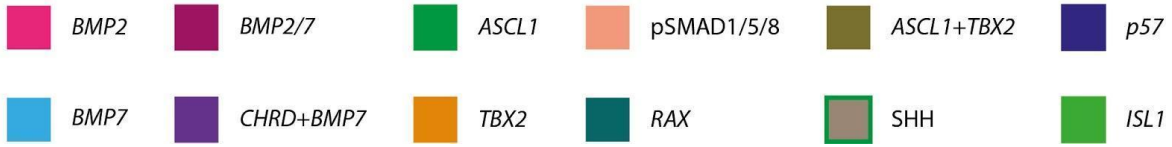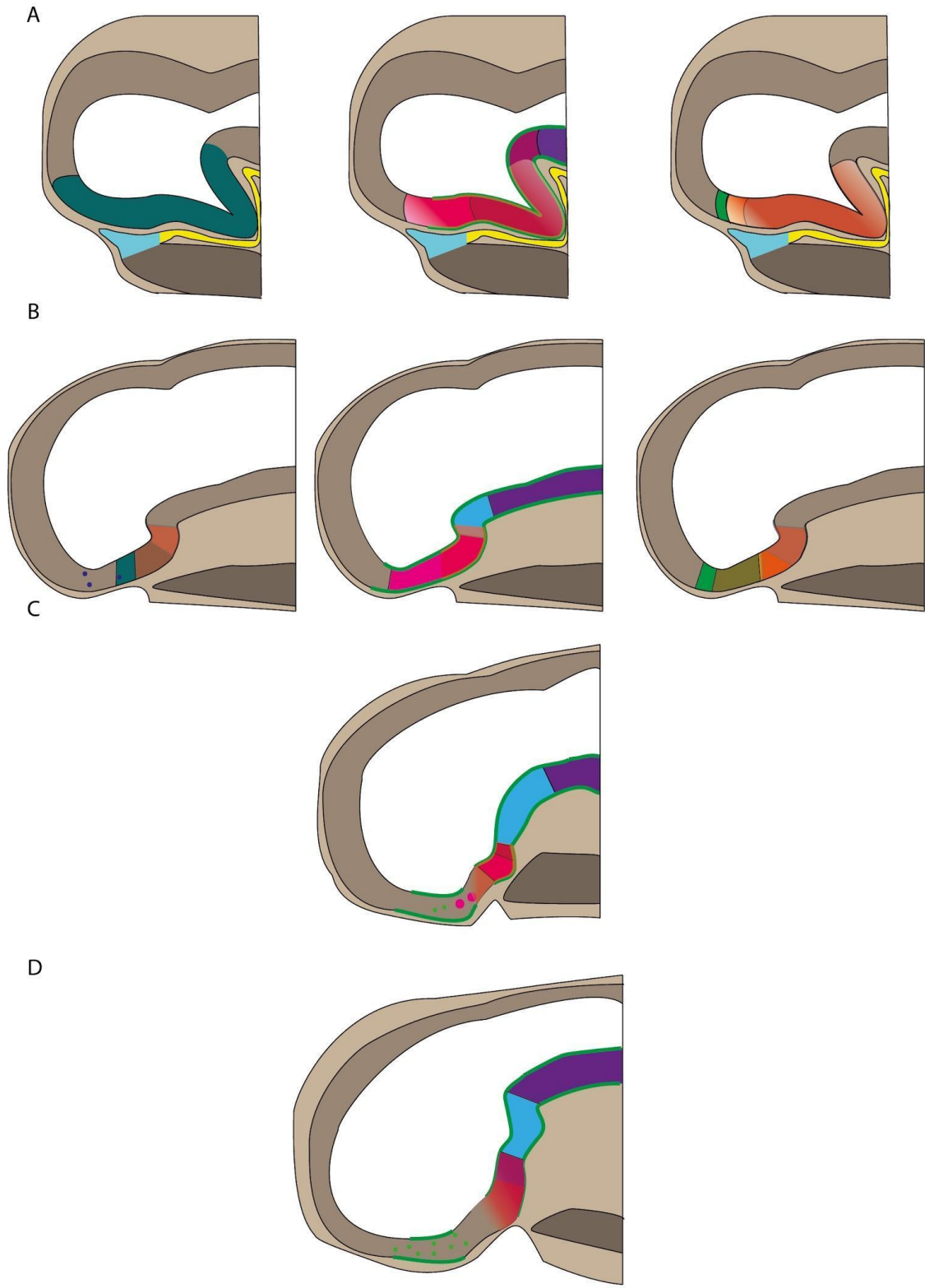
Figure 5.13: Summary schematic of the expression profiles between 10 and 20 somites. A) At 10s *RAX* is expressed throughout the ventral neuroectoderm. pBHyp cells express pSMAD1/5/8+ SHH+ and there is an anterior population of that has already begun to upregulate *TBX2* and *ASCL1*. B) At 14s there is now a SHH+/BMP2+/RAX+/ASCL1+/p57+ pAnt region which partially overlaps with the SHH+/BMP2+/RAX+/pSMAD1/5/8+ pVT region with resolution beginning. C) By 17s there is now a clear SHH+/ISL1+ pAnt region and posteriorly a pSMAD1/5/8+ pVT region. B) At 20s these regions have grown and elaborated.

5.3. Discussion

In this chapter I have performed an in-depth analysis of BMP family members, pSMAD1/5/8, SHH and a number of transcription factors over the period at which pAnt cells emerge from pBHyp cells, and at which a subset of pBHyp cells downregulate SHH to give rise to pVT cells. My results show that pSMAD1/5/8 is retained in posterior *FGF10*+ cells: these are cells that derive from pBHyp cells, but downregulate SHH. At the same time, BMPs and BMP signalling are excluded from differentiating anterior progenitors, which instead upregulate/maintian SHH, *RAX, ASCL1* and *p57.* Over time, the anterior progenitor domain lengthens and anterior progenitors begin to upregulate ISL1. Together, these studies support the anisotropic growth model of hypothalamic development. Below I briefly discuss the key observations made in this chapter.

5.3.1. *BMP2* and *BMP7* continue to show dynamic expression

My studies show a highly dynamic pattern to BMP2/7 expression as pBHyp cells give rise to pVT and pAnt cells. At 14 somites, BMP2 is expressed in pVT and telencephalic progenitors, but is then detected in mammillary pouch and telencephalic progenitors. The distance

between telencephalic and hypothalamic *BMP2* expression domains increases steadily from 14s to 20s, i.e. *BMP2+* telencephalic progenitors are gradually displaced from the mammillary pouch by emerging anterior (*BMP2-*) progenitors. This supports the anisotropic growth model of hypothalamic development, i.e. the idea that anterior progenitors form through the division of anterior-most pBHyp cells, with some daughter cells undergoing an anterior differentiation programme while others are retained as pBHyp/pVT cells.

5.3.2. BMP signalling is progressively more excluded from more committed anterior progenitors

My studies suggest that particular markers are expressed sequentially as some pBHyp cells commit to pAnt fates. They indicate that the uncommitted pBHyp population, marked by pSMAD1/5/8, initially express *TBX2* and *RAX*, then upregulate *ASCL1* and SHH while maintaining *RAX* becoming rapidly cycle pAnt cells, then upregulate markers of terminal differentiation, *p57* and ISL1 (Muthu et al., 2016; Nasif et al., 2015; Fu et al., 2017). My results confirm and extend a previous study (Fu et al., 2017), showing that differentiation is linked to space: thus the more differentiated an anterior progenitor cell, the further displaced it is from the *FGF10*+ pSMAD1/5/8+ pVT population. Of the markers analysed, *ASCL1* is clearly detected in anterior-most pBHyp/pVT cells that express weakest levels of pSMAD1/5/8. This suggests that *ASCL1* might act at a choice point, at which progenitors begin to commit to an anterior progenitor identity rather than a pVT identity.

For technical reasons, I was unable to examine the precise spatial relationship of *TBX2* and pSMAD1/5/8. However, the close proximity of these markers suggest that pSMAD1/5/8 is responsible for *TBX2* upregulation in the chick hypothalamus. These and past studies suggest that BMP signalling in highly important for the proper specification of the pVT region of the hypothalamus, a region that will later give rise to the infundibulum and pMam cells.

RAX is a homeodomain transcription factor. In fish, *rx3* is required to select anterior progenitors and drive their anisotropic growth during hypothalamic development (Muthu et al., 2016). Although not formally proved, it is likely to play a similar role in mouse (Orquera et al., 2016). Studies in fish have shown that Rax is first induced, then downregulated by SHH. This complex relationship is required for the generation of anterior progenitors and ultimately for the generation of multiple cell types in anterior and 'tuberal' domains (Muthu et al., 2016; Orquera et al., 2016). The relationship between RAX and BMP signalling has received little study, although it has been shown that recombinant human BMP4 soaked beads are capable of down-regulating *RAX* in the optic vesicle when implanted at 4 somites (Teraoka et al., 2009). Together, these studies might have predicted that as pBHyp cells resolve into pAnt versus pVT, RAX is detected only in anterior progenitors. However, I do not see evidence for this, i.e. I do not see a clear relationship between chick *RAX* and SHH+ pAnt cells. Thus, *RAX* appears to be expressed in both pVT and pAnt, albeit that there is the possibility that expression is detected in cells that express lower levels of pSMAD1/5/8, at least at 14s. Future studies are needed to better examine the spatial relationship of *RAX*, SHH and pSMAD1/5/8, including multiplexing labelling studies**.**

Chapter 6:

BMP7 inhibits anterior progenitor development

6.1. Introduction

As outlined in the main Introduction, previous studies in chick show that pAnt cells develop from pBHyp cells through a mechanism that involves a SHH-mediated mediated effect on growth and cell cycle (Introduction section 1.2.3. and Fu et al., 2017). Studies in mouse and zebrafish suggest that such a mechanism may be conserved (Muthu et al., 2016; Orquera et al., 2016). However, in the embryo, pBHyp cells are entirely surrounded by SHH-expressing cells (Fu et al., 2017). An unknown question is therefore that of why anterior progenitors emerge and grow anteriorly, rather than in all directions. One possibility is that pBHyp cells are not a homogeneous population, but instead are heterogeneous. My findings in Chapters 3 and 4 provide evidence for this, showing that *BMP2/BMP7/Chordin* and pSMAD1/5/8 are expressed differentially in RDVM and pBHyp cells. Thus, my results show that from the time of their induction at 10 somites, anterior-most pBHyp cells show strong *BMP2* expression, central pBHyp cells express show low levels of *BMP2* and *BMP7* and posterior pBHyp cells express *BMP7* strongly; cells posterior to these also show strong expression of *BMP7* (Figs.3.2, Fig.3.6). This differential expression appears to affect BMP signalling, with

particularly low levels of pSMAD1/5/8 detected in cells that abut the telencephalon, and strongest levels in central pBHyp cells (Fig.3.3, Fig.3.4). Anterior progenitors begin to form almost as soon as pBHyp cells are detected (Chapter 5 and Fu et al., 2017).

One explanation for the anisotropic growth of pAnt cells is that BMP signalling, potentially that mediated by BMP7, inhibits the specification of pAnt cells from pBHyp cells. My results in Chapter 5 support this idea: I showed progressive separation of pSMAD1/5/8 and early-specified anterior progenitors (*RAX*), anterior neuronal progenitors (*ASCL1*), and committed anterior cells (ISL1 and *p57*). I therefore hypothesised that BMP7 acts via pSMAD1/5/8 to inhibit pAnt development (growth and specification) from pBHyp cells.

Therefore the questions I aim to address in this chapter are:

- Does ectopic BMP7 inhibit anterior progenitor growth and specification?
- Does a reduction in the levels of BMP signalling in pBHyp cells enhance anterior progenitor growth and specification?

To elucidate these questions I performed in vivo studies, implanting beads in the prosencephalic vesicle in defined positions relative to pBHyp cells; I allowed embryos to continue developing in ovo, before sagittal or transverse sectioning and analyses with a

range of markers selected to interrogate anterior progenitor growth and specification. These experiments were performed together with M.P.

6.1 Results

Ectopic hBMP7 is capable of inducing pSMAD1/5/8 in vivo

First I examined the ability of hBMP7 to induce pSMAD1/5/8 in vivo. Briefly, beads were soaked in 50μg/ml hBMP7 overnight at 4°C before being implanted into the prosencephalic vesicle of 10 somites embryos, placing them adjacent to the apical surface of pBHyp cells. Control beads, soaked in PBS, were implanted into a second subset of 10 somites embryos. As previously shown (Fu et al., 2017) the position of pBHyp cells can be accurately determined at 10 somites, based on the position of the prechordal mesendoderm. I therefore positioned beads adjacent to the anterior-most pBHyp domain (Figure 6.1.A). In this way, implanted embryos would be exposed to ectopic anterior hBMP7 in addition to endogenous BMP7 deriving from posterior pBHyp cells (schematised in Figure 6.1.B). Embryos were then re-incubated to the desired stage, between HH14-15, i.e. the time when anterior progenitors are normally growing and are differentiating (Chapter 5 and Fu et al., 2017).
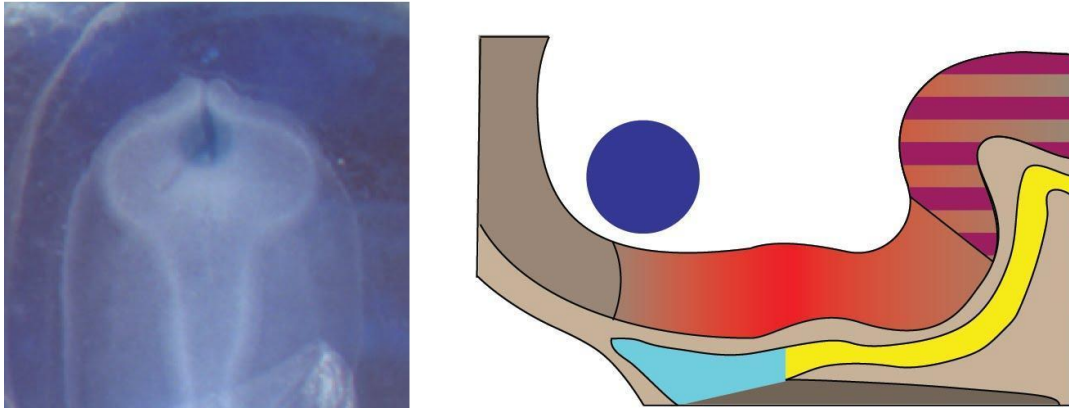
Figure 6.1: Figure showing implantation of hBMP7 beads above anterior pBHyp cells. Anterior pBHyp cells have low levels of pSMAD1/5/8 (red region) in unimplanted embryos and are distant from endogenous *BMP7* expression (purple barred region).

I first ascertained that hBMP7 was able to induce pSMAD1/5/8 in vivo. Analysis of sagittal sections showed that when the hBMP7 bead remained in contact with the anterior ventral neuroectoderm its was able to induce ectopic pSMAD1/5/8 compared to control beads (Fig.6.2). Thus, in embryos implanted with control beads at 10 somites and analysed at HH14-15, pSMAD1/5/8 was detected as in wild-type embryos, i.e. in *FGF10+* pVT cells (n=2; Fig.6.2.A and compare to Fig.5.3). In contrast, in embryos implanted with hBMP7-soaked beads at 10 somites and analysed at HH14-15, ectopic pSMAD1/5/8 was detected, adjacent to the endogenous pSMAD1/5/8 domain (n=4 beads induce pSMAD1/5/8 somewhere in the neuroectoderm; Fig.6.2.B; ectopic cells shown by bracket).

This clearly shows that hBMP7 is capable of inducing ectopic pSMAD1/5/8 in the forming hypothalamus in vivo.
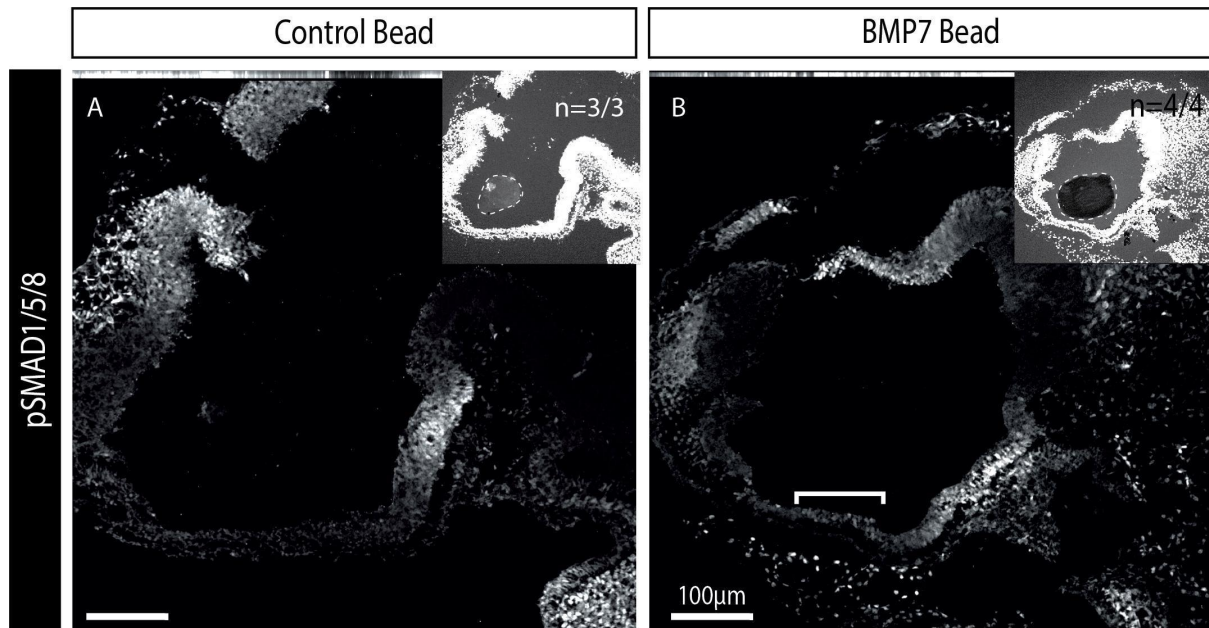
Figure 6.2: hBMP7 beads induce pSMAD1/5/8. A-B) pSMAD1/5/8 is detected in the area in contact with the hBMP7 bead (B) but not the control bead (A). Insets show position of the bead outlined in white dashed line.

Ectopic hBMP7 inhibits anterior hypothalamic differentiation and SHH expression

To determine if ectopic hBMP7/ectopic pSMAD1/5/8 inhibits pAnt cells differentiation I examined similar embryos for expression of ISL1, a marker of anterior neuronal progenitors (Chapter 5). I observed a reduction in the number of ISL1 positive cells in embryos with ectopic pSMAD1/5/8, compared to control embryos (n=2 control; Fig.6.3, C', D', white bracket). In two hBMP7-exposed embryos, the sagittal section showed a complete absence of ISL1 cells (not shown); in the third hBMP7-exposed embryo, the sagittal section showed a 50% reduction in ISL1 cells (Fig.6.3, D'). Overall, quantitative analyses (one section/embryo) showed a statistically significant reduction in the number of ISL1-positive cells after

exposure to ectopic hBMP7 (19.3+/-2.9 for controls; 4+/-4 for BMP-exposed embryos; p=0.03). Further, in the embryo in which ISL1 cells were still detected, they occupied a reduced anterior-posterior domain, compared to a control (Fig.6.3 C', D', white bracket). In order to confirm these observations it would be necessary to perform more of these experiments but these initial results support the hypothesis that BMP7 inhibits pAnt cell differentiation.

Our working hypothesis is that anterior neuronal progenitors, including ISL1-expressing cells, derive from pBHyp cells via SHH-expressing anterior progenitor cells (see Introduction, section 1.2.3). In the forming pVT hypothalamus, *SHH* is known to be inhibited by BMP7 (and to a lesser extent BMP2) via a TBX2/TBX3-dependent pathway (Manning et al., 2006; Trowe et al., 2013). However, no study has yet asked whether SHH-expressing anterior progenitor cells are inhibited by BMP7. Given the loss/reduction of ISL1-expressing anterior progenitors, I therefore predicted that implanting hBMP7 beads in vivo would also inhibit the anterior SHH expression.

To test this, I performed double-label immunohistochemistry on control or hBMP7-exposed embryos (n=3 control, n=1 hBMP7 bead remaining in contact with anterior region) to simultaneously detect pSMAD1/5/8 and SHH. Embryos analysed at HH14 after implantation of a control-soaked beads show an identical pattern of expression of pSMAD1/5/8 and SHH as wild type embryos: pSMAD1/5/8 and SHH are in the spatially-distinct progenitor populations; SHH demarcates early-forming pAnt cells and pSMAD1/5/8 demarcates *FGF10+* pVT cells (Fig. 6.3.A). SHH is also detected in the posterior mammillary hypothalamus, and abutting floor plate. By contrast, a very different pattern of SHH is detected after

implantation of a hBMP7-soaked bead. In particular hBMP7 beads inhibited SHH expression in regions anterior to the pVT (Fig.6.3.A-B; compare green bracketed region). This inhibition was restricted to sites of ectopic pSMAD1/5/8 induction: thus, normal SHH expression was detected in the posterior mammillary hypothalamus (Fig.6.3).

Anterior progenitor growth is inhibited by hBMP7 beads in vivo

A previous study has shown that SHH directs the differentiation of anterior hypothalamic progenitor cells through a mechanism that is intimately linked to their proliferation and growth. Thus, exposure of embryos to cyclopamine, a pharmacological inhibitor of SHH, reduces anterior progenitor growth (Fu et al., 2017). This predicts that the elimination of anterior SHH expression, provoked by ectopic hBMP7/BMP signalling, will lead to a reduction in proliferation of pAnt cells, and a reduction/loss of the anterior progenitor territory. To test this, I analysed one control-bead, and one hBMP7-exposed embryo for phospho-histone H3 (pH3), a marker of mitosis: sections were double-labelled to detect pH3 and ISL1, and were serial adjacent to those analysed with pSMAD1/5/8 and SHH). Qualitative analyses showed a reduction in pH3 labelling within the anterior hypothalamus close to the location of the implanted bead compared to control beads (Fig.6.3.C-D). Notably, this embryo appeared to show an overall shorter hypothalamus, along the anterior-posterior axis.

Overall these results support the anisotropic growth model of hypothalamic development, which suggests that the pAnt cells develop through SHH-driven growth. In particular my

results suggest a role for BMP signalling in this process: ectopic hBMP7/BMP signalling eliminates SHH expression in pAnt cells and reduces their proliferation. Therefore, my results suggest that pAnt cells normally form in regions where BMP/BMP signalling is low (see Discussion).
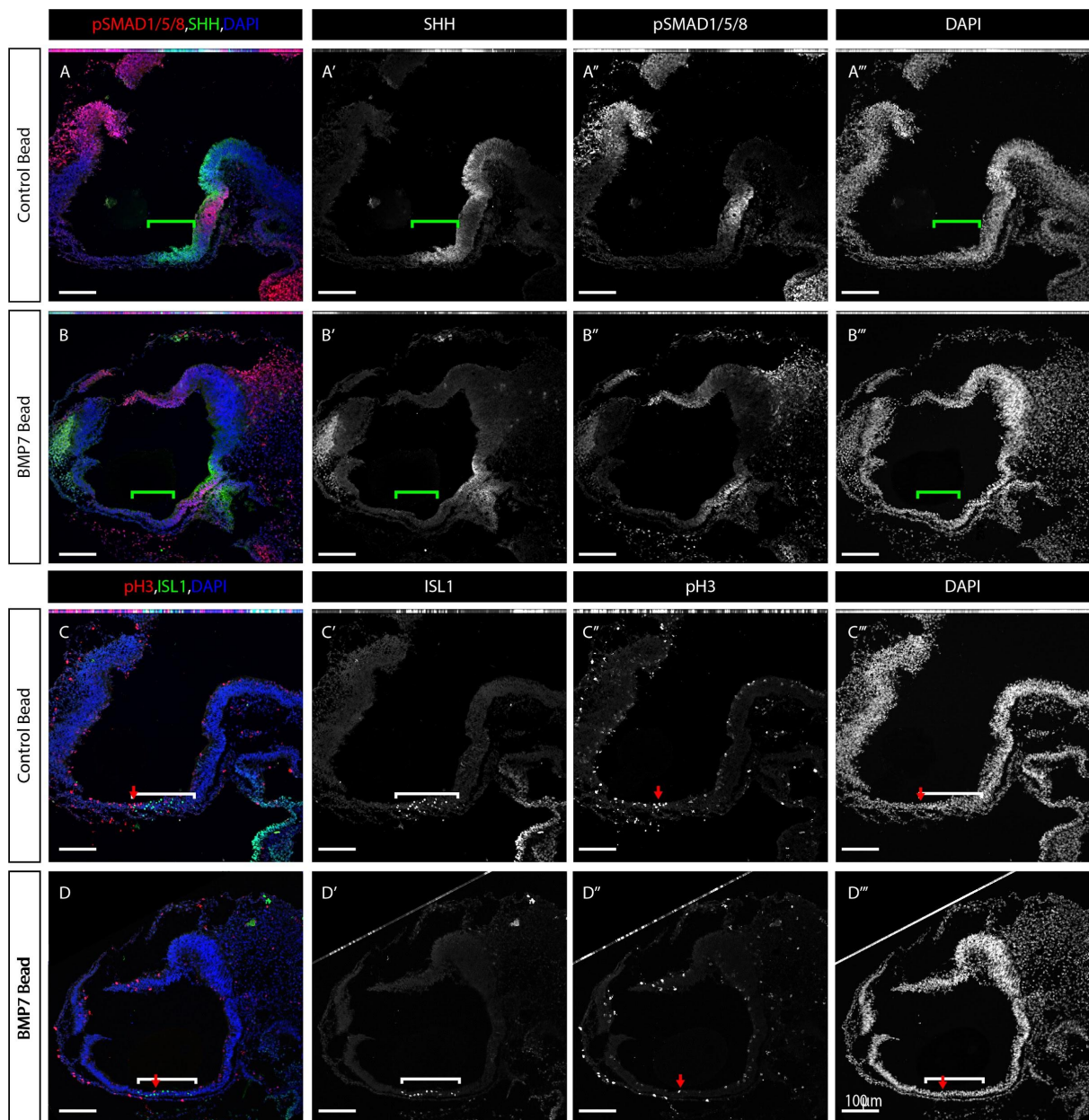
Figure 6.3: hBMP7 beads appear to inhibit SHH and proliferation/specification in/of the Anterior Hypothalamus. A-B) Green bracket indicates anterior SHH expression (in B this is the distance between the anterior limit of pSMAD1/5/8 and some weak remaining SHH expression). Compared to control embryos (A') hBMP7 beads (B') appear to to express little to no SHH in the region of the bead, this corresponds with a reduction in anterior length,

122µm to 111µm, respectively. C-D) White brackets indicate ISL1 distribution. hBMP7 beads appear to reduce the number of ISL1 positive cells and the distance over which they are located. Control bead implanted embryo shows numerous ISL1 positive cells in the anterior region measuring 170µm (C'). hBMP7 bead implanted embryo shows fewer ISL1 positive cells in the anterior region measuring 150µm (D'). Quantitative analyses (one section/embryo) showed a statistically significant reduction in the number of ISL1-positive cells after exposure to ectopic hBMP7 (19.3+/-2.9 for controls; 4+/-4 for BMP-exposed embryos; p=0.03). C-D) Red arrow indicates area of lots of pH3 expression in control bead embryo and analogous region in hBMP7 bead embryo. Control embryos show a region in the Anterior Hypothalamus that has many pH3 labelled cells (C''), however this region does not appear to be present in hBMP7 bead treated embryos (D''). A-D) Multichannel view followed by SHH (A'-B')/ISL1 (C'-D'), pSMAD1/5/8 (A''-B'')/pH3 (C''-D''), and DAPI (A'''-D''').

Lateral hBMP7 beads only induce pSMAD1/5/8 and downregulate SHH and ISL1 in their immediate vicinity

As described above, beads did not always remain in the position in which they were implanted. Due to this in some embryos the bead drifted to one side of the ventricle during development. This however allowed me to effectively perform an experiment with a control and experimental side within the same embryo.

Embryos exposed to a lateral hBMP7 bead showed a similar (but not identical) phenotype to those exposed to a midline hBMP7 bead. pSMAD1/5/8 was induced, but on only one side of the hypothalamus, and adjacent to the bead (Fig.6.4.A red arrow). SHH was downregulated in these cells (Fig.6.4.A, red arrow), but was expressed in its usual lateral location on the non-exposed side (Fig.6.4.A, green arrow) These embryos also showed a loss of ISL1+ cells on the side with the bead (Fig.6.4.B, red arrow). However, in contrast to midline-exposed embryos, where pH3 was reduced (Fig.6.3), in lateral-exposed embryos, there appeared to be more pH3-expressing cells in the vicinity of the bead (Fig.6.4.B, red arrow). Further, many

hBMP7 treated embryos in this experiment appeared to have either underdeveloped of absent eyes on the side of the embryo that was not exposed to the bead (Fig.6.4 green arrow side). This complex and unexpected phenotype suggests that BMP7 exerts asymmetric effects that impact not just on the hypothalamus, but more generally on development of the prosencephalon.
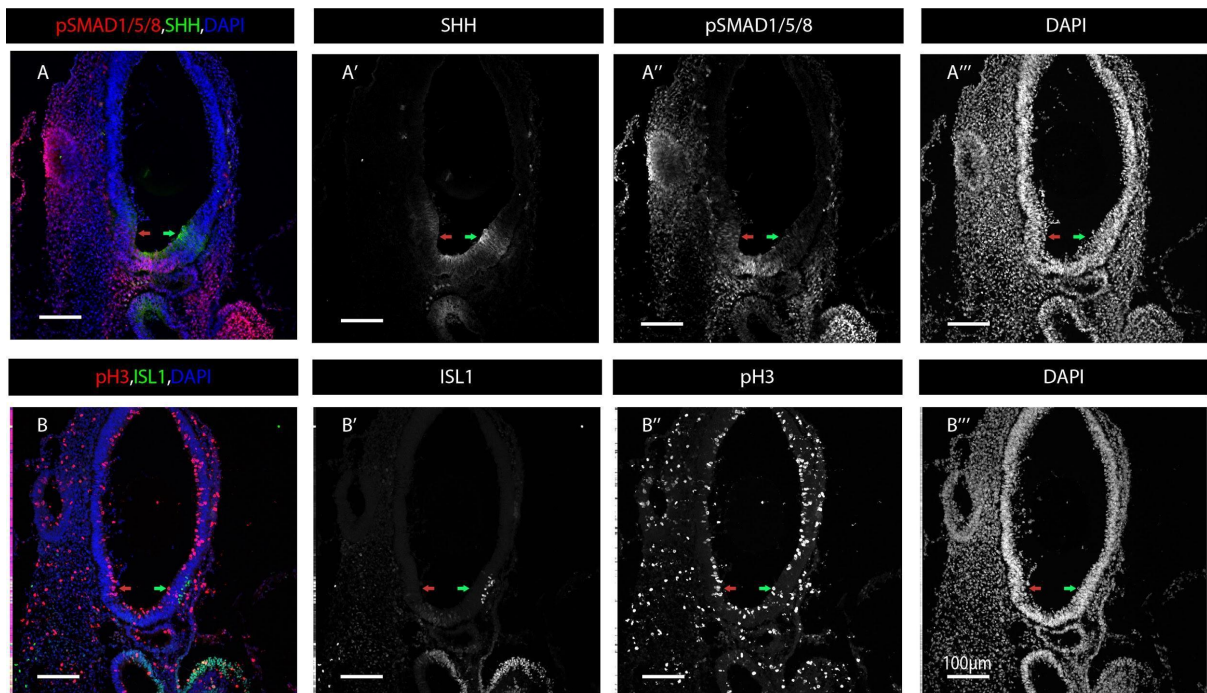
Figure 6.4: Lateral hBMP7 beads show asymmetric effects. A) SHH is downregulated and pSMAD1/5/8 is upregulated on the treated (red arrow) compared to the control side (green arrow). B) There is a complete loss of ISL1 on the treated side (red arrow) compared to the control side (green arrow). In this case there appears to be an increase in pH3 labelling on the treated (red arrow) compared to the control side (green arrow) (B''). A-B) Multichannel view followed by SHH (A')/ISL1 (B'), pSMAD1/5/8 (A'')/pH3 (B''), and DAPI (A'''-B''').

Noggin beads downregulate pSMAD1/5/8 but do not induce any other obvious phenotype

With these observed effects in the gain-of-function experiments I next performed loss-of-function experiments, aiming to inhibit BMP activity and reduce pSMAD1/5/8 in

pBHyp cells. To achieve this aim I first used Noggin protein soaked onto beads at a concentration of 200µg/ml and implanted them in a similar manner to the hBMP7 beads; however, instead of positioning the bead adjacent to anterior-most pBHyp cells, I positioned the bead adjacent to central-most pBHyp cells (Fig.6.5; full description in Chapter 2). Beads were implanted in embryos at 10 somites and embryos examined at HH14 or HH15 for expression of pSMAD1/5/8; in parallel, a subset of embryos were exposed to control beads and analysed in a similar manner.

Noggin-soaked beads reduced pSMAD1/5/8 labelling within pBHyp cells in embryos analysed at 10 somites, 1.5 hours after implantation (n= 3; Fig.6.6). However the reduction in pSMAD1/5/8 was transient, and embryos analysed at HH15 did not show a clear reduction in pSMAD1/5/8 (n =3; data not shown). This led me to hypothesise that due to the expression of multiple BMPs in pBHyp cells at this time there may be a requirement to use multiple inhibitors in order to obtain a stronger phenotype.
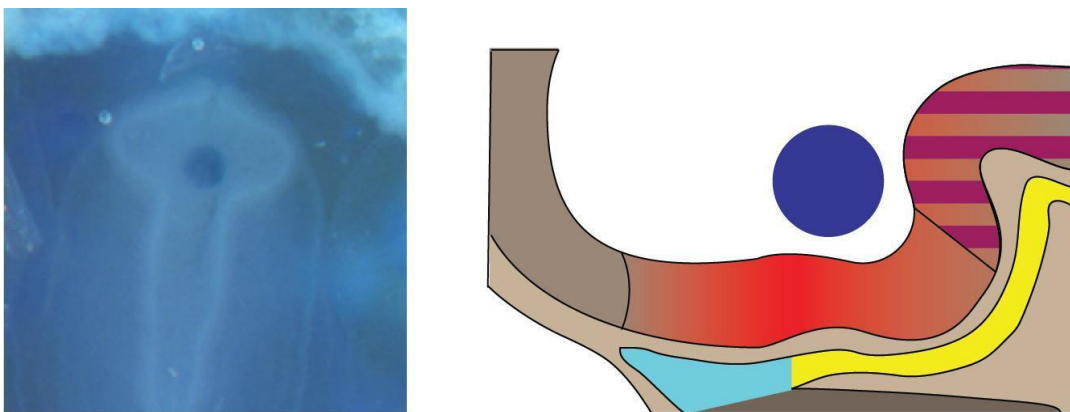
Figure 6.5: N+C beads were implanted above the centre of the pBHyp domain. pSMAD1/5/8 is strongest in central pBHyp cells (red region) and close to *BMP7* expression (purple barred region).
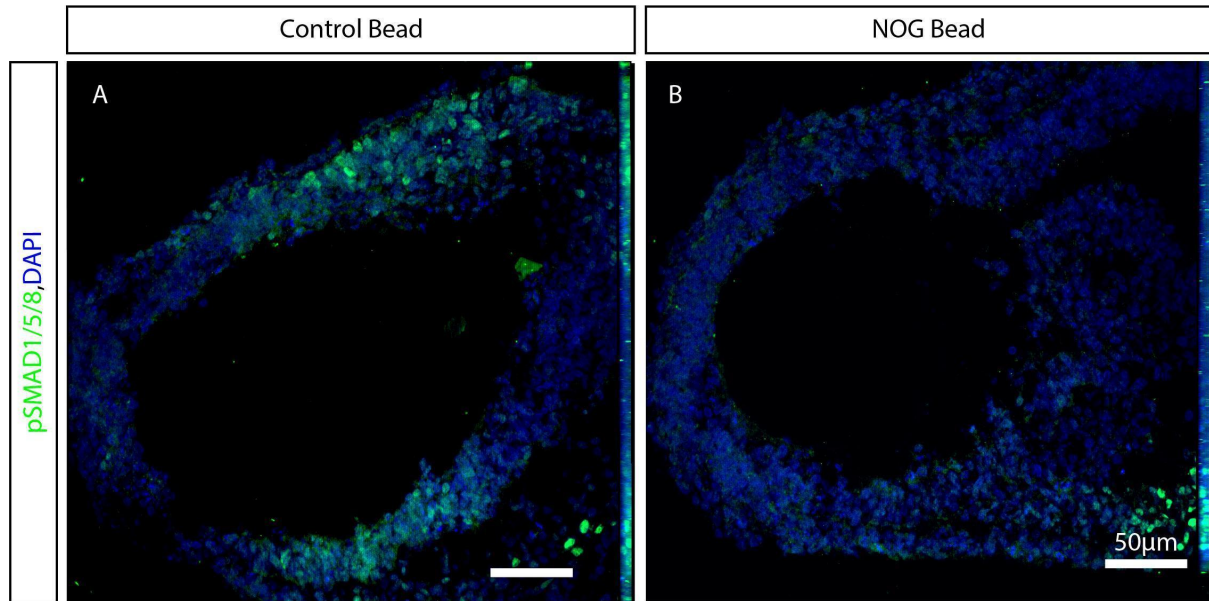
Figure 6.6: Noggin beads are capable of down regulating pSMAD1/5/8 in pBHyp cells but fails to induce another clear phenotype. A-B) Control (A) beads showed no effect on pSMAD1/5/8 compared to unimplanted embryos (Fig.5.4.A) however N+C beads showed a clear down regulation of pSMAD1/5/8 (B) 1.5 hours after implantation but this was transient and BMP signalling was present in pVT cells at 20s (data not shown).

Noggin and Chordin beads appear to have some effect on Anterior Hypothalamic development

Using a combination of Noggin (200µg/ml) and Chordin (20µg/ml) protein soaked onto beads (N+C bead) will provide a greater range of inhibition, as Noggin binds preferentially to BMP2/4 but also BMP7 and Chordin has similar dynamics, but may show a preference for BMP4/7 heterodimers over BMP4 homodimers (Groppe et al., 2002; Piccolo et al., 1996). Using two, albeit similar, inhibitors should provide a stronger inhibition of BMP signalling.

Preliminary studies (n=2) show that this combination appears to show some effect on the differentiation of pAnt cells. The distance over which both SHH and ISL1 were expressed appeared to be increased in N+C bead treated embryos compared to controls (Fig.6.7.A-D). There was also a non-significant increase in ISL1+ cells within the anterior region (19.3+/-2.9 for controls; 32.5+/-2.5 for N-C-exposed embryos; p=0.0745). This however was accompanied by no clear phenotypic differences in pSMAD1/5/8 or pH3 labelling (Fig.6.7.A-D). Future experiments are needed to strengthen any conclusions from this experiment.
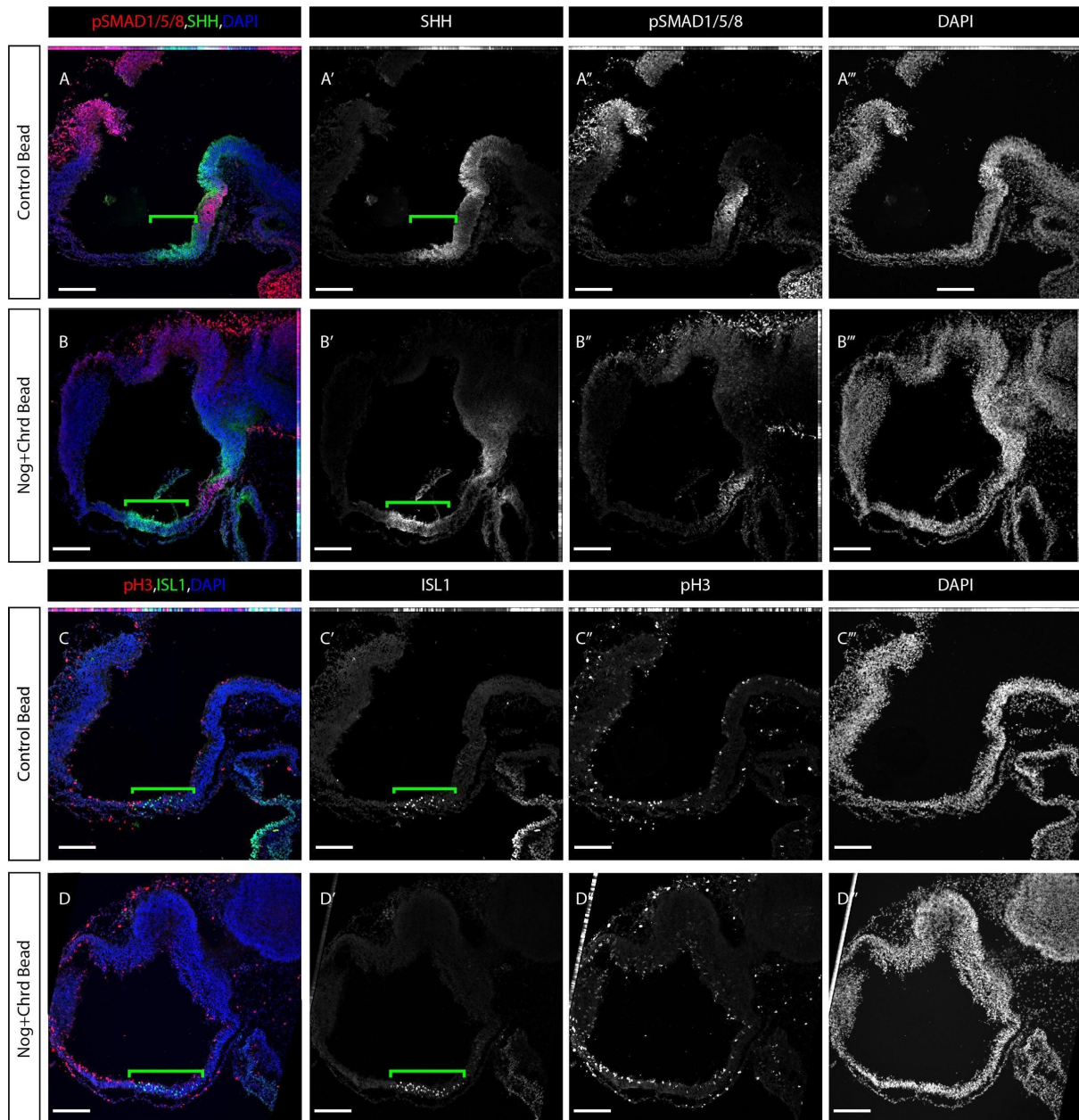
Figure 6.7: Noggin and Chordin beads appear to increase the length of the anterior hypothalamus. A-B) Green bracket indicates anterior SHH expression distance or (C-D) distance over which ISL1+ cells are detected. A-B) Anterior hypothalamic SHH appeared to show an increase in N+C bead treated embryos compared to controls, Control 122µm, N+C 166µm. No difference was observed in pSMAD1/5/8 labelling. C-D) ISL1 was also detected over a longer distance in N+C bead treated embryos compared to controls, Control 170µm, N+C 195µm. A-D) Multichannel view followed by SHH (A'-B')/ISL1 (C'-D'), pSMAD1/5/8 (A''-B'')/pH3 (C''-D''), and DAPI (A'''-D'''). There was a non-significant increase in ISL1+ cells within the anterior region (19.3+/-2.9 for controls; 32.5+/-2.5 for N-C-exposed embryos; p=0.0745).

6.3. Discussion

In this chapter I begin to provide evidence that BMP signalling inhibits anterior progenitor differentiation. Using in vivo techniques, that enable both temporal and spatial manipulation of BMP/BMP signalling, I have shown that an ectopic increase in BMP signalling in the anterior-most part of pBHyp cells, at the time that anterior progenitor first emerge, inhibits the expression of markers of pAnt cells, such as SHH and ISL1. I have also performed the converse experiment which appears to support this theory: a decrease in BMP signalling during anterior progenitor emergence leads to a longer anterior hypothalamus perhaps generated by more anterior differentiation.

6.3.1. hBMP7 Beads appear to reduce SHH and ISL1 expression in the Anterior Hypothalamus

As I have discussed previously SHH can be downregulated in the pVT hypothalamus by BMP signalling via induction of *TBX2* (Manning et al., 2006, Trowe et al., 2013). My gain of function experiments indicate that BMP7 can also downregulate SHH in emerging pAnt cells. In order to show whether the loss of SHH expression is due to a loss of cells with anterior character or a respecification of cells, markers such as TBX2 could be used in future studies. The simultaneous use of a marker of telencephalic progenitors, such as FOXG1, would likewise help to distinguish whether ectopic BMP7/BMP signalling leads to a change in pattern, or a change in growth. Is there a reduction in the length of the anterior region, the

distance between telencephalic and pVT markers, or is there an anterior expansion of pVT markers, or both? BMPs have also been shown to inhibit proliferation and promote cell death at high concentration in mouse neural progenitors (Mehler et al., 2000). This raises the possibility that rather than respecified some anterior progenitors may have never been born or induced to apoptose. All of these mechanisms would likely affect ISL1 expression. I address this further in the final discussion.

The transcription factor ISL1 is involved in the specification of many cell types around the body, including motor neurones, cardiac progenitors and the developing limb (Thaler et al., 2002; Yang et al., 2006). In the hypothalamus it is essential for the proper specification of many arcuate nucleus neurons (Lee et al., 2016). Here I show that ISL1 is detected in differentiating anterior progenitors. But is there a relationship between BMP signalling and ISL1 in the chick hypothalamus? BMP signalling has been shown to repress ISL1 expression in the developing chick spinal cord in a cell-autonomous manner (Timmer et al., 2002). However electroporation of constitutively-active BMP receptors BMPR1b into the diencephalon at 4 to 7 somites assayed three days later showed a marked increase in the number of cells expressing ISL1 in the region of the electroporated cells (Lim et al., 2005). The former study showed that cells surrounding the normal expression region had been successfully electroporated, the later study however failed to show clear co-expression of the constituently active BMP signalling construct with ISL1. This allows the possibility that what is being seen is some downstream effect of increased BMP signalling at an early stage leading to an increase in ISL1 expressing cells at a later stage without there being and inductive relationship between BMP signalling and ISL1. Results from this paper show no

increase in proliferation 16 hours post electroporation. What was not assessed was the fate of electroporated daughter cells. Given it has now been shown that increased BMP signalling can result in a mode shift of stem cells to self expanding divisions away from self consuming divisions, this could result in more ISL1 positive cells without increasing the replication rate or directly inducing ISL1 expression (Dréau et al., 2014).

Chapter 7:
Discussion

7.1. Discussion

In the studies presented in this thesis I have:

1. shown that pSMAD1/5/8 is the earliest known marker of RDVM cells and prefigures and predicts the expression of the pBHyp cell marker *FGF10*. pSMAD1/5/8 also shows complementary expression with *FOXG1*, a marker of the telencephalon, giving weight to the case that it marks all pBHyp cells. But pSMAD1/5/8 is not uniform within pBHyp cells, it shows a low-high-low pattern along the anterio-posterior axis (Fig. 7.1).

2. demonstrated a continued requirement for, and a dose dependent relationship to, canonical BMP signalling in the upregulation of *FGF10* in RDVM explants. This work showed that endogenous BMP expression was capable of directing *FGF10* upregulation and that this must continue through BMP type 1 receptors in order for *FGF10* to be upregulated.

3. investigated the expression profiles of markers likely to contribute to the emergence of differentiating progenitors from pBHyp. I have shown that by 10 somites, anterior most cells within the pBHyp region have already begun to upregulate ASCL1, a marker of pAnt neuronal cells and that slightly more posterior/medial cells within the pBHyp region have begun to upregulate *TBX2,* a marker of pVT cells. By examining

successive stages of development, from 10 somites to HH16, I have shown that there appears to be a clear progression from pBHyp *FGF10+* pSMAD1/5/8+ progenitors to a *RAX+FGF10-* pSMAD1/5/8- rapidly cycling pAnt cell, to a non-cycling anterior cell, expressing *p57* and/or ISL1 (Fig. 7.2, 7.3).

4. generated preliminary studies that show that BMP signalling must be downregulated in order for pAnt cells to be specified/induced. Thus, ectopic BMP7/BMP signalling leads to an apparent loss of anterior territory, loss of SHH+ pAnt cells and loss of differentiating ISL1+ anterior cells. It would also appear that the converse is true, that decreased BMP signalling in the pBHyp cells leads to more ISL1+ cells and a larger anterior hypothalamus.

7.1.1. Expression of pSMAD1/5/8, *BMP2* and *BMP7* in RDVM, pBHyp and pVT cells

pSMAD1/5/8 is the first marker I am aware of that selectively marks RDVM and pBHyp cells from their induction to when they begin to generate pAnt cells and pVT cells. However this expression is not uniform and I see a low-high-low pattern of intensity along the anteroposterior axis from 7 somites (Fig.3.3). This becomes clear at 10 somites, with a region with weak pSMAD1/5/8 labelling abutting the telencephalon (Fig.3.4). The existence of some form of patterning and heterogeneity within pBHyp cells provides an explanation for how these cells grow anisotropically to generate, first, pAnt cells, which I will discuss in the section below. Here I will focus on heterogeneity within pBHyp cells.

The simplest explanation for the differences I detect in pSMAD1/5/8 labelling would be differences in either the amount or type of upstream activation of BMP signalling that triggers SMAD1/5/8 phosphorylation. To begin with type: I have shown that *BMP2* begins to be expressed more anteriorly than *BMP7* from around 7s. Previous in vitro work has shown that BMP2/7 heterodimers have a greatly increased ability to induce alkaline phosphatase expression compared to homodimers (Israel et al., 1996). A similar conclusion has been drawn through in vivo studies: in zebrafish, Bmp2/7 heterodimers have great enough receptor affinity to overcome endogenous inhibition and activate downstream signalling compared to homodimers (Little and Mullins, 2009). The other simple explanation is that central pBHyp cells are exposed to greater amounts of ligand than anterior or posterior pBHyp cells. This could well be the case, their central location means that not only are they expressing BMPs, all the surrounding neuroectoderm cells also express BMPs. Similarly they are located above the centre of the underlying PM, a source of BMP7. Together with their distance from endogenous inhibitor expression (Fig.3.2), it could simply be a matter of being exposed to greater levels of signalling ligand that lead central pBHyp cells to label most intensely for pSMAD1/5/8.

After ligand composition and availability the next logical step is to look at differential receptor activation. However the loop of type 1 receptors that interacts with SMAD1/5/8, Loop 45, shows no amino acid differences between BMPR1A and BMPR1B (Persson et al., 1998). These receptor show highly different expression patterns in the chick neuroectoderm during pBHyp specification and pAnt generation and in the spinal cord have been shown to have pro-proliferation, BMPR1A, and pro-cell cycle arrest, BMPR1B, functions (Lim et al., 2005; Panchision et al., 2001). These observations leave open the possibility of co-receptors

and other downstream signal modulation, careful analysis focused on the hypothalamic

primordium with reference to exactly when and where these receptors are active to help

elucidate their functions during hypothalamic development.

Intracellular SMAD regulation could also lead to differential SMAD activation. SMADs have a

highly diverse region known as the linker region, which can be modified by phosphorylation,

ubiquitination, SUMOylation and actylation (Wrighton, Lin, and Feng 2009; Xu, Liu, and

Derynck 2012). This provides both a means of specific SMAD modulation and the specific

activities of SMADs that have been discovered through knockout models (Dick et al., 1999).

Making use of single cell techniques such as single cell sequencing and proteomics could

begin to answer whether these potential modifications are present and how they may

impact hypothalamic development.

7.1.2. A pSMAD1/5/8 prepattern in pBHyp cells may explain the anisotropic growth of basal hypothalamic progenitors

As alluded to above, the presence of a pSMAD1/5/8 prepattern would provide a simple

mechanism to explain how pBHyp cells are first directed to proliferate and be

displaced/migrate anteriorly, giving rise to pAnt cells. The idea is that there is a SHH (high

anterior) – BMP7 (high posterior) signalling gradient in pBHyp cells, and pAnt cells are

generated when SHH signalling is highest and BMP signalling is lowest (Fig. 7.1, 7.2). The

idea that subtle alterations in the balance of SHH/BMP signalling can affect pBHyp cells,

and/or pBHyp cell development is well-founded. Previous studies have demonstrated that

BMP2 and BMP7 downregulate SHH in the hypothalamus via the induction of *TBX2* in a

concentration dependant manner ex vivo and that this can be inhibited by Chordin, an extracellular BMP inhibitor (Manning et al., 2006; Troilo et al., 2014). This suggests BMP signalling must be tightly constrained for pBHyp cells to resolve to pAnt and pVT cells. As outlined in the Introduction, in the mouse, SHH downregulation in pVT cells appears to be under the control of *Tbx3*: deletions of *Tbx3* leads to a hypoplastic hypothalamus that fails to properly downregulate SHH (Trowe et al., 2013). Inhibition is achieved at a transcriptional level by TBX2/3 preventing SOX2 from binding to the SHH brain enhancer 2 (*SBE2*). SHH is still downregulated in the more caudal portion of the developing hypothalamus in this Tbx3Δ model, suggesting that this may not be the only mechanism by which SHH is downregulated. This could be due to the ability of BMP7, which in chick induces *GLI3* which can inhibit SHH signalling, and at the same time, promote expression of Pax7, a marker of pMam cells (Ohyama et al., 2008). Alternatively this could show some partial redundancy between Tbx3 and Tbx2 in mouse. Thus, previous studies have described a role for BMPs in development of the pVT and pMam regions of the hypothalamus.

A

B

C

FOXG1	*BMP2*	*BMP2/7*	pSMAD1/5/8
FGF10	*BMP7*	SHH	*CHRD+BMP7*
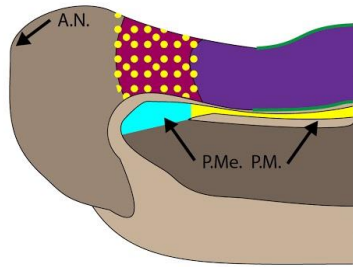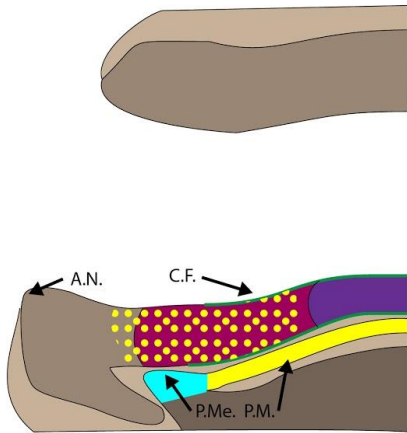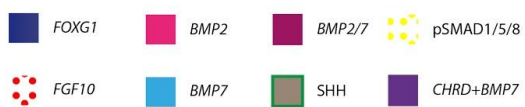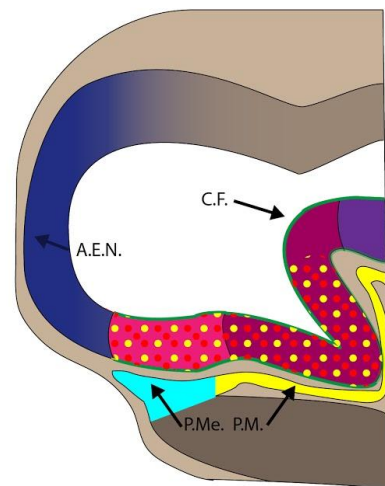
Figure 7.1: Summary schematic of RVDM/pBHyp cell development from 4s to 10s. Please see key for colour/gene relations. A) At 1 somite BMP7 from the PM/PME induces BMP2 and BMP7 expression in overlying ventral midline cells, pSMAD1/5/8 is confined to a region anterior to *CHRD* expression. B) By 7 somites as *CHRD* is downregulated/displaced pSMAD1/5/8 extends posteriorly. C) Continued BMP signalling then induces *FGF10+* pBHyp character at 10 somites. AN anterior neuropore, AEN anterior extent of neuroectoderm, CF cephalic flexure, PME prechordal mesendoderm, PM prechordal mesoderm.

A

B

C

D

BMP2	*BMP2/7*	*ASCL1*	pSMAD1/5/8	*ASCL1+TBX2*	*p57*
BMP7	*CHRD+BMP7*	*TBX2*	*RAX*	SHH	*ISL1*
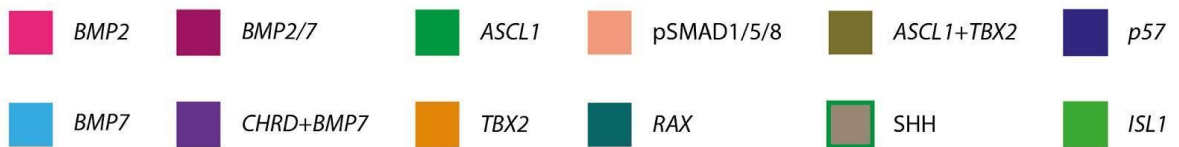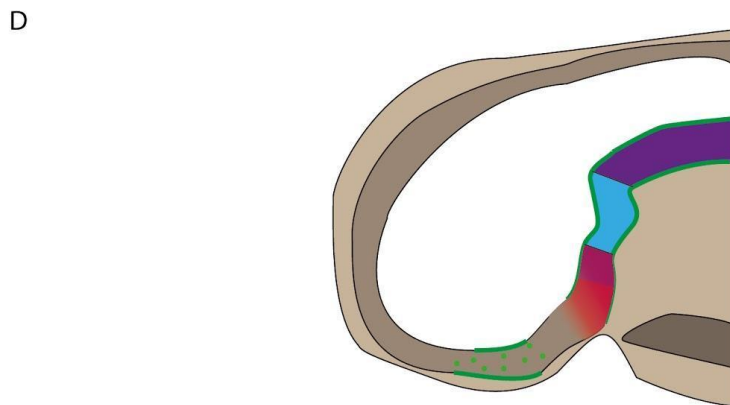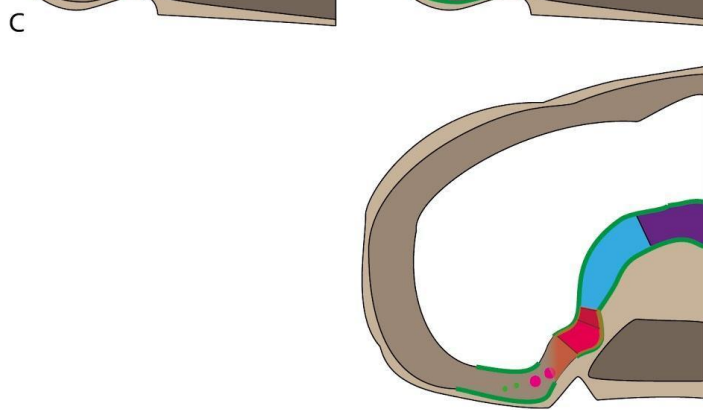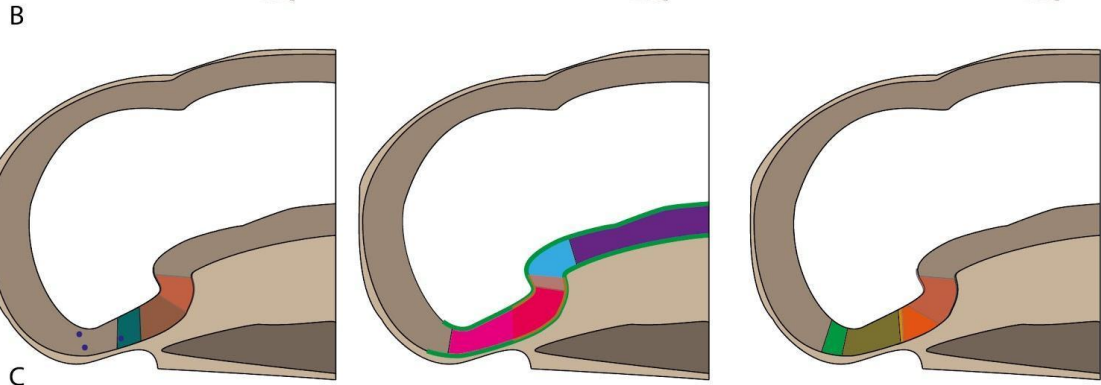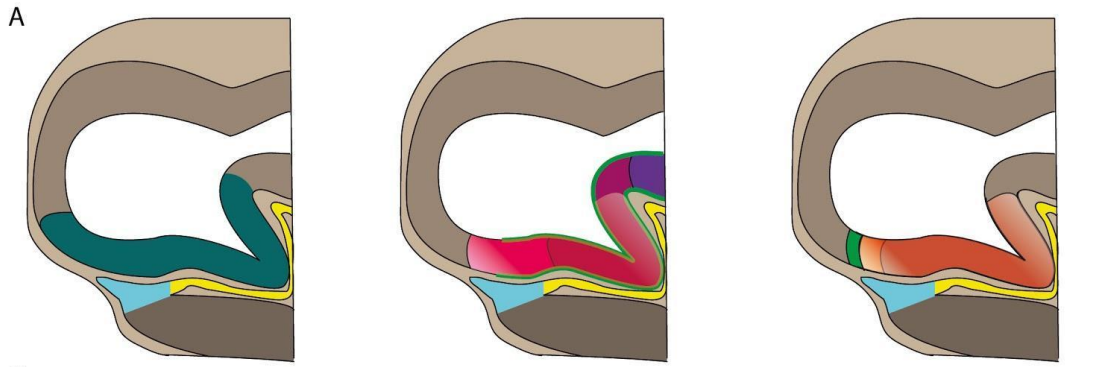
Figure 7.2: Summary schematic of the expression profiles between 10 and 20 somites. A) At 10s *RAX* is expressed throughout the ventral neuroectoderm. pBHyp cells express pSMAD1/5/8+ SHH+ and there is an anterior population of that has already begun to upregulate *TBX2* and *ASCL1*. B) At 14s there is now a SHH+/BMP2+/RAX+/ASCL1+/p57+ pAnt region which partially overlaps with the SHH+/BMP2+/RAX+/pSMAD1/5/8+ pVT region with resolution beginning. C) By 17s there is now a clear SHH+/ISL1+ pAnt region and posteriorly a pSMAD1/5/8+ pVT region. B) At 20s these regions have grown and elaborated.

My studies now add to this, indicating that BMP signalling inhibits anterior hypothalamic differentiation/specification. I have shown that ectopic BMP signalling appears to lead to a loss of pAnt cell specification/proliferation. My study builds on previous work that suggests that BMP signalling must be highly regulated during hypothalamic development. Studies show that Noggin and Chordin, endogenous inhibitors of BMP signalling expressed in and around the hypothalamic primordia, most likely act in a semi-redundant manner to affect early hypothalamic development: *CHRDΔ/Δ* mutants show normal early development but have ear defects and are stillborn and *NOGΔ/Δ* mutants show neural tube closure and limb defects as well as loss of caudal vertebrae (Bachiller et al., 2000; McMahon et al., 1998). However, when simultaneously deleted in mouse models there is a failure to induce *NKX2.1*, a marker of the hypothalamic primordia, and a loss of anterior hypothalamic expression of *SHH* (Anderson et al., 2002; Bachiller et al., 2000). These mutants show similarities to *SHHΔ/Δ* phenotype, including holoprosencephaly, in which the hemispheres fail to separate, and cyclopia, the presence of only a single eye (Chiang et al., 1996). Potentially, the increase in BMP signalling – due to lack of endogenous inhibition - prematurely downregulates *SHH* expression, leading to a holoprosencephaly phenotype. Conversely, increasing BMP inhibition also has marked effects of hypothalamic development. Chordin-soaked beads, implanted close to the PM in vivo, prevent the induction of *TBX2* in pBHyp cells, presumably because BMP signalling is decreased (Manning et al., 2006). This

paper appears to show a BMP-induced cell cycle arrest at 10 somites in pBHyp cells which

can be inhibited by Chordin in vivo; however prolonged SHH exposure inhibits proliferation

in vitro (Manning et al., 2006). This points to a model in which SHH must be downregulated

in pVT cells in order for them to proliferate following cell cycle arrest but must be

maintained in anterior progenitors for their specification/proliferation.

7.1.3. pAnt development

Previous studies in chick, zebrafish and mouse have suggested that SHH signalling is required

for the differentiation of pAnt cells from pBHyp cells (Muthu et al., 2016; Orquera et al 2016;

Fu et al., 2017). In zebrafish and mouse, a potential mechanism has been identified: studies

suggest that Shh induce pAnt development via the transcription factor, Rax2/rx3 (Muthu et

al., 2016; Orquera et al., 2016). Deletion of *Rax* in mouse throughout hypothalamic

progenitors leads to loss of many anterior and ventro-tuberal cell types (Lu et al., 2013). In

zebrafish *rx3* has been shown to be required for the anisotropic growth and specification of

anterior progenitors and the neurons that arise from them (Muthu et al., 2016). When *rx3*

expression is knocked down with a morpholino there is a marked loss of anterior cell

territory. My studies provide preliminary evidence that this mechanism is widely-conserved

and operates in chick. *RAX* expression in chick appear to be similar located between pAnt

and pVT regions (Fig.5.7). This opens the possibility that *RAX* performs a similar function in

the chick. Additionally, my studies add weight to the anisotropic growth and differentiation

of pAnt cells: I detect an increasing distance between pVT cells and committed anterior cells

over time. As suggested by previous studies (Muthu et al., 2016; Fu et al., 2017) I suggest

that RAX selects them pAnt cells, that then can upregulate *ASCL1* when committing to neural

progenitor identity, followed by upregulation of committed anterior markers such as ISL1 and *p57.*

7.2. Future Directions

7.2.1. Heterogeneity of RDVM/pBHyp cells

To better understand the heterogeneity of RDVM/pBHyp cells, more complex multiprobe in situ hybridisation could be performed. This would allow the exact relationship between *BMP2* and *BMP7* to be understood, which would begin to build evidence for the presence of BMP2/7 heterodimers in the developing hypothalamus. In order to show these heterodimers where sufficient and necessary to induce RDVM/pBHyp cells one would have to perform a knockdown of both BMP2 and BMP7 and then test the heterodimer against both homodimers in their ability to rescue the knockdown.

Another avenue to explore looking at heterogeneity of RDVM/pBHyp cells is the use of slice culture to investigate the role of differential SMAD activation by electroplating in reporter constructs that show SMAD activation level and markers of progenitor/neuron cells, such as in (Dréau et al, 2014). This would elucidate the role of differential SMAD activation in the hypothalamic primordium. In the spinal cord high levels of SMAD activation are associated with self-expanding (progenitor-progenitor) divisions (Dréau et al., 2014). If this were also the case in the developing hypothalamus it would integrate well with the theory that the low-high-low pattern of SMAD1/5/8 is at least partially responsible for the anisotropic growth seen during pAnt cell generation. Using sagittal slice culture of pBHyp cells one

would expect to see high SMAD1/5/8 levels centrally displace cells anteriorly through self

expanding divisions, these anterior cells with low SMAD1/5/8 levels exhaust themselves

through self consuming (neuron-neuron) divisions, leading to the reduced proliferation seen

in the pAnt region as it is displaced/migrates away from BMP signalling (Fig. 7.3) (Fu et al.,

2017).

Figure 7.3: The Anisotropic Growth Model of Hypothalamic development. Groups of progenitors are represented by coloured balls, with time progressing from top to bottom and anterior to the left and posterior to the right. The initial SHH+/BMP7+/FGF10+/pSMAD1/5/8+ pBHyp population first gives rise to SHH+/RAX+/FGF10-/BMP7- rapidly proliferative pAnt cells, followed by SHH-/BMP7+/FGF10+ pVT cells, while being centrally retained. pAnt cells then give rise to committed p57+/ISL1+ pAnt cells while pVT cells generate FGF10-/BMP7+ pMam cells. During this there continues to be a centrally retained FGF10+/pSMAD1/5/8+ pBHyp population.

7.2.2. Expression of BMP receptors

As mentioned in the Introduction, BMP receptors assemble tetrameric complexes of two type 1 and two type 2 receptors prior to the initiation of downstream signalling (Introduction section 1.3.1.). There is some evidence of differential expression of BMP type 1 receptors within the developing chick hypothalamus. At RDVM stages there is little expression of either BMPR1A or BMPR1B in RDVM cells, however at 16 somites there is widespread expression of BMPR1A in the ventral neuroectoderm but specific BMPR1B expression within the ventral midline at the height of the hypothalamus (Lim et al., 2005). Along with this is data suggesting that BMPR1A signalling induces proliferation induced the expression of BMPR1B, which is also induced by exposure to BMP2 (Panchision et al., 2001). BMPR1B then inhibits proliferation and induces apoptosis at early stages and differentiation at later stages in the developing neuroectoderm in mouse embryos (Panchision et al., 2001). Induction by BMP2 and induction of differentiation implicated BMPR1B as a potential mediator of pAnt development based on my data (Fig.3.2. and Fig.5.12.). Therefore a line of inquiry into the requirement for BMP signalling in chick hypothalamic development would be a close examination of BMP receptors in the context of the anisotropic growth model. If it were the case in pBHyp cells that initially express BMPR1A give rise to pAnt cells that upregulate BMPR1B and are then directed to differentiate, then inhibition of BMPR1B should lead to excessive proliferation and growth of the anterior region.

Electroporating dominant negative or constitutively active forms of SMADs or BMP receptors could be used to decipher the required for these highly similar proteins. Would a constitutively active form of SMAD1 or BMPR1A prevent the generation of pAnt cells?

Similarly, would a dominant negative form of BMPR1B prevent the cell cycle arrest seen at 7 somites? Conversely, would a constitutively active form of BMPR1B prevent the waves of sequential proliferation required for the generation of the hypothalamus?

7.2.3. BMP signalling during the emergence of Anterior and Mammillary progenitors

Another interesting avenue to explore would be to test the requirement for pSMAD1/5/8 downregulation in pAnt emergence. This could be tested via the electroporation of a constitutively active form of pSMAD1/5/8 into pBHyp cells. If pSMAD1/5/8 does prevent pAnt proliferation/differentiation then one would expect electroporated cells not to contribute to the anterior hypothalamus or to result in a smaller anterior region.

These are important questions as we understand the physiological roles of specific BMPs both in development and adult life. Single nucleotide polymorphisms in BMP2 and BMP7 have been shown to affect fertility in sheep, raising the possibility that BMP2 and BMP7 may play similar roles in humans and be of potential therapeutic use such as in fertility treatments (Zhang et al., 2019). These insights are already being translated into possible treatments, intracerebroventricular injection of FGF1 has been shown to alleviate type 2 diabetes pathology (Scarlett et al., 2019). Similar injections of recombinant BMP7 in mice can reduce food intake by ~45%, opening the possibility of a treatment for obesity as a possible use of BMP7 (Townsend et al., 2012). However, before exploring the therapeutic possibilities of BMPs and other signalling ligands a thorough understanding of their activity, both in the embryo and adult brain, is required to inform any medical trial of potential side effects, therapeutic windows and the effects of long term exposure or delayed effects.

References

Asa, S.L., and S. Ezzat. 2004. 'Molecular Basis of Pituitary Development and Cytogenesis'. In *Frontiers of Hormone Research*, edited by G. Kontogeorgos and K. Kovacs, 32:1–19. Basel: KARGER. https://doi.org/10.1159/000079035.

Adelmann, H.B., 1922. The significance of the prechordal plate: An interpretative study. Am. J. Anat. 31, 55–101. https://doi.org/10.1002/aja.1000310104

Anderson, D.J., 2016. Circuit modules linking internal states and social behaviour in flies and mice. Nat. Rev. Neurosci. 17, 692–704. https://doi.org/10.1038/nrn.2016.125

Anderson, R.M., Lawrence, A.R., Stottmann, R.W., Bachiller, D., Klingensmith, J., 2002. Chordin and noggin promote organizing centers of forebrain development in the mouse. Development 129, 4975–4987.

Aoto, K., Shikata, Y., Imai, H., Matsumaru, D., Tokunaga, T., Shioda, S., Yamada, G., Motoyama, J., 2009. Mouse Shh is required for prechordal plate maintenance during brain and craniofacial morphogenesis. Dev. Biol. 327, 106–120. https://doi.org/10.1016/j.ydbio.2008.11.022

Bachiller, D., Klingensmith, J., Kemp, C., Belo, J.A., Anderson, R.M., May, S.R., McMahon, J.A., McMahon, A.P., Harland, R.M., Rossant, J., De Robertis, E.M., 2000. The organizer factors Chordin and Noggin are required for mouse forebrain development. Nature 403, 658–661. https://doi.org/10.1038/35001072

Barahona, M.J., Llanos, P., Recabal, A., Escobar-Acuña, K., Elizondo-Vega, R., Salgado, M., Ordenes, P., Uribe, E., Sepúlveda, F.J., Araneda, R.C., García-Robles, M.A., 2018. Glial hypothalamic inhibition of GLUT2 expression alters satiety, impacting eating behavior. Glia 66, 592–605. https://doi.org/10.1002/glia.23267

Benford, H., Bolborea, M., Pollatzek, E., Lossow, K., Hermans-Borgmeyer, I., Liu, B., Meyerhof, W., Kasparov, S., Dale, N., 2017. A sweet taste receptor-dependent mechanism of glucosensing in hypothalamic tanycytes. Glia n/a-n/a. https://doi.org/10.1002/glia.23125

Briscoe, J., Pierani, A., Jessell, T.M., Ericson, J., 2000. A Homeodomain Protein Code Specifies Progenitor Cell Identity and Neuronal Fate in the Ventral Neural Tube. Cell 101, 435–445. https://doi.org/10.1016/S0092-8674(00)80853-3

Cannon, W. B. (1929) 'Organization for physiological homeostasis', *Physiological Reviews*. American Physiological Society, 9(3), pp. 399–431. doi: 10.1152/physrev.1929.9.3.399.

Carreno, G., Apps, J.R., Lodge, E.J., Panousopoulos, L., Haston, S., Gonzalez-Meljem, J.M., Hahn, H., Andoniadou, C.L., Martinez-Barbera, J.P., 2017. Hypothalamic sonic hedgehog is required for cell specification and proliferation of LHX3/LHX4 pituitary embryonic precursors. Dev. Camb. Engl. 144, 3289–3302. https://doi.org/10.1242/dev.153387

Castro, D.S., Martynoga, B., Parras, C., Ramesh, V., Pacary, E., Johnston, C., Drechsel, D., Lebel-Potter, M., Garcia, L.G., Hunt, C., Dolle, D., Bithell, A., Ettwiller, L., Buckley, N., Guillemot, F., 2011. A novel function of the proneural factor Ascl1 in progenitor proliferation identified by genome-wide characterization of its targets. Genes Dev. 25, 930–945. https://doi.org/10.1101/gad.627811

Chaikuad, A., Alfano, I., Kerr, G., Sanvitale, C.E., Boergermann, J.H., Triffitt, J.T., Delft, F. von, Knapp, S., Knaus, P., Bullock, A.N., 2012. Structure of the Bone Morphogenetic

Protein Receptor ALK2 and Implications for Fibrodysplasia Ossificans Progressiva. J. Biol. Chem. 287, 36990–36998. https://doi.org/10.1074/jbc.M112.365932

Chapman, S.C., Schubert, F.R., Schoenwolf, G.C., Lumsden, A., 2002. Analysis of Spatial and Temporal Gene Expression Patterns in Blastula and Gastrula Stage Chick Embryos. Dev. Biol. 245, 187–199. https://doi.org/10.1006/dbio.2002.0641

Chiang, C., Litingtung, Y., Lee, E., Young, K.E., Corden, J.L., Westphal, H., Beachy, P.A., 1996. Cyclopia and defective axial patterning in mice lacking Sonic hedgehog gene function. Nature 383, 407–413. https://doi.org/10.1038/383407a0

Chuang, J.C., Mathers, P.H., Raymond, P.A., 1999. Expression of three Rx homeobox genes in embryonic and adult zebrafish. Mech. Dev. 84, 195–198.

Corman, T.S., Bergendahl, S.E., Epstein, D.J., 2018. Distinct temporal requirements for Sonic hedgehog signaling in development of the tuberal hypothalamus. Dev. Camb. Engl. 145. https://doi.org/10.1242/dev.167379

Couly, G.F., Le Douarin, N.M., 1987. Mapping of the early neural primordium in quail-chick chimeras: II. The prosencephalic neural plate and neural folds: Implications for the genesis of cephalic human congenital abnormalities. Dev. Biol. 120, 198–214. https://doi.org/10.1016/0012-1606(87)90118-7

Cuny, G.D., Yu, P.B., Laha, J.K., Xing, X., Liu, J.-F., Lai, C.S., Deng, D.Y., Sachidanandan, C., Bloch, K.D., Peterson, R.T., 2008. Structure-activity relationship study of bone morphogenetic protein (BMP) signaling inhibitors. Bioorg. Med. Chem. Lett. 18, 4388–4392. https://doi.org/10.1016/j.bmcl.2008.06.052

Dale, J.K., Vesque, C., Lints, T.J., Sampath, T.K., Furley, A., Dodd, J., Placzek, M., 1997. Cooperation of BMP7 and SHH in the induction of forebrain ventral midline cells by prechordal mesoderm. Cell 90, 257–269.

Dale, K., Sattar, N., Heemskerk, J., Clarke, J.D., Placzek, M., Dodd, J., 1999. Differential patterning of ventral midline cells by axial mesoderm is regulated by BMP7 and chordin. Dev. Camb. Engl. 126, 397–408.

Davis, S.W., Camper, S.A., 2007. Noggin regulates Bmp4 activity during pituitary induction. Dev. Biol. 305, 145–160. https://doi.org/10.1016/j.ydbio.2007.02.001

Dick, Alexander, Andrea Meier, and Matthias Hammerschmidt. 1999. 'Smad1 and Smad5 Have Distinct Roles during Dorsoventral Patterning of the Zebrafish Embryo'. *Developmental Dynamics* 216 (3): 285–98. https://doi.org/10.1002/(SICI)1097-0177(199911)216:3<285::AID-DVDY7>3.0.CO;2-L

Dijke, P. ten, Miyazono, K., Heldin, C.-H., 1996. Signaling via hetero-oligomeric complexes of type I and type II serine/threonine kinase receptors. Curr. Opin. Cell Biol. 8, 139–145. https://doi.org/10.1016/S0955-0674(96)80058-5

Dréau, G.L., Saade, M., Gutiérrez-Vallejo, I., Martí, E., 2014. The strength of SMAD1/5 activity determines the mode of stem cell division in the developing spinal cord. J Cell Biol 204, 591–605. https://doi.org/10.1083/jcb.201307031

Ebisawa, T., Fukuchi, M., Murakami, G., Chiba, T., Tanaka, K., Imamura, T., Miyazono, K., 2001. Smurf1 Interacts with Transforming Growth Factor-β Type I Receptor through Smad7 and Induces Receptor Degradation. J. Biol. Chem. 276, 12477–12480. https://doi.org/10.1074/jbc.C100008200

Ellis, P.S., Burbridge, S., Soubes, S., Ohyama, K., Ben-Haim, N., Chen, C., Dale, K., Shen, M.M., Constam, D., Placzek, M., 2015. ProNodal acts via FGFR3 to govern duration of Shh expression in the prechordal mesoderm. Dev. Camb. Engl. 142, 3821–3832. https://doi.org/10.1242/dev.119628

Epstein, D.J., McMahon, A.P., Joyner, A.L., 1999. Regionalization of Sonic hedgehog

transcription along the anteroposterior axis of the mouse central nervous system is regulated by Hnf3-dependent and -independent mechanisms. Development 126, 281–292.

Ericson, J., Norlin, S., Jessell, T.M., Edlund, T., 1998. Integrated FGF and BMP signaling controls the progression of progenitor cell differentiation and the emergence of pattern in the embryonic anterior pituitary. Development 125, 1005–1015.

Filosa, S., Rivera-Perez, J.A., Gomez, A.P., Gansmuller, A., Sasaki, H., Behringer, R.R., Ang, S.L., 1997. Goosecoid and HNF-3beta genetically interact to regulate neural tube patterning during mouse embryogenesis. Development 124, 2843–2854.

Fu, T., Pearson, C., Towers, M., Placzek, M., 2019. Development of the basal hypothalamus through anisotropic growth. J. Neuroendocrinol. 31, e12727. https://doi.org/10.1111/jne.12727

Fu, T., Towers, M., Placzek, M.A., 2017. Fgf10+ progenitors give rise to the chick hypothalamus by rostral and caudal growth and differentiation. Dev. Camb. Engl. 144, 3278–3288. https://doi.org/10.1242/dev.153379

Fuentealba, L.C., Eivers, E., Ikeda, A., Hurtado, C., Kuroda, H., Pera, E.M., De Robertis, E.M., 2007. Integrating Patterning Signals: Wnt/GSK3 Regulates the Duration of the BMP/Smad1 Signal. Cell 131, 980–993. https://doi.org/10.1016/j.cell.2007.09.027

Furukawa, T., Kozak, C.A., Cepko, C.L., 1997. rax, a novel paired-type homeobox gene, shows expression in the anterior neural fold and developing retina. Proc. Natl. Acad. Sci. 94, 3088–3093.

García-Calero, E., Fernández-Garre, P., Martínez, S., Puelles, L., 2008. Early mammillary pouch specification in the course of prechordal ventralization of the forebrain tegmentum. Dev. Biol. 320, 366–377. https://doi.org/10.1016/j.ydbio.2008.05.545

Gautron, L., Elmquist, J.K., 2011. Sixteen years and counting: an update on leptin in energy balance. J. Clin. Invest. 121, 2087–2093. https://doi.org/10.1172/JCI45888

Groppe, J., Greenwald, J., Wiater, E., Rodriguez-Leon, J., Economides, A.N., Kwiatkowski, W., Affolter, M., Vale, W.W., Izpisua, B., Choe, S., 2002. Structural basis of BMP signalling inhibition by the cystine knot protein Noggin. Nature 420, 636–642. https://doi.org/10.1038/nature01245

González-Gaitán, M., M. P. Capdevila, and A. García-Bellido. 1994. 'Cell Proliferation Patterns in the Wing Imaginal Disc of Drosophila'. *Mechanisms of Development* 46 (3): 183–200. https://doi.org/10.1016/0925-4773(94)90070-1.

Haan, N., Goodman, T., Najdi-Samiei, A., Stratford, C.M., Rice, R., Agha, E.E., Bellusci, S., Hajihosseini, M.K., 2013. Fgf10-Expressing Tanycytes Add New Neurons to the Appetite/Energy-Balance Regulating Centers of the Postnatal and Adult Hypothalamus. J. Neurosci. 33, 6170–6180. https://doi.org/10.1523/JNEUROSCI.2437-12.2013

Hamburger, V., Hamilton, H.L., 1951. A series of normal stages in the development of the chick embryo. J. Morphol. 88, 49–92.

Hao, J., Ho, J.N., Lewis, J.A., Karim, K.A., Daniels, R.N., Gentry, P.R., Hopkins, C.R., Lindsley, C.W., Hong, C.C., 2010. In Vivo Structure−Activity Relationship Study of Dorsomorphin Analogues Identifies Selective VEGF and BMP Inhibitors. ACS Chem. Biol. 5, 245–253. https://doi.org/10.1021/cb9002865

Harrelson, Z., Kaestner, K.H., Evans, S.M., 2012. Foxa2 mediates critical functions of prechordal plate in patterning and morphogenesis and is cell autonomously required for early ventral endoderm morphogenesis. Biol. Open 1, 173–181. https://doi.org/10.1242/bio.2012040

Hashikawa, K., Hashikawa, Y., Lischinsky, J., Lin, D., 2018. The Neural Mechanisms of Sexually Dimorphic Aggressive Behaviors. Trends Genet. https://doi.org/10.1016/j.tig.2018.07.001

Hassel, S., Schmitt, S., Hartung, A., Roth, M., Nohe, A., Petersen, N., Ehrlich, M., Henis, Y.I., Sebald, W., Knaus, P., 2003. Initiation of Smad-Dependent and Smad-Independent Signaling via Distinct BMP-Receptor Complexes. JBJS 85, 44.

Hayashi, H., Abdollah, S., Qiu, Y., Cai, J., Xu, Y.-Y., Grinnell, B.W., Richardson, M.A., Topper, J.N., Gimbrone, M.A., Wrana, J.L., Falb, D., 1997. The MAD-Related Protein Smad7 Associates with the TGFβ Receptor and Functions as an Antagonist of TGFβ Signaling. Cell 89, 1165–1173. https://doi.org/10.1016/S0092-8674(00)80303-7

Heldin, C.-H., Miyazono, K., Dijke, P. ten, 1997. TGF-β signalling from cell membrane to nucleus through SMAD proteins. Nature 390, 465–471. https://doi.org/10.1038/37284

Hoodless, P.A., Haerry, T., Abdollah, S., Stapleton, M., O'Connor, M.B., Attisano, L., Wrana, J.L., 1996. MADR1, a MAD-Related Protein That Functions in BMP2 Signaling Pathways. Cell 85, 489–500. https://doi.org/10.1016/S0092-8674(00)81250-7

Israel, D.I., Nove, J., Kerns, K.M., Kaufman, R.J., Rosen, V., Cox, K.A., Wozney, J.M., 1996. Heterodimeric Bone Morphogenetic Proteins Show Enhanced Activity In Vitro and In Vivo. Growth Factors 13, 291–300. https://doi.org/10.3109/08977199609003229

Iwasaki, S., Iguchi, M., Watanabe, K., Hoshino, R., Tsujimoto, M., Kohno, M., 1999. Specific Activation of the p38 Mitogen-activated Protein Kinase Signaling Pathway and Induction of Neurite Outgrowth in PC12 Cells by Bone Morphogenetic Protein-2. J. Biol. Chem. 274, 26503–26510. https://doi.org/10.1074/jbc.274.37.26503

Kawabata, M., Imamura, T., Miyazono, K., 1998. Signal transduction by bone morphogenetic proteins. Cytokine Growth Factor Rev. 9, 49–61.

Kawabata, M., Inoue, H., Hanyu, A., Imamura, T., Miyazono, K., 1998. Smad proteins exist as monomers in vivo and undergo homo- and hetero-oligomerization upon activation by serine/threonine kinase receptors. EMBO J. 17, 4056–4065. https://doi.org/10.1093/emboj/17.14.4056

Kitamura, K., Miura, H., Yanazawa, M., Miyashita, T., Kato, K., 1997. Expression patterns of Brx1 (Rieg gene), Sonic hedgehog, Nkx2.2, Dlx1 and Arx during zona limitans intrathalamica and embryonic ventral lateral geniculate nuclear formation. Mech. Dev. 67, 83–96.

Koenig, B.B., Cook, J.S., Wolsing, D.H., Ting, J., Tiesman, J.P., Correa, P.E., Olson, C.A., Pecquet, A.L., Ventura, F., Grant, R.A., Chen, G.-X., Wrana, J.L., Massagué, J., Rosenbaum, J.S., 1994. Characterization and cloning of a receptor for BMP-2 and BMP-4 from NIH 3T3 cells. Mol. Cell. Biol. 14, 5961–5974. https://doi.org/10.1128/MCB.14.9.5961

Koshida, S., Shinya, M., Nikaido, M., Ueno, N., Schulte-Merker, S., Kuroiwa, A., Takeda, H., 2002. Inhibition of BMP Activity by the FGF Signal Promotes Posterior Neural Development in Zebrafish. Dev. Biol. 244, 9–20. https://doi.org/10.1006/dbio.2002.0581

Kretzschmar, M., Doody, J., Massagu, J., 1997. Opposing BMP and EGF signalling pathways converge on the TGF-β family mediator Smad1. Nature 389, 618–622. https://doi.org/10.1038/39348

Lee, B., Lee, S., Lee, S.-K., Lee, J.W., 2016. The LIM-homeobox transcription factor Isl1 plays crucial roles in the development of multiple arcuate nucleus neurons. Dev. Camb. Engl. 143, 3763–3773. https://doi.org/10.1242/dev.133967

Lee, K.J., Jessell, T.M., 1999. The Specification of Dorsal Cell Fates in the Vertebrate Central Nervous System. Annu. Rev. Neurosci. 22, 261–294. https://doi.org/10.1146/annurev.neuro.22.1.261

Li, Y., Dulac, C., 2018. Neural coding of sex-specific social information in the mouse brain. Curr. Opin. Neurobiol., Developmental Neuroscience 53, 120–130. https://doi.org/10.1016/j.conb.2018.07.005

Liem, K.F., Jessell, T.M., Briscoe, J., 2000. Regulation of the neural patterning activity of sonic hedgehog by secreted BMP inhibitors expressed by notochord and somites. Development 127, 4855–4866.

Lillien, L., Raphael, H., 2000. BMP and FGF regulate the development of EGF-responsive neural progenitor cells. Development 127, 4993–5005.

Lim, Y., Cho, G., Minarcik, J., Golden, J., 2005. Altered BMP signaling disrupts chick diencephalic development. Mech. Dev. 122, 603–620. https://doi.org/10.1016/j.mod.2004.12.001

Little, S.C., Mullins, M.C., 2009. Bone morphogenetic protein heterodimers assemble heteromeric type I receptor complexes to pattern the dorsoventral axis. Nat. Cell Biol. 11, 637–643. https://doi.org/10.1038/ncb1870

Lu, F., Kar, D., Gruenig, N., Zhang, Z.W., Cousins, N., Rodgers, H.M., Swindell, E.C., Jamrich, M., Schuurmans, C., Mathers, P.H., Kurrasch, D.M., 2013. Rax Is a Selector Gene for Mediobasal Hypothalamic Cell Types. J. Neurosci. 33, 259–272. https://doi.org/10.1523/JNEUROSCI.0913-12.2013

Lyons, K.M., Hogan, B.L.M., Robertson, E.J., 1995. Colocalization of BMP 7 and BMP 2 RNAs suggests that these factors cooperatively mediate tissue interactions during murine development. Mech. Dev. 50, 71–83. https://doi.org/10.1016/0925-4773(94)00326-I

Macdonald, R., Barth, K.A., Xu, Q., Holder, N., Mikkola, I., Wilson, S.W., 1995. Midline signalling is required for Pax gene regulation and patterning of the eyes. Development 121, 3267–3278.

Manning, L., Ohyama, K., Saeger, B., Hatano, O., Wilson, S.A., Logan, M., Placzek, M., 2006. Regional Morphogenesis in the Hypothalamus: A BMP-Tbx2 Pathway Coordinates Fate and Proliferation through Shh Downregulation. Dev. Cell 11, 873–885. https://doi.org/10.1016/j.devcel.2006.09.021

Marti, E., Bumcrot, D.A., Takada, R., McMahon, A.P., 1995. Requirement of 19K form of Sonic hedgehog for induction of distinct ventral cell types in CNS explants. Nature 375, 322–325. https://doi.org/10.1038/375322a0

McMahon, J.A., Takada, S., Zimmerman, L.B., Fan, C.-M., Harland, R.M., McMahon, A.P., 1998. Noggin-mediated antagonism of BMP signaling is required for growth and patterning of the neural tube and somite. Genes Dev. 12, 1438–1452. https://doi.org/10.1101/gad.12.10.1438

Mehler, M.F., Mabie, P.C., Zhu, G., Gokhan, S., Kessler, J.A., 2000. Developmental Changes in Progenitor Cell Responsiveness to Bone Morphogenetic Proteins Differentially Modulate Progressive CNS Lineage Fate. Dev. Neurosci. 22, 74–85. https://doi.org/10.1159/000017429

Meyer, N. éva P., Roelink, H., 2003. The amino-terminal region of Gli3 antagonizes the Shh response and acts in dorsoventral fate specification in the developing spinal cord. Dev. Biol. 257, 343–355. https://doi.org/10.1016/S0012-1606(03)00065-4

Muthu, V., Eachus, H., Ellis, P., Brown, S., Placzek, M., 2016. Rx3 and Shh direct anisotropic growth and specification in the zebrafish tuberal/anterior hypothalamus. Development dev.138305. https://doi.org/10.1242/dev.138305

Nasif, S., Souza, F.S.J. de, González, L.E., Yamashita, M., Orquera, D.P., Low, M.J., Rubinstein, M., 2015. Islet 1 specifies the identity of hypothalamic melanocortin neurons and is critical for normal food intake and adiposity in adulthood. Proc. Natl. Acad. Sci. 112, E1861–E1870. https://doi.org/10.1073/pnas.1500672112

Nguyen, V.H., Trout, J., Connors, S.A., Andermann, P., Weinberg, E., Mullins, M.C., 2000. Dorsal and intermediate neuronal cell types of the spinal cord are established by a BMP signaling pathway. Development 127, 1209–1220.

Ohuchi, H., Hori, Y., Yamasaki, M., Harada, H., Sekine, K., Kato, S., Itoh, N., 2000. FGF10 acts as a major ligand for FGF receptor 2 IIIb in mouse multi-organ development. Biochem. Biophys. Res. Commun. 277, 643–649. https://doi.org/10.1006/bbrc.2000.3721

Ohuchi, H., Tomonari, S., Itoh, H., Mikawa, T., Noji, S., 1999. Identification of chick rax/rx genes with overlapping patterns of expression during early eye and brain development. Mech. Dev. 85, 193–195.

Ohyama, K., Das, R., Placzek, M., 2008. Temporal progression of hypothalamic patterning by a dual action of BMP. Dev. Camb. Engl. 135, 3325–3331. https://doi.org/10.1242/dev.027078

Ohyama, K., Ellis, P., Kimura, S., Placzek, M., 2005. Directed differentiation of neural cells to hypothalamic dopaminergic neurons. Dev. Camb. Engl. 132, 5185–5197. https://doi.org/10.1242/dev.02094

Orquera, D.P., Nasif, S., Low, M.J., Rubinstein, M., de Souza, F.S.J., 2016. Essential function of the transcription factor Rax in the early patterning of the mammalian hypothalamus. Dev. Biol. 416, 212–224. https://doi.org/10.1016/j.ydbio.2016.05.021

Panchision, D.M., Pickel, J.M., Studer, L., Lee, S.-H., Turner, P.A., Hazel, T.G., McKay, R.D.G., 2001. Sequential actions of BMP receptors control neural precursor cell production and fate. Genes Dev. 15, 2094–2110. https://doi.org/10.1101/gad.894701

Patten, I., Kulesa, P., Shen, M.M., Fraser, S., Placzek, M., 2003. Distinct modes of floor plate induction in the chick embryo. Development 130, 4809–4821. https://doi.org/10.1242/dev.00694

Patten, I., Placzek, M., 2002. Opponent Activities of Shh and BMP Signaling during Floor Plate Induction In Vivo. Curr. Biol. 12, 47–52. https://doi.org/10.1016/S0960-9822(01)00631-5

Pearson, C.A., Ohyama, K., Manning, L., Aghamohammadzadeh, S., Sang, H., Placzek, M., 2011. FGF-dependent midline-derived progenitor cells in hypothalamic infundibular development. Dev. Camb. Engl. 138, 2613–2624. https://doi.org/10.1242/dev.062794

Pearson, C.A., Placzek, M., 2013. Development of the medial hypothalamus: forming a functional hypothalamic-neurohypophyseal interface. Curr. Top. Dev. Biol. 106, 49–88. https://doi.org/10.1016/B978-0-12-416021-7.00002-X

Peng, C.-Y., Mukhopadhyay, A., Jarrett, J.C., Yoshikawa, K., Kessler, J.A., 2012. BMP Receptor 1A Regulates Development of Hypothalamic Circuits Critical for Feeding Behavior. J. Neurosci. Off. J. Soc. Neurosci. 32, 17211–17224. https://doi.org/10.1523/JNEUROSCI.2484-12.2012

Pera, E.M., Kessel, M., 1997. Patterning of the chick forebrain anlage by the prechordal plate. Development 124, 4153–4162.

Persson, Urban, Hiroto Izumi, Serhiy Souchelnytskyi, Susumu Itoh, Susanne Grimsby, Ulla Engström, Carl-Henrik Heldin, Keiko Funa, and Peter ten Dijke. 1998. 'The L45 Loop in Type I Receptors for TGF-β Family Members Is a Critical Determinant in Specifying

Smad Isoform Activation'. *FEBS Letters* 434 (1–2): 83–87.
https://doi.org/10.1016/S0014-5793(98)00954-5.

Piccolo, S., Sasai, Y., Lu, B., De Robertis, E.M., 1996. Dorsoventral Patterning in Xenopus: Inhibition of Ventral Signals by Direct Binding of Chordin to BMP-4. Cell 86, 589–598. https://doi.org/10.1016/S0092-8674(00)80132-4

Placzek, M., Briscoe, J., 2005. The floor plate: multiple cells, multiple signals. Nat. Rev. Neurosci. 6, 230–240. https://doi.org/10.1038/nrn1628

Placzek, M., Dale, K., 1999. Tissue Recombinations in Collagen Gels, in: Sharpe, P.T., Mason, I. (Eds.), Molecular Embryology: Methods and Protocols, Methods in Molecular Biology™. Humana Press, Totowa, NJ, pp. 293–304. https://doi.org/10.1385/1-59259-270-8:293

Pronobis, M.I., Deuitch, N., Peifer, M., 2016. The Miraprep: A Protocol that Uses a Miniprep Kit and Provides Maxiprep Yields. PLOS ONE 11, e0160509. https://doi.org/10.1371/journal.pone.0160509

Puelles, L., Rubenstein, J.L.R., 2015. A new scenario of hypothalamic organization: rationale of new hypotheses introduced in the updated prosomeric model. Front. Neuroanat. 9. https://doi.org/10.3389/fnana.2015.00027

Ratié, L., Ware, M., Barloy-Hubler, F., Romé, H., Gicquel, I., Dubourg, C., David, V., Dupé, V., 2013. Novel genes upregulated when NOTCH signalling is disrupted during hypothalamic development. Neural Develop. 8, 25. https://doi.org/10.1186/1749-8104-8-25

Rios, I., Alvarez-Rodríguez, R., Martí, E., Pons, S., 2004. Bmp2 antagonizes sonic hedgehog-mediated proliferation of cerebellar granule neurones through Smad5 signalling. Development 131, 3159–3168. https://doi.org/10.1242/dev.01188

Rizzoti, K., Lovell-Badge, R., 2017. Pivotal role of median eminence tanycytes for hypothalamic function and neurogenesis. Mol. Cell. Endocrinol., Stem cells of endocrine glands 445, 7–13. https://doi.org/10.1016/j.mce.2016.08.020

Robins, S.C., Stewart, I., McNay, D.E., Taylor, V., Giachino, C., Goetz, M., Ninkovic, J., Briancon, N., Maratos-Flier, E., Flier, J.S., Kokoeva, M.V., Placzek, M., 2013. α-Tanycytes of the adult hypothalamic third ventricle include distinct populations of FGF-responsive neural progenitors. Nat. Commun. 4, 2049. https://doi.org/10.1038/ncomms3049

Rozbicki, Emil, Manli Chuai, Antti I. Karjalainen, Feifei Song, Helen M. Sang, René Martin, Hans-Joachim Knölker, Michael P. MacDonald, and Cornelis J. Weijer. 2015. 'Myosin-II-Mediated Cell Shape Changes and Cell Intercalation Contribute to Primitive Streak Formation'. *Nature Cell Biology* 17 (4): 397–408. https://doi.org/10.1038/ncb3138.

Ruiz i Altaba, A., 1998. Combinatorial Gli gene function in floor plate and neuronal inductions by Sonic hedgehog. Dev. Camb. Engl. 125, 2203–2212.

Sagai, T., Amano, T., Maeno, A., Ajima, R., Shiroishi, T., 2019. SHH signaling mediated by a prechordal and brain enhancer controls forebrain organization. Proc. Natl. Acad. Sci. https://doi.org/10.1073/pnas.1901732116

Saper, C.B., Lowell, B.B., 2014. The hypothalamus. Curr. Biol. CB 24, R1111-1116. https://doi.org/10.1016/j.cub.2014.10.023

Scarlett, J.M., Muta, K., Brown, J.M., Rojas, J.M., Matsen, M.E., Acharya, N.K., Secher, A., Ingvorsen, C., Jorgensen, R., Høeg-Jensen, T., Stefanovski, D., Bergman, R.N., Piccinini, F., Kaiyala, K.J., Shiota, M., Morton, G.J., Schwartz, M.W., 2019. Peripheral Mechanisms Mediating the Sustained Antidiabetic Action of FGF1 in the Brain. Diabetes 68, 654–664. https://doi.org/10.2337/db18-0498

Schier, A.F., Neuhauss, S.C., Helde, K.A., Talbot, W.S., Driever, W., 1997. The one-eyed pinhead gene functions in mesoderm and endoderm formation in zebrafish and interacts with no tail. Dev. Camb. Engl. 124, 327–342.

Schliermann, A., Nickel, J., 2018. Unraveling the connection between fibroblast growth factor and bone morphogenetic protein signaling. Int. J. Mol. Sci. 19, 3220.

Shi, W., Sun, C., He, B., Xiong, W., Shi, X., Yao, D., Cao, X., 2004. GADD34–PP1c recruited by Smad7 dephosphorylates TGFβ type I receptor. J. Cell Biol. 164, 291–300. https://doi.org/10.1083/jcb.200307151

Shibuya, H., Iwata, H., Masuyama, N., Gotoh, Y., Yamaguchi, K., Irie, K., Matsumoto, K., Nishida, E., Ueno, N., 1998. Role of TAK1 and TAB1 in BMP signaling in early Xenopus development. EMBO J. 17, 1019–1028. https://doi.org/10.1093/emboj/17.4.1019

Shimogori, T., Lee, D.A., Miranda-Angulo, A., Yang, Y., Wang, H., Jiang, L., Yoshida, A.C., Kataoka, A., Mashiko, H., Avetisyan, M., Qi, L., Qian, J., Blackshaw, S., 2010. A genomic atlas of mouse hypothalamic development. Nat. Neurosci. 13, 767–775. https://doi.org/10.1038/nn.2545

Shirai, M., Imanaka-Yoshida, K., Schneider, M.D., Schwartz, R.J., Morisaki, T., 2009. T-box 2, a mediator of Bmp-Smad signaling, induced hyaluronan synthase 2 and Tgfβ2 expression and endocardial cushion formation. Proc. Natl. Acad. Sci. 106, 18604–18609. https://doi.org/10.1073/pnas.0900635106

Singh Reena, Horsthuis Thomas, Farin Henner F., Grieskamp Thomas, Norden Julia, Petry Marianne, Wakker Vincent, Moorman Antoon F.M., Christoffels Vincent M., Kispert Andreas, 2009. Tbx20 Interacts With Smads to Confine Tbx2 Expression to the Atrioventricular Canal. Circ. Res. 105, 442–452. https://doi.org/10.1161/CIRCRESAHA.109.196063

Sirard, C., Pompa, J.L. de la, Elia, A., Itie, A., Mirtsos, C., Cheung, A., Hahn, S., Wakeham, A., Schwartz, L., Kern, S.E., Rossant, J., Mak, T.W., 1998. The tumor suppressor gene Smad4/Dpc4 is required for gastrulation and later for anterior development of the mouse embryo. Genes Dev. 12, 107–119. https://doi.org/10.1101/gad.12.1.107

Srinivasan, S., Hu, J.S., Currle, D.S., Fung, E.S., Hayes, W.B., Lander, A.D., Monuki, E.S., 2014. A BMP-FGF Morphogen Toggle Switch Drives the Ultrasensitive Expression of Multiple Genes in the Developing Forebrain. PLOS Comput. Biol. 10, e1003463. https://doi.org/10.1371/journal.pcbi.1003463

Streit, A., Lee, K.J., Woo, I., Roberts, C., Jessell, T.M., Stern, C.D., 1998. Chordin regulates primitive streak development and the stability of induced neural cells, but is not sufficient for neural induction in the chick embryo. Dev. Camb. Engl. 125, 507–519.

Sun, Y., Hu, J., Zhou, L., Pollard, S.M., Smith, A., 2011. Interplay between FGF2 and BMP controls the self-renewal, dormancy and differentiation of rat neural stem cells. J Cell Sci 124, 1867–1877. https://doi.org/10.1242/jcs.085506

Szabó, N.-E., Zhao, T., Çankaya, M., Theil, T., Zhou, X., Alvarez-Bolado, G., 2009. Role of Neuroepithelial Sonic hedgehog in Hypothalamic Patterning. J. Neurosci. 29, 6989–7002. https://doi.org/10.1523/JNEUROSCI.1089-09.2009

Takuma, N., H. Z. Sheng, Y. Furuta, J. M. Ward, K. Sharma, B. L. Hogan, S. L. Pfaff, H. Westphal, S. Kimura, and K. A. Mahon. 1998. 'Formation of Rathke's Pouch Requires Dual Induction from the Diencephalon'. *Development* 125 (23): 4835–40.

Teraoka, M.E., Paschaki, M., Muta, Y., Ladher, R.K., 2009. Rostral paraxial mesoderm regulates refinement of the eye field through the bone morphogenetic protein (BMP) pathway. Dev. Biol. 330, 389–398. https://doi.org/10.1016/j.ydbio.2009.04.008

Tessmar-Raible, K., Raible, F., Christodoulou, F., Guy, K., Rembold, M., Hausen, H., Arendt, D.,

2007. Conserved Sensory-Neurosecretory Cell Types in Annelid and Fish Forebrain: Insights into Hypothalamus Evolution. Cell 129, 1389–1400. https://doi.org/10.1016/j.cell.2007.04.041

Thaler, J.P., Lee, S.-K., Jurata, L.W., Gill, G.N., Pfaff, S.L., 2002. LIM Factor Lhx3 Contributes to the Specification of Motor Neuron and Interneuron Identity through Cell-Type-Specific Protein-Protein Interactions. Cell 110, 237–249. https://doi.org/10.1016/S0092-8674(02)00823-1

Timmer, J.R., Wang, C., Niswander, L., 2002. BMP signaling patterns the dorsal and intermediate neural tube via regulation of homeobox and helix-loop-helix transcription factors. Development 129, 2459–2472.

Townsend, K.L., Suzuki, R., Huang, T.L., Jing, E., Schulz, T.J., Lee, K., Taniguchi, C.M., Espinoza, D.O., McDougall, L.E., Zhang, H., He, T.-C., Kokkotou, E., Tseng, Y.-H., 2012. Bone morphogenetic protein 7 (BMP7) reverses obesity and regulates appetite through a central mTOR pathway. FASEB J. 26, 2187–2196. https://doi.org/10.1096/fj.11-199067

Treier, M., A. S. Gleiberman, S. M. O'Connell, D. P. Szeto, J. A. McMahon, A. P. McMahon, and M. G. Rosenfeld. 1998. 'Multistep Signaling Requirements for Pituitary Organogenesis in Vivo'. *Genes & Development* 12 (11): 1691–1704.

Treier, M., O'Connell, S., Gleiberman, A., Price, J., Szeto, D.P., Burgess, R., Chuang, P.T., McMahon, A.P., Rosenfeld, M.G., 2001. Hedgehog signaling is required for pituitary gland development. Dev. Camb. Engl. 128, 377–386.

Treier, M., and Rosenfeld, M., 1996. 'The Hypothalamic-Pituitary Axis; Co-Development of Two Organs'. *Current Opinion in Cell Biology* 8 (6): 833–43. https://doi.org/10.1016/S0955-0674(96)80085-8.

Troilo, H., Zuk, A.V., Tunnicliffe, R.B., Wohl, A.P., Berry, R., Collins, R.F., Jowitt, T.A., Sengle, G., Baldock, C., 2014. Nanoscale structure of the BMP antagonist chordin supports cooperative BMP binding. Proc. Natl. Acad. Sci. 111, 13063–13068. https://doi.org/10.1073/pnas.1404166111

Trowe, M.-O., Zhao, L., Weiss, A.-C., Christoffels, V., Epstein, D.J., Kispert, A., 2013. Inhibition of Sox2-dependent activation of Shh in the ventral diencephalon by Tbx3 is required for formation of the neurohypophysis. Dev. Camb. Engl. 140, 2299–2309. https://doi.org/10.1242/dev.094524

Urist, M.R., 1965. Bone: Formation by Autoinduction. Science 150, 893–899. https://doi.org/10.1126/science.150.3698.893

Vesque, C., Ellis, S., Lee, A., Szabo, M., Thomas, P., Beddington, R., Placzek, M., 2000. Development of chick axial mesoderm: specification of prechordal mesoderm by anterior endoderm-derived TGFbeta family signalling. Development 127, 2795–2809.

Walsh, D.W., Godson, C., Brazil, D.P., Martin, F., 2010. Extracellular BMP-antagonist regulation in development and disease: tied up in knots. Trends Cell Biol. 20, 244–256. https://doi.org/10.1016/j.tcb.2010.01.008

Ware, M., Hamdi-Rozé, H., Dupé, V., 2014. Notch signaling and proneural genes work together to control the neural building blocks for the initial scaffold in the hypothalamus. Front. Neuroanat. 8. https://doi.org/10.3389/fnana.2014.00140

Wrighton, Katharine H., Xia Lin, and Xin-Hua Feng. 2009. 'Phospho-Control of TGF-β Superfamily Signaling'. *Cell Research* 19 (1): 8–20. https://doi.org/10.1038/cr.2008.327.

Xu, Pinglong, Jianming Liu, and Rik Derynck. 2012. 'Post-Translational Regulation of TGF-β Receptor and Smad Signaling'. *FEBS Letters*, Sorting the TGF-β Labyrinth, 586 (14):

1871–84. https://doi.org/10.1016/j.febslet.2012.05.010.

Yamaguchi, K., Nagai, S., Ninomiya-Tsuji, J., Nishita, M., Tamai, K., Irie, K., Ueno, N., Nishida, E., Shibuya, H., Matsumoto, K., 1999. XIAP, a cellular member of the inhibitor of apoptosis protein family, links the receptors to TAB1–TAK1 in the BMP signaling pathway. EMBO J. 18, 179–187. https://doi.org/10.1093/emboj/18.1.179

Yamaguchi, K., Shirakabe, K., Shibuya, H., Irie, K., Oishi, I., Ueno, N., Taniguchi, T., Nishida, E., Matsumoto, K., 1995. Identification of a Member of the MAPKKK Family as a Potential Mediator of TGF-β Signal Transduction. Science 270, 2008–2011. https://doi.org/10.1126/science.270.5244.2008

Yamashita, H., ten Dijke, P., Huylebroeck, D., Sampath, T.K., Andries, M., Smith, J.C., Heldin, C.H., Miyazono, K., 1995. Osteogenic protein-1 binds to activin type II receptors and induces certain activin-like effects. J. Cell Biol. 130, 217–226. https://doi.org/10.1083/jcb.130.1.217

Yang, L., Cai, C.-L., Lin, L., Qyang, Y., Chung, C., Monteiro, R.M., Mummery, C.L., Fishman, G.I., Cogen, A., Evans, S., 2006. Isl1Cre reveals a common Bmp pathway in heart and limb development. Development 133, 1575–1585. https://doi.org/10.1242/dev.02322

Yates, D., 2015. Going on the defensive. Nat. Rev. Neurosci. 16, 247–247. https://doi.org/10.1038/nrn3952

Yoo, Sooyeon, and Seth Blackshaw. 2018. 'Regulation and Function of Neurogenesis in the Adult Mammalian Hypothalamus'. *Progress in Neurobiology*, April. https://doi.org/10.1016/j.pneurobio.2018.04.001.

Yu, P.B., Hong, C.C., Sachidanandan, C., Babitt, J.L., Deng, D.Y., Hoyng, S.A., Lin, H.Y., Bloch, K.D., Peterson, R.T., 2008. Dorsomorphin inhibits BMP signals required for embryogenesis and iron metabolism. Nat. Chem. Biol. 4, 33–41. https://doi.org/10.1038/nchembio.2007.54

Zhang, J.-L., Huang, Y., Qiu, L.-Y., Nickel, J., Sebald, W., 2007. Von Willebrand factor type C domain-containing proteins regulate bone morphogenetic protein signaling through different recognition mechanisms. J. Biol. Chem. 282, 20002–20014. https://doi.org/10.1074/jbc.M700456200

Zhang, Y., Proenca, R., Maffei, M., Barone, M., Leopold, L., Friedman, J.M., 1994. Positional cloning of the mouse obese gene and its human homologue. Nature 372, 425–432. https://doi.org/10.1038/372425a0

Zhang, Z., Liu, Q., Di, R., Hu, W., Wang, X., He, X., Ma, L., Chu, M., 2019. Single nucleotide polymorphisms in BMP2 and BMP7 and the association with litter size in Small Tail Han sheep. Anim. Reprod. Sci. 204, 183–192. https://doi.org/10.1016/j.anireprosci.2019.04.001

Zhao, L., Zevallos, S.E., Rizzoti, K., Jeong, Y., Lovell-Badge, R., Epstein, D.J., 2012. Disruption of SoxB1-Dependent Sonic hedgehog Expression in the Hypothalamus Causes Septo-optic Dysplasia. Dev. Cell 22, 585–596. https://doi.org/10.1016/j.devcel.2011.12.023

Zhou, G., Myers, R., Li, Y., Chen, Y., Shen, X., Fenyk-Melody, J., Wu, M., Ventre, J., Doebber, T., Fujii, N., Musi, N., Hirshman, M.F., Goodyear, L.J., Moller, D.E., 2001. Role of AMP-activated protein kinase in mechanism of metformin action. J. Clin. Invest. 108, 1167–1174. https://doi.org/10.1172/JCI13505